WANGANUI RIVER
Flood Modelling
Report

5 March 2024

Client: West Coast Regional Council

Report by: Rose Beagley & Matthew Gardner
Land River Sea Consulting Limited
www.landriversea.com

Land River Sea CONSULTING

THE WEST COAST REGIONAL COUNCIL

REVISION HISTORY

Author:	Rose Beagley Geomorphologist / Water Resources Scientist	Matthew Gardner Water Resources Engineer, CMEngNZ, CPEng
Signature:		
Date:	5 March 2024	(Final DRAFT published 27 July 2023)
Revision:	03	
Authorised by:	Kent Jacobsen / Darryl Lew	
Signature:		
Organisation:	West Coast Regional Council	
Date:		

Land River Sea Consulting Limited

5/245 St Asaph Street

Christchurch

M: +64 27 318 9527

E: matthew@landriversea.com

W: landriversea.com

EXECUTIVE SUMMARY

Land River Sea Consulting has been contracted by the West Coast Regional Council (WCRC) to develop a detailed flood model of the Wanganui River to allow a better understanding of the current level of service of the Wanganui protection scheme; investigate breach scenarios, potential areas of erosion and aggradation; and develop a general understanding of both the historic and current behaviour of the river to assist with advice around future management of the scheme.

SCHEME HISTORY

The first protection works on the Wanganui River were instigated by severe flooding of the Hari Hari Flat in 1913, resulting in a 400 m stopbank immediately downstream from the old SH6 bridge abutment on the true left.

There is no record of further work until the late 1950's when both sides of the river received the bulk of the protections. Between 1958 and 1976 hook groynes, training walls and the main stopbank scheme were completed along approximately 8 km of the true left bank, and a small section of eroding bank approximately 2 to 3 km downstream of the SH6 bridge on the true right received hook groynes and a training wall.

Further stopbanks, groynes and training walls were constructed on the true left in 1982, and due to flood damage, repairs and additions were made to the protection works on the true right between 1980 and 1987. Construction of the true right stopbanks have resulted in approximately 40% of the active riverbed being converted to pasture since the mid 1980's.

GEOMORPHOLOGY

The Wanganui River behaves like a typical braided river, shifting back and forth across the active braidplain as it moves its high volume of sediment and water from source to sea.

The protective network constructed largely during the 20th century has affected the natural behaviour of the river by reducing the braidplain, resulting in less space to deposit sediment and absorb floodwaters, as well as narrowing the corridor the river has access to and so changing the behaviour of the main channel of flow. This has exacerbated river bed aggradation resulting in a decreased level of service from the existing stopbanks.

In addition to human influence, the Wanganui River appears to be influenced by the positive and negative phases of the Interdecadal Pacific Oscillation (IPO) which result in active and quiescent phases, respectively. The bulk of the true left side of the scheme was built in a quiescent phase (1950s to 1970s), whilst the true right side was constructed in a more active phase (1980s to 1990s) and as such experienced repeated damage at the time, due to large and more frequent flood events.

The IPO is believed to have switched to a positive phase around 2020, and climate change projections forecast a wetter West Coast, which will result in an increased sediment supply from greater amounts of catchment erosion, and increased flood event frequency and intensity.

The combination of increased sediment supply and flow variability, as well as the potential for further additions to the network seems likely to exacerbate the current situation, resulting in continued network damage and chances of breach or overtopping.

Comparison of cross sections from 2012 with the latest LiDAR data shows that the river is actively aggrading, and this is most likely due to confinement caused by the construction of stopbanks. This is most notable between 7 km and 10 km downstream of the SH6 bridge where the main channel has become perched above the floodplain.

The trend of increasing bed levels will further reduce the capacity of the flood protection network over time, increasing the chance of breach or overtopping during events. As a result of this ongoing aggradation, past behaviour of the river cannot be relied upon as a reliable indicator of future behaviour.

HYDRAULIC MODELLING

A detailed 2D model has been built of the river system based on a combination of the latest LiDAR survey data (2020) as well as topographical drone survey (2022). The model has been constructed using industry best practice techniques, however the model is uncalibrated due to the lack of available hydrological data, and as a result has a greater level of uncertainty in comparison to a calibrated model (e.g. the Buller River Model). The model is still considered an excellent tool for better understanding likely flood risk and assessing the impacts of changes in the catchment. It is a significant improvement on the previous 1D modelling (Gardner & Wallace, 2013).

Limitations of the model, particularly due to the fact that it is a fixed bed model and does not simulate sediment transport do need to be kept in mind, with the results being interpreted by experienced professionals.

Detailed flood maps showing depth, speed and hazard have been produced for a number of annual exceedance probability (AEP) events ranging from a 10% AEP (10-year ARI) to a 1% AEP (100-year ARI) event including an estimate for the potential impacts of climate change.

MODEL RESULTS

BASE RUNS

Results show that the scheme performs reasonably well for 10% AEP and 5% AEP events with no overtopping visible on the true left bank, however inundation is visible on the true right bank, spilling between the gaps in existing banks as well as some minor overtopping visible in select locations.

The true left stopbank has several low spots which are likely to begin to overtop in a 2% AEP flow. Much of the bank has little to no freeboard available with the current bed levels. There is significant overtopping of the true right stopbanks, and it is pointed out that these banks would have a high probability of collapse should they overtop.

Flood flow velocities are very high in locations, particularly where the braid alignment bounces off the existing banks, and where structures such as groynes etc are impeding the flow. Velocities are sufficient to damage even large rockwork, and ongoing failures can be expected, particularly where rock work has been damaged or loosened in previous flood events.

BREACH SCENARIOS

Breach failures on the true left stopbank have the potential to flood large sections of farmland as well as causing significant damage due to scour with high velocities.

Breach failures on the true right stopbanks don't show significant changes in flood extent due to the fact that significant water already spills on the true right through the existing gaps in the network, as well as from the tributaries, however results do show significant increases in flood flow velocities, indicating that the banks are providing significant protection to the adjacent land by preventing scour.

GENERAL CONCLUSIONS

The existing 2D model of the river is a useful tool which can be used to investigate the impact of potential changes to the flood protection network allowing likely impacts to be assessed before they are considered for construction.

The current management regime for the river is likely to be financially unsustainable in the long term. The river has been severely constrained and whilst the stopbank network has survived until now, the climate appears to have been in a quiescent stage since the late 1990's. However, it seems reasonable that we can expect a continuation of the active river behaviour from the last few years in at least the coming decade.

Expanding the protective network to fill in gaps between stopbanks may serve only to exacerbate the current situation, resulting in continued network damage and increasing the likelihood of breaches or overtopping.

Removal of all or part of the right bank protection works may assist in slowing the rate of aggradation, reducing the pressure on the true left protection works, and decreasing the chance of a breach or overtopping. This would however have significant negative impact on the existing land users and would require further study.

RECOMMENDATIONS

Investigate installing a flow gauge in the catchment to allow an accurate estimate of flow at the State Highway 6 bridge to be determined.

Collect peak water levels down the full length of the river immediately after a flood event to assist with calibration of the model and to improve our understanding of river behaviour.

Keeping detailed logs of recollections of flood events from local residents / flood photos on file will assist in improving our understanding of the river behaviour.

Breach scenarios predict significant impacts. It is recommended that geotechnical investigations are carried out to assess the condition of the existing banks and to better determine their likelihood of failure.

Further investigations in order to better understand the long term aggradation trends as well as river characteristics would be worthwhile.

Minor earthworks to raise low spots on the true left bank could add significant resilience to the scheme by reducing the risk of an overtopping failure.

Regular inspections of the entire scheme are recommended after each high flow event in order to determine if there is any minor damage which could be further exacerbated in future events. Model results indicate that there are very high velocities in locations and potential for scour failure is high should any rockwork be damaged.

Serious thought and discussion needs to be had around realistic long-term management of the scheme. Consideration needs to be given to affordability / return on investment for long term protection. Trade-offs in regard to protection of the right / left bank may need to be considered.

Decisions around the desired level of service for the scheme will be necessary, with the scheme currently providing less than a 2% annual exceedance probability (AEP; 50-year ARI) level of service based on the historic climate. This level of service is actively decreasing with ongoing aggradation as well as a warming climate bringing more intense and larger flood events.

TABLE OF CONTENTS

1. INTRODUCTION

1.1. SCOPE

Land River Sea Consulting has been contracted by the West Coast Regional Council (WCRC) to develop a detailed flood model of the Wanganui River for approximately 24 km immediately downstream of the SH6 bridge to the sea (Figure 1-1) including input from the tributaries labelled in Figure 1-2.

The purpose of the model is to:

- allow a better understanding of the current level of service of the Wanganui protection scheme;
- investigate breach scenarios, and potential areas of erosion and aggradation; and
- develop a general understanding of both the historic and current behaviour of the river to assist with advice around future management of the scheme.

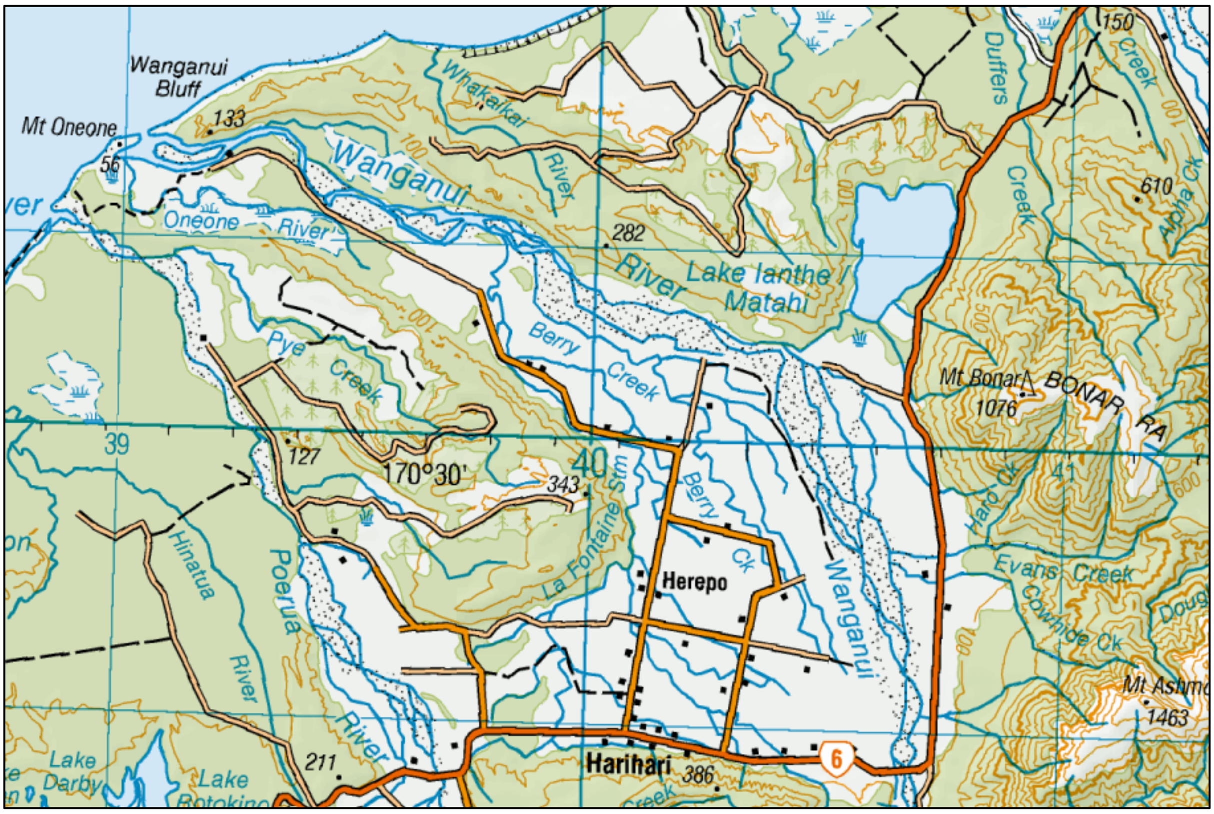

Figure 1-1: Area of Interest

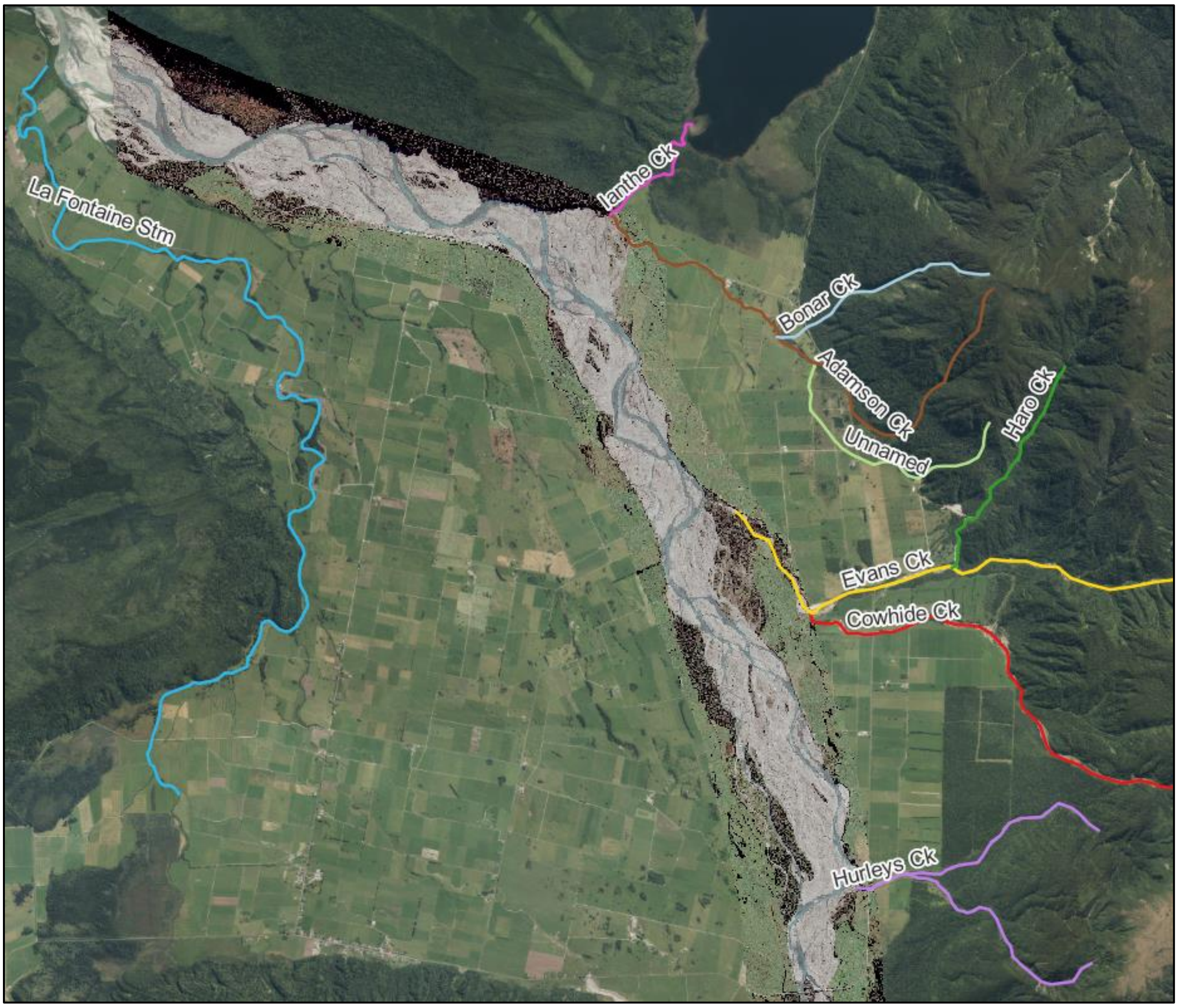

Figure 1-2: Tributaries included in the Wanganui River model.

The scope of the project involves:

- Building a detailed MIKE 21 model of the reach based on the 2021 LiDAR as well as cross section survey data.
- Creating maps of flood depth, extent and hazard for 2% and 1% annual exceedance probability (AEP; 50- and 100-year ARI) event scenarios under the current climate.
- Simulating separate breach and banks down scenarios.
- Investigating the historic and geomorphic setting of the river using the available aerial imagery from 1948 to 2022.

1.2. PREVIOUS MODELLING

The only modelling completed previously was by Matthew Gardner and Philip Wallace of River Edge Consulting Limited in June 2013. The modelling was carried out using the MIKE 11 software by DHI, which solves the 1D Saint-Venant equations to determine flow characteristics.

The inflow hydrology was based on consideration of at-site records from nearby catchments and the regional flood estimation methods, with the hydrograph shape taken from a consideration of recorded flow hydrographs at the Whataroa Rv @ SH6 site.

The modelling simulated 2%, 1% and 0.25% AEP (50, 100 and 400-year ARI) events and provided design levels for the three stopbanks on the true right bank of the Wanganui River, as well as advising that the existing left bank stopbank is lower than a 2% AEP design level.

The report did not specifically model the impact of climate change.

1.3. SITE VISIT

On the 30th of May 2013, Matthew Gardner and Phillip Wallace from River Edge Consulting were accompanied by Wayne Moen from the WCRC to visit the general scheme area. The purpose of the visit was to observe the catchment on the ground to assist with the representation of the river in the model.

On the 6th and 7th of October 2022, Matthew Gardner and Bilu Susan Babu were accompanied by James Bell from WCRC to visit the general scheme area. The purpose of the visit was to capture drone footage of the area not captured by the 2021 LiDAR and to view the river, including observations of gravel characteristics, stopbank locations, berm vegetation and evidence of previous flood levels.

A selection of site visit photos are included in Appendix A.

1.4. RATING DISTRICT

The Wanganui Rating District is broken up into six rateable classifications (Figure 1-3), all of which are detailed in the Wanganui Rating District 2021-2024 Asset Management Plan (West Coast Regional Council, 2022).

The objectives of the district are (quoted from the Asset Management Plan):

1. *To reduce bank erosion and flooding of the existing structures between the State Highway Bridge and the end of the stopbank 13 kilometres downstream.*
2. *To maintain existing creeks and drains included in the La Fontaine and Lower La Fontaine and Hari Hari Township Drainage Schemes to their original plan specifications.*

The level of service provided by the asset network and council to ensure these objectives are met is aligned with community values including affordability, quality, safety, community engagement, reliability, and sustainability.

A map of the assets included in the plan is shown below in Figure 1-4.

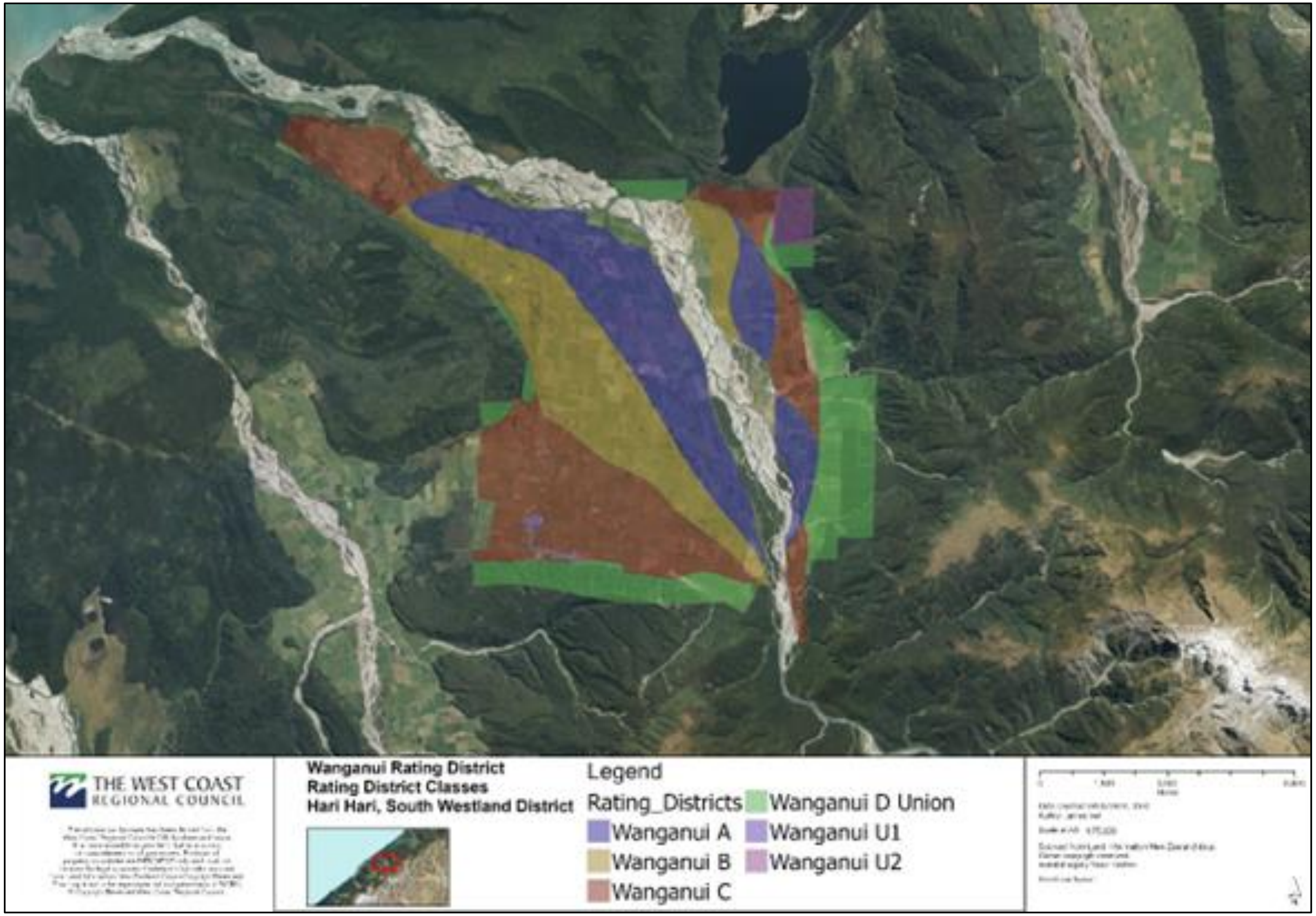

Figure 1-3: WCRC provided map. Wanganui rating district classes in Hari Hari, South Westland.

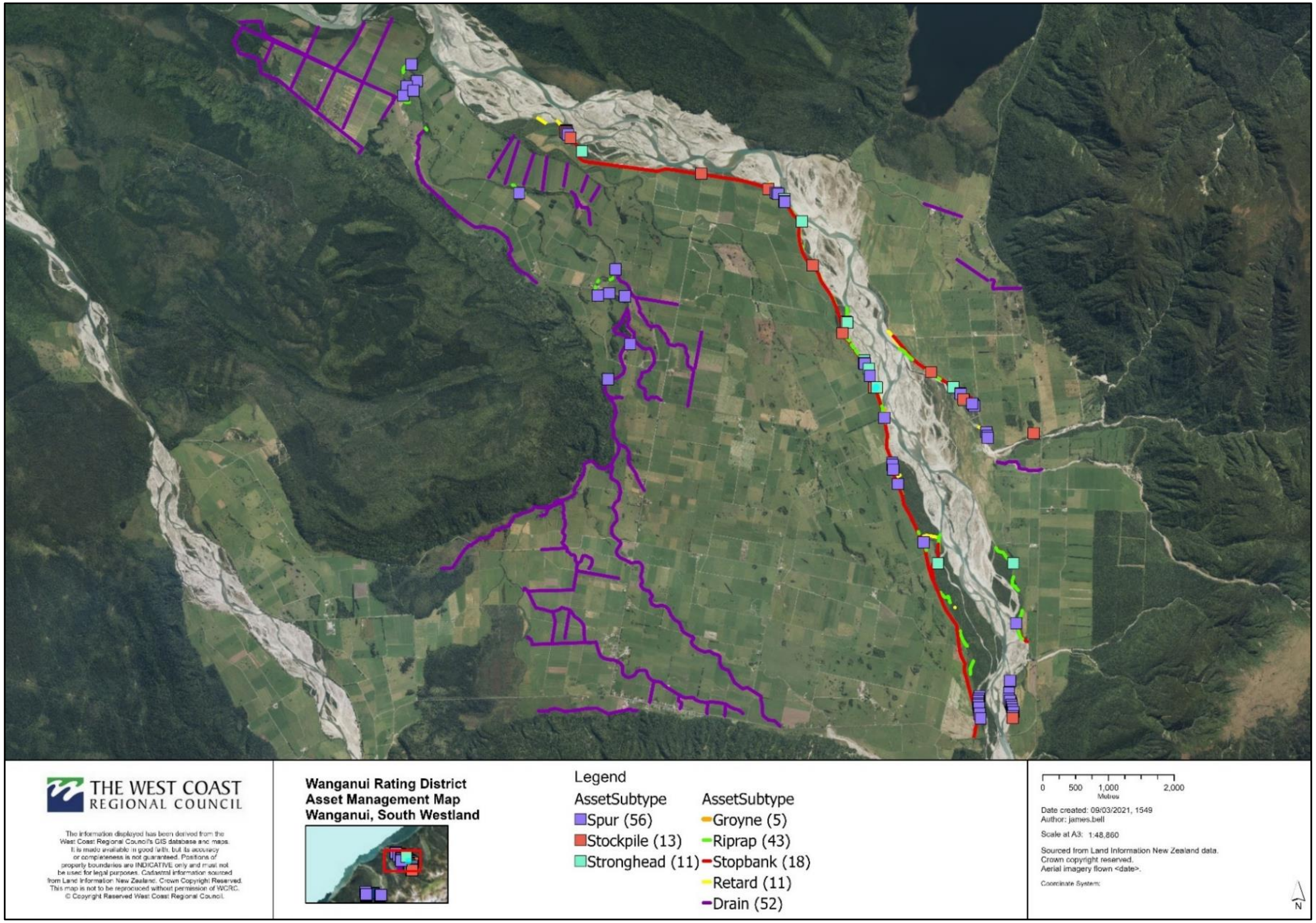

Figure 1-4: WCRC provided map. Not all assets have been added to the map due to WCRC not having the spatial data to represent them.

2. LIMITATIONS OF STUDY

This study has been carried out using the information and data made available to the consultancy at the time of this study. There are number of uncertainties which should be acknowledged which include but are not limited to:

- LiDAR data – whilst there is good coverage, LiDAR data comes with a degree of vertical uncertainty typically considered to be in the range of +\-0.15 m.
- The river bathymetry has not been surveyed and has been interpolated.
- There is significant uncertainty in the input hydrology estimates due to lack of any flow data for the river.
- The model is a fixed bed model and does not allow for bed mobilisation / gravel transport.
- The model is uncalibrated due to the lack of flow gauging as well as a lack of historic water level information.

3. HISTORICAL PERSPECTIVE

3.1. PROTECTION SCHEME

A detailed discussion of the Wanganui River protection scheme can be found in the WCRC "Wanganui Rating District 2021-2024 Asset Management Plan" (West Coast Regional Council, 2022). However, the main periods of historic work from this document are summarised below:

- The first protection works on the Wanganui River were instigated by severe flooding of the Hari Hari Flat in 1913, resulting in a 400 m stopbank immediately downstream from the old SH6 bridge abutment on the true left (Figure 3-1). There is earlier mention of a rock groyne in 1905 near where the ferry used to operate before the old bridge was built (Benn, 1990).

Figure 3-1 – The 400 m long true left stopbank immediately downstream of the old SH6 bridge.

- There is no record of further work until the late 1950's from when both sides of the river received the bulk of the protections. Between 1958 and 1976 hook groynes, training walls and the main stopbank scheme were completed along ~8 km of the true left bank, and a small section of eroding bank ~2 to 3 km downstream of the SH6 bridge on the true right received hook groynes and a training wall.
- Further stopbank, groynes and training walls were constructed on the true left in 1982, and due to flood damage, repairs and additions were made to the protection works on the true right between 1980 and 1987.

Breakout points have been identified from where protection works were focussed historically and the recorded damage from flood events (Figure 3-2).

True left

- A) 200 m immediately up and downstream of the current SH6 bridge: severe flooding of Hari Hari Flat in 1913.

- B) 2.8 km downstream of the SH6 bridge (downstream of Peterson Rd end): erosion threatening main scheme in 1972.
- C) 6.6 km downstream of the SH6 bridge (downstream of Haddock Rd end): washout of the stopbank in 1982 (evident in the 1984 imagery), and damage to the groyne stronghead in 1994.

True right

- D) 1.7 km downstream of the SH6 bridge: erosion in 1966, riverbank on the inside of the hook groyne washed out in 1980, and hook groyne and training wall destroyed in 1985. This area is currently actively eroding.

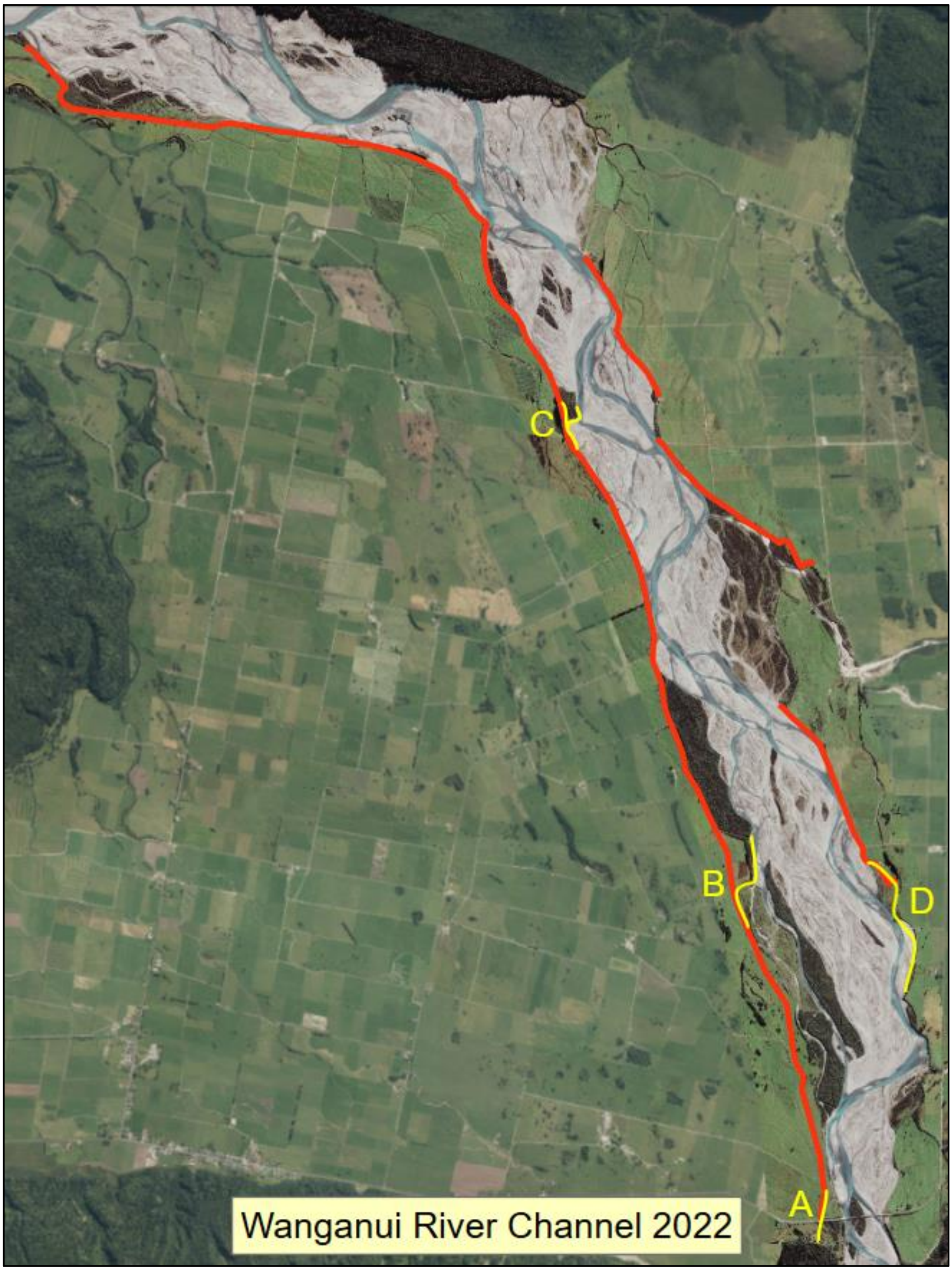

Figure 3-2: Breakout points identified from where historical protection works were focussed.

3.2. GEOMORPHOLOGY

Over the 74-year period of which we have imagery available (see Appendix B for the full set of imagery), the Wanganui River has been behaving like a typical braided river. Its many channels actively adjusting as the main channel shifts back and forth across the active braidplain, whilst occupying the northeast side of the fan that has formed downstream of the SH6 bridge.

However, there are some stark differences between the imagery pre and post 1984, which appear to be largely due to the confinement of the river by the protection scheme discussed in Section 3.1. This scheme has reduced the area of braidplain the river has access to and as a result influenced the behaviour of the system.

Further analysis of the imagery shows that there appears to be more exposed sediment present throughout the catchment (from landslides) in the 1980's imagery which coincides with a more complex braidplain as well as with the frequency and intensity of reported damage to the protection network from the late 1970s to mid-1990s.

Braidplain

The historic aerial imagery from 1948 to 1984 shows that the river used to have access to a far greater area of braidplain than it is currently restricted to:

- Up until the late 1960s, protection works were focussed predominantly on the true left. In 1948 this side of the main river channel between the SH6 bridge and about 12 km downstream is mosaiced with light vegetation, small areas of active braidplain, and paleochannels in recent braidplain. However, by 1964, this area was being developed into farmland with protective structures present along the true left bank, and by the time the 1981 imagery is taken, the entire area (~6.4 km^2) is occupied by pasture (Figure 3-3). The loss of access of the river to this true left side would have put pressure on the true right, as blocked from the left the river would have been forced in that direction. Subsequently, protective works intensified on the true right to regain control of a river that was trying to find space to move.

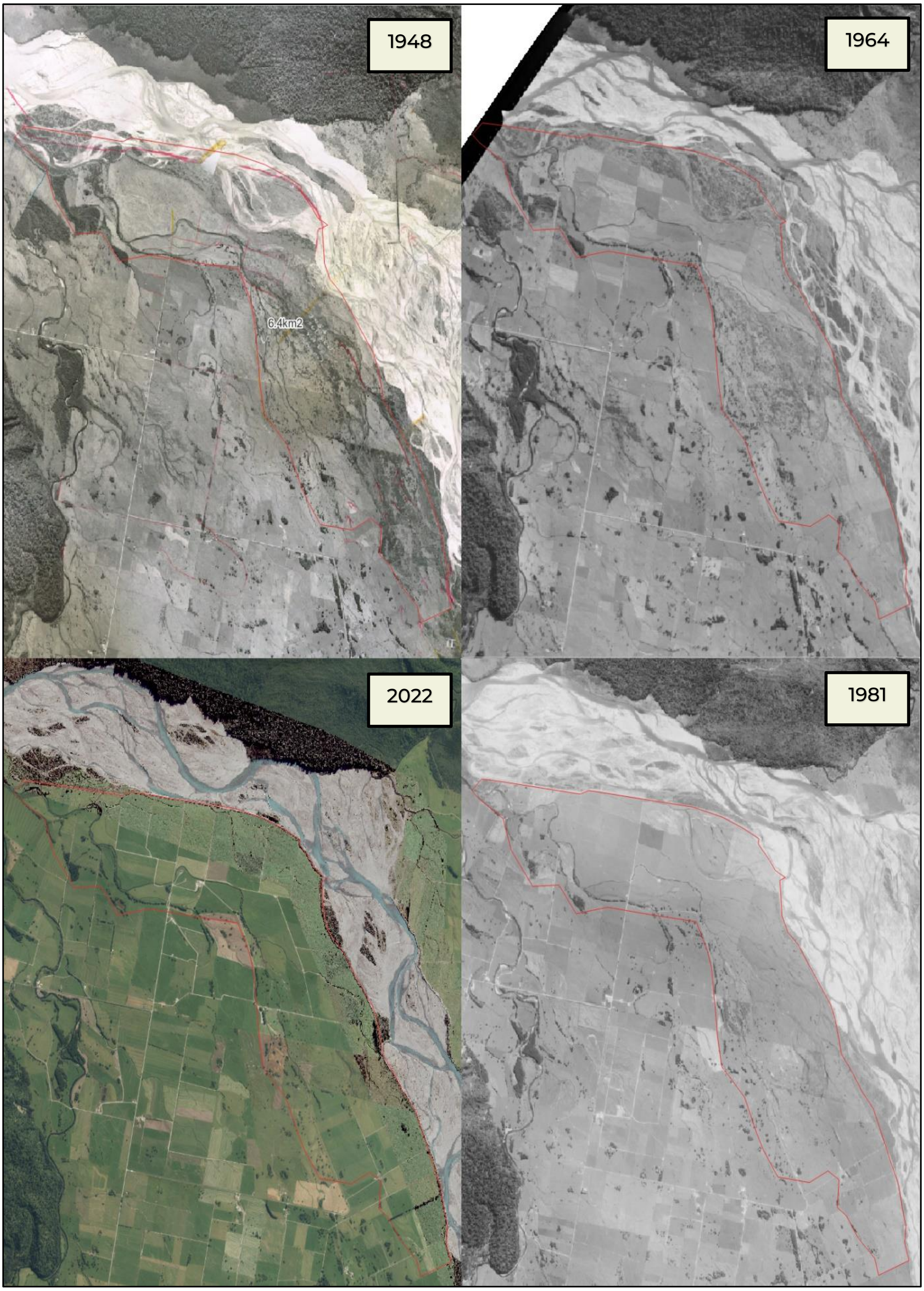

Figure 3-3: comparison of historic to present day imagery to show the change in land use from 1948 to 2022. Clockwise from the top left image - 1948, 1964, 1981 and 2022.

- More significant, is the loss of approximately 40% of active braidplain on the true right (Figure 3-4). Pre 1984, between 2.3 km and 8.0 km downstream of the SH6 bridge, the active braidplain used to extend further to the NE into the Lake Ianthe valley which acted as a depositional area for the river, as well encroaching into the toe of the true right tributary fan between Cowhide and Hurleys Creeks (Figure 3-5). This gave the river access to an extra 3.8 km^2 (40%) of braidplain.

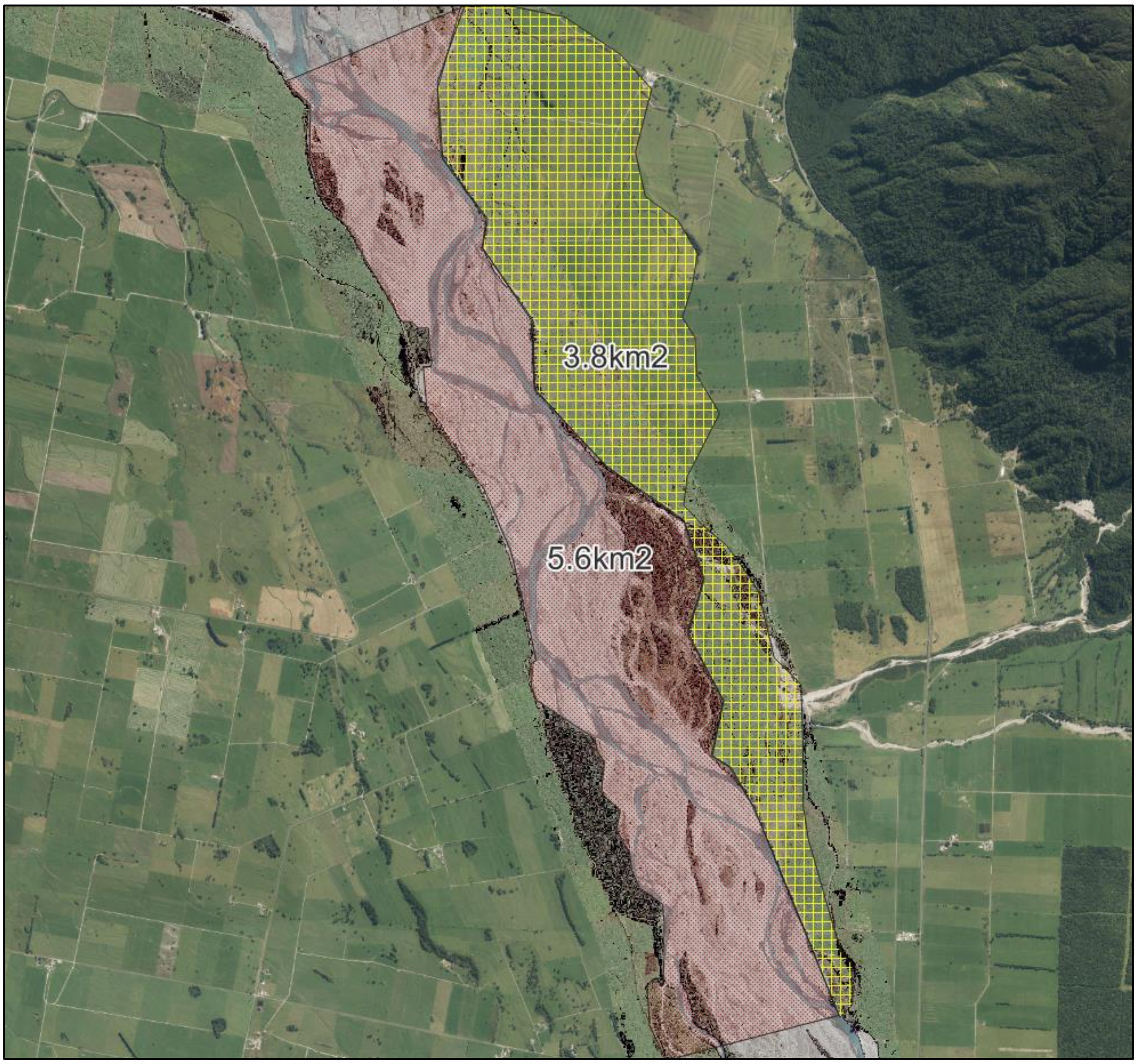

Figure 3-4: 2022 Imagery of the Wanganui River overlain with dense red points for the current active braidplain, and yellow thatching for the historically active braidplain (prior to the construction of the protection network on the true right).

- Then, sometime after the 1984 imagery was captured, in order to protect the land for farming, stopbanks were extended along the true right side (Figure 3-5). This reduced the active braidplain in this reach from 9.4 km^2 to 5.6 km^2, and therefore reduced the amount of braidplain available to move sediment through and to absorb floodwaters.

Land River Sea
CONSULTING

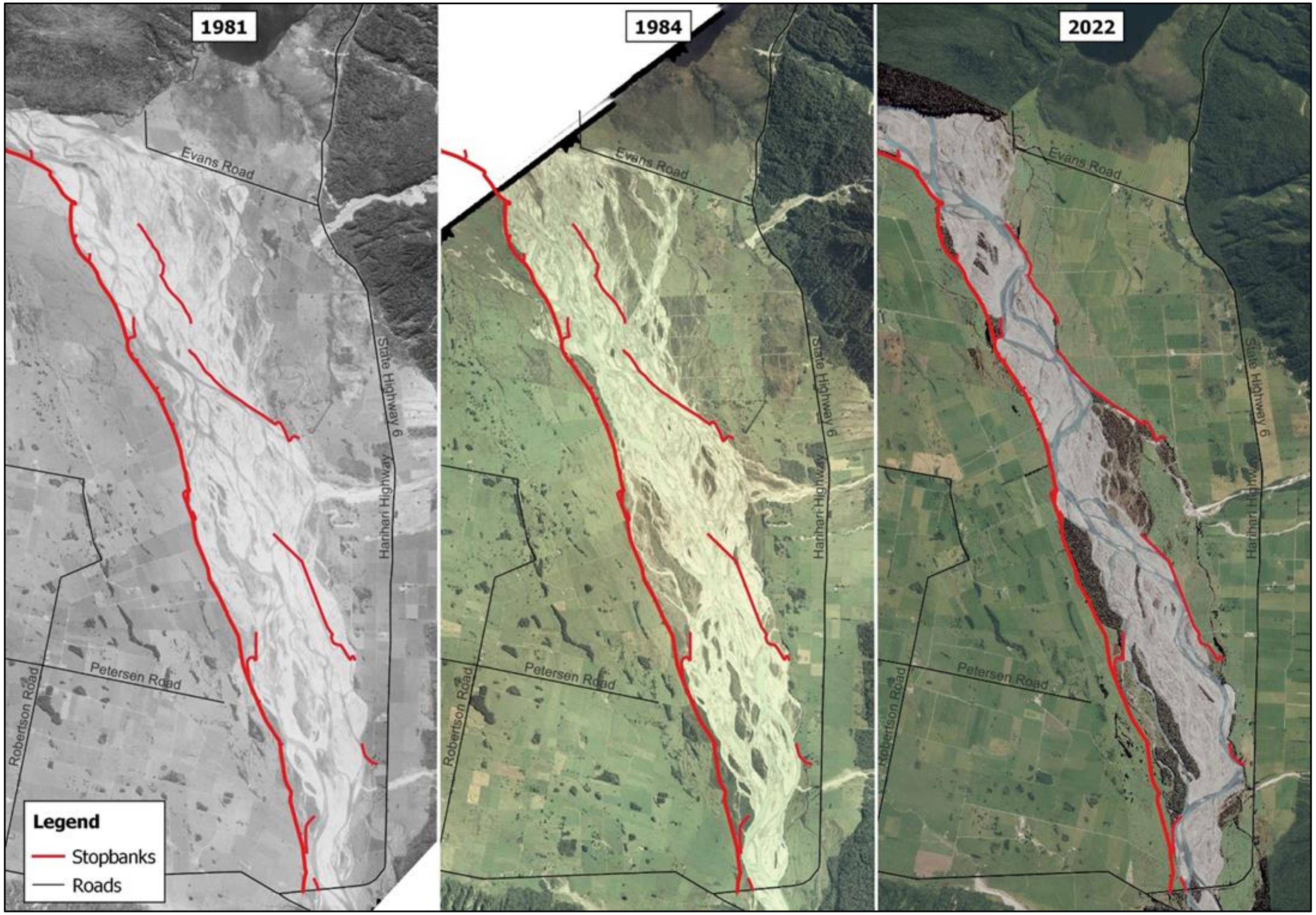

Figure 3-5: Comparison of aerial imagery from 1981, 1984, and 2022 to show the historic width of the active channel between 2.3 and 8.0 km downstream of the SH6 Bridge, and its present day confinement.

Furthermore, when contours from the most recent LiDAR (2020) are laid over the 2022 imagery, the elongated valley fan that begins at the SH6 bridge is not uniform across its surface, rather it appears to be becoming somewhat perched where the braidplain is confined.

This perched area occurs on both sides of the active river corridor from about 5.5 km downstream of the SH6 bridge to where the river corridor is pushed left by the piedmont terraces (a complex adjustment in its own right). In this section the contours of the braid corridor that the river operates within extend further downstream than those either side of it, thus breaking the relatively smooth continuity of the contours like those further upstream on the fan (Figure 3-6).

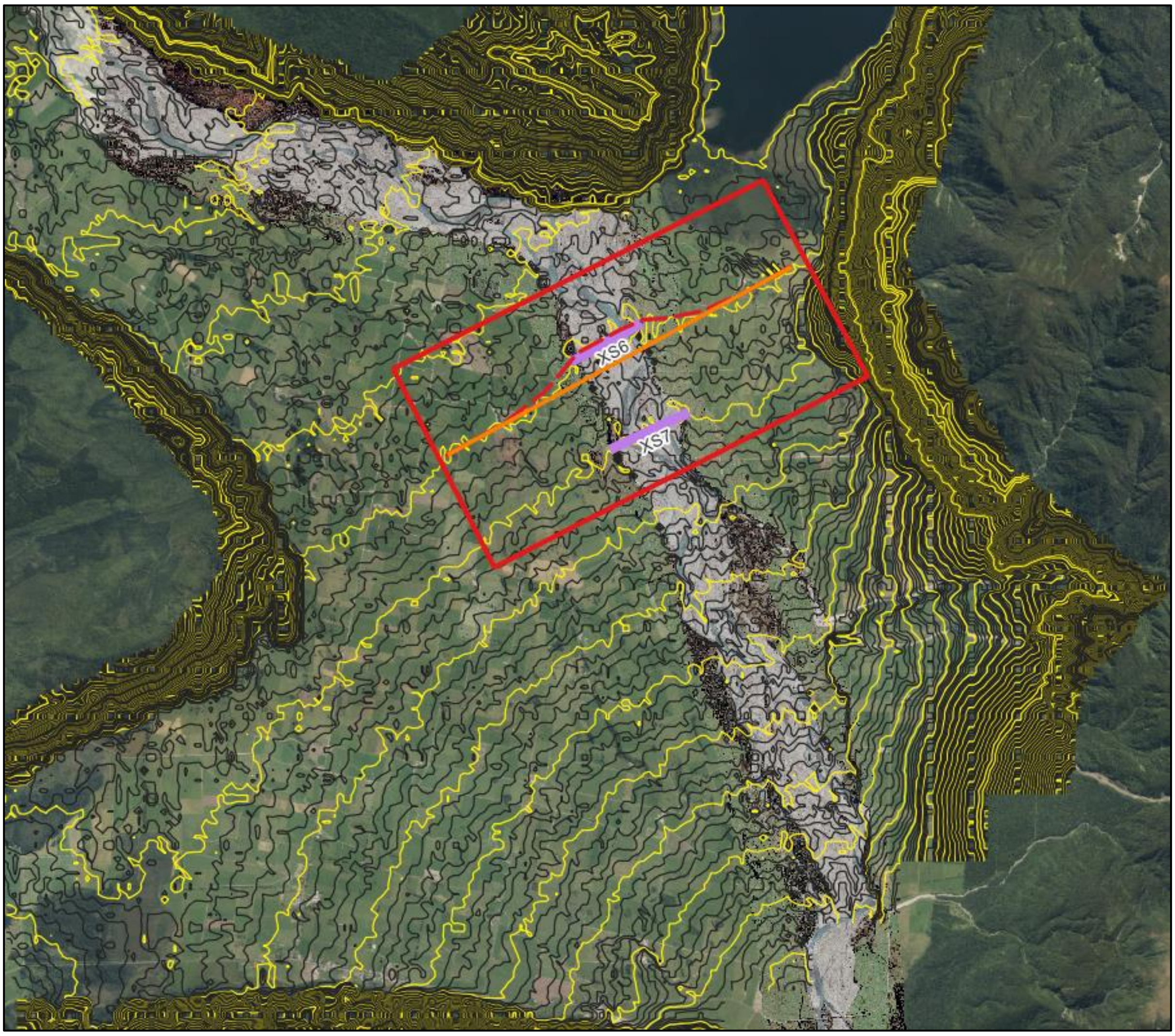

Figure 3-6: contour lines and imagery taken from the recently flown LiDAR (2021). Of interest is the true right and left of the main channel, 5.5km downstream of the SH6 bridge (red outline), where the active river corridor is becoming somewhat perched (red dashed) compared to the valley contours on either side (orange line). Cross sections 6 and 7 shown by purple lines.

Cross section comparisons between the 2012 survey and the 2020 LiDAR also show that the active river corridor in this section (7 to 10 km downstream of the SH6 bridge) has aggraded significantly since 2012, with aggradation filling the lower parts of the channel on the true left of each section (Figure 3-7 and Figure 3-8; additional cross sections in Appendix C). This will further encourage the channel to put pressure on the right bank in these locations. Locations for cross sections (XS) 6 and 7 are shown in Figure 3-6.

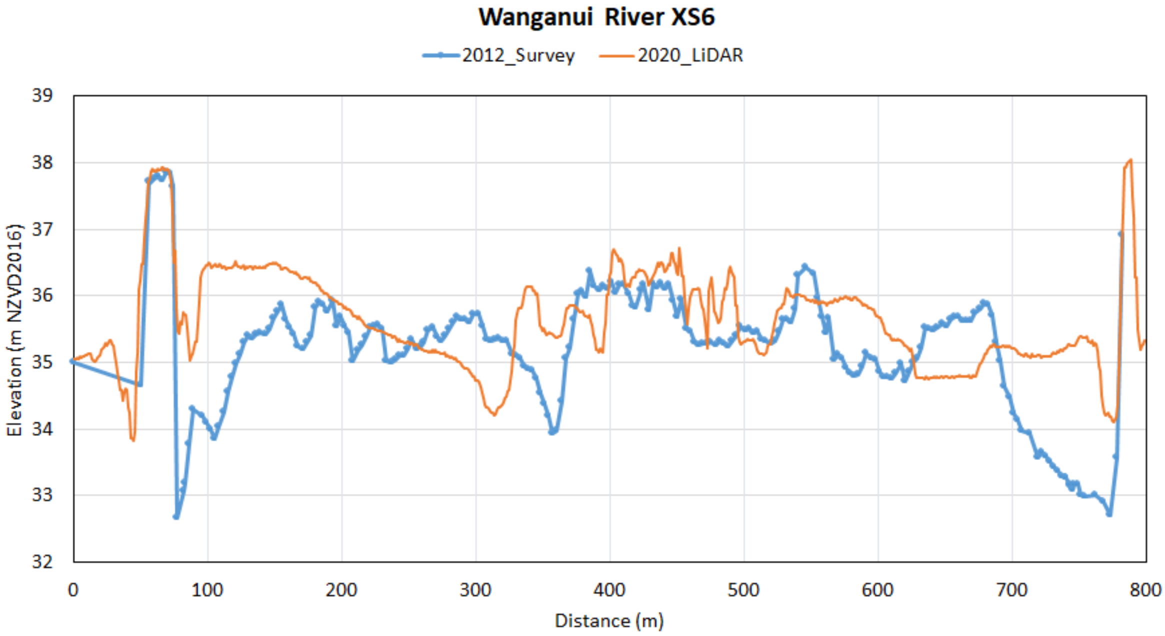

Figure 3-7: Cross section 6 comparison between 2012 and 2020. The active channel in the 2020 LiDAR data can be seen where the plot flatlines between 600 and 700m. The LiDAR would have captured the water surface, and not the channel which would likely be about 1 to 2m deep.

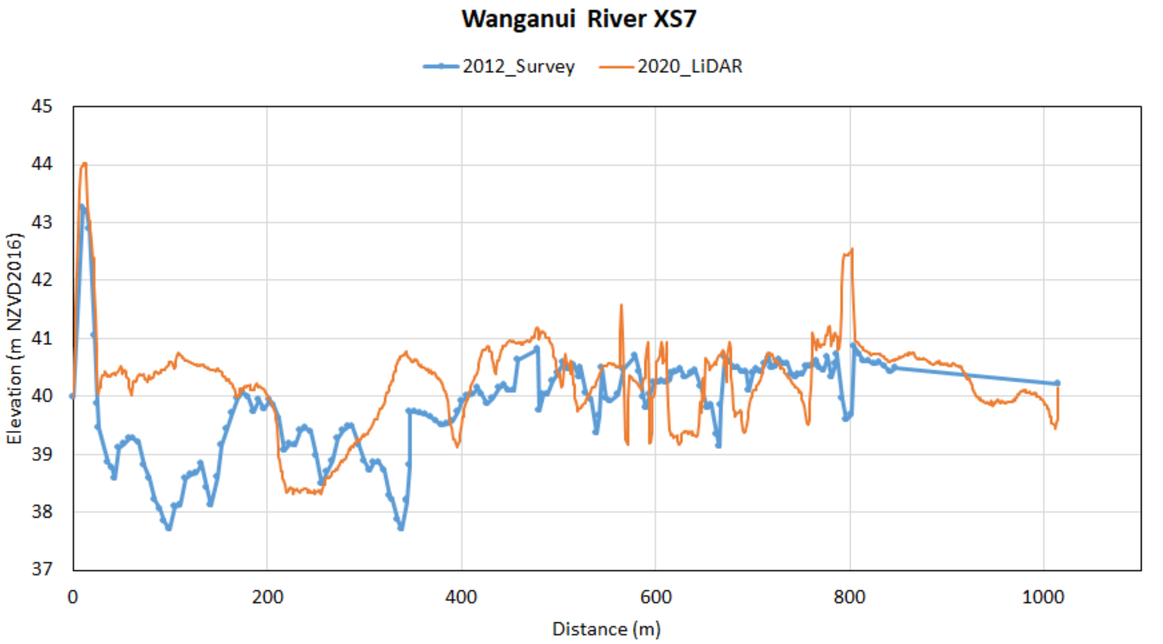

Figure 3-8: Cross section 7 comparison between 2012 and 2020. The active channel in the LiDAR data can be seen where the plot flatlines between 200 and 300m. The LiDAR would have captured the water surface, and not the channel which would likely be about 1 to 2m deep.

This means that the areas of braidplain that were actively used by the Wanganui River prior to the construction of the stopbank network (as discussed earlier in this section) are now at slightly lower elevations to the corridor the river is currently occupying (i.e. the channel is perched above the floodplain). And so, given the tendency of rivers to gravitate towards areas of lower elevation, it seems likely that the Wanganui River will continue to try and access these previously active areas of braidplain.

Narrow corridor and bend curvature

In the pre-1984 imagery, with more room, the main river channel weaves across the active braidplain, gradually changing direction by itself without always reaching a bank (Figure 3-9). However, in more recent imagery, the stopbanks have confined this corridor, with width reductions of up to half (and more) what they used to be compared to the present-day narrowest reaches (Figure 3-9). This confinement not only reduces the amount of space the river has to absorb flood waters but can also affect sediment deposition. It seems likely that the perched appearance of the contours in the downstream reach shown in Figure 3-6 could be attributed to the confinement and then the subsequent loss of space to deposit sediment, leading to localised aggradation.

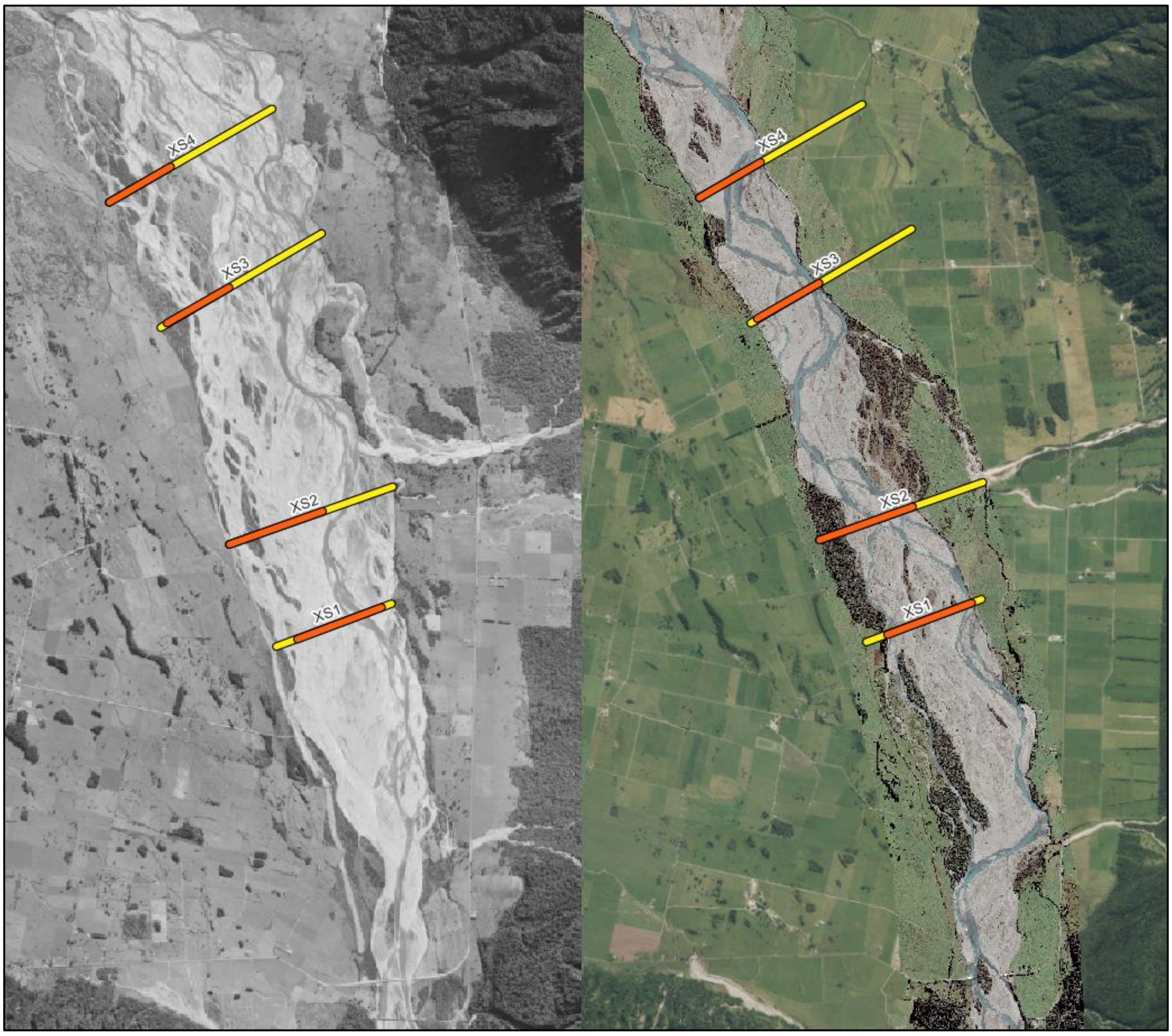

Figure 3-9: 1964 aerial and 2022 satellite imagery with four cross sections showing the most dramatic changes in width from braidplain to confined corridor. Orange is the 2022 width, whilst behind it and extending beyond it in yellow is the 1964 width.

The narrowed corridor also forces the braids and main channel back and forth between the banks, resulting in sudden changes in direction. These points of contact between channel bend and stopbank become pressure points, and as the curvature of the bend increases, the potential for thalweg (the deepest part of the channel) scour also increases, which can lead to greater bank erosion, more rapid rates of lateral migration and floodplain reworking (Fryirs & Brierley, 2013).

On the true right about 1.0 km downstream of the SH6 bridge, the Wanganui River has eroded approximately 76 m^2 of bank since the 1984 aerial imagery, after being deflected from protective structures on the true left to the right (Figure 3-9).

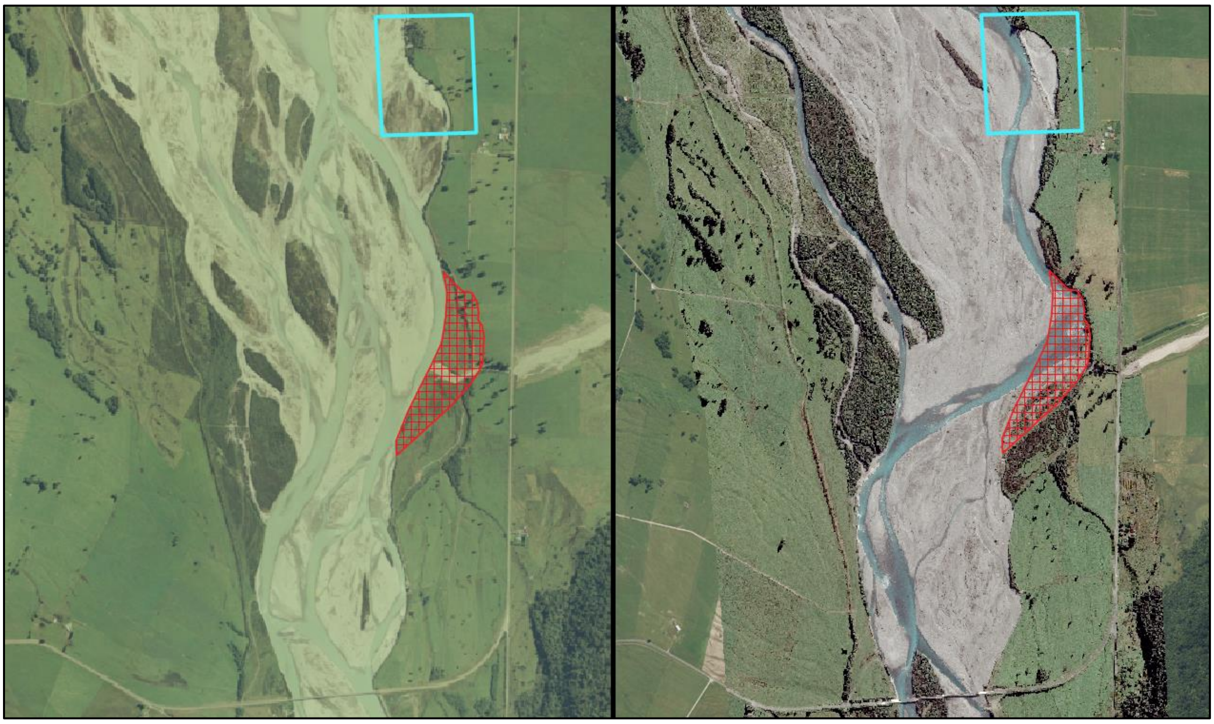

Figure 3-10: 1984 aerial and 2022 satellite imagery to show erosion between 1km and 2.2km downstream of the SH6 bridge on the true right. 76m^2 of erosion in thatched red, and Raymond's stopbank outlined in blue.

The main channel then remains on the true right before connecting with the downstream Raymond's stopbank. In 2022, this stopbank was damaged by two separate events. In February the stopbank was washed away, and then after being repaired it was again damaged in another flood in July (Figure 3-11), a repeating pattern it seems, as this area also experienced similar damage in the 1980s.

Figure 3-11: Raymond's stopbank during the 2022 July 18th/19th flood.

Most recently in 2023, a section of stopbank 2 was damaged three times in the space of six weeks. The section is where the river is it as its most confined, and the main channel is pushed from the left onto the right bank. Additionally, as shown in Figure 3-12, the area was part of the active braidplain before the stopbank was constructed, restricting the rivers braidplain.

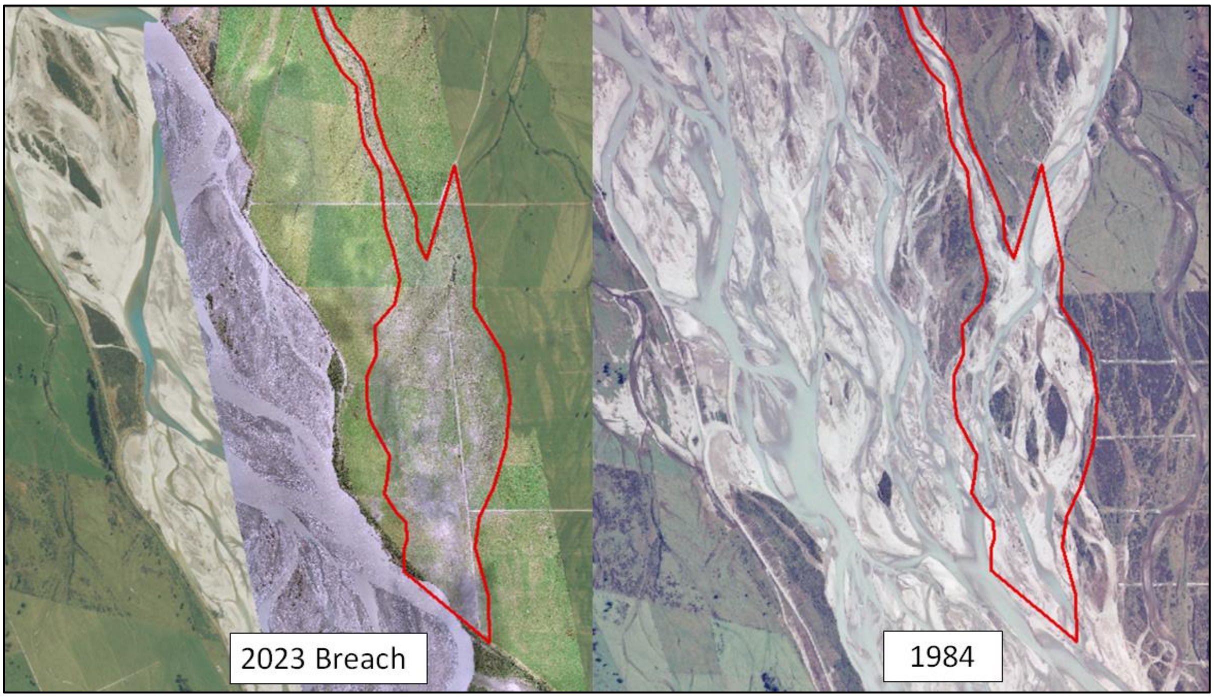

Figure 3-12: Location of the 2023 breach and flow path across farmland which used to be active braidplain in 1984 before the stopbank was constructed.

Sediment supply and flood frequency

Braided river development is thought to be the result of several conditions: an abundant bed load, erodible banks, a highly variable flow, and steep valley slopes (Knighton, 1998). Whilst none of these conditions appear to be able to produce braiding on their own, fluctuations in the bed transport rate because of changes in sediment supply and flow variability have a noticeable effect on the braid morphology (Knighton, 1998) as shown by the imagery of the Wanganui River.

The Interdecadal Pacific Oscillation (IPO) is the long-term oscillation of sea surface temperatures in the Pacific Ocean which affects the strength and frequency of El Niño and La Niña cycles. When in a positive IPO phase, New Zealand receives stronger west to southwest winds which means the West Coast is wetter than average. So, it experiences more extreme rainfall and therefore more frequent flooding than average (Wratt et al., 2022). This increase in rainfall also results in increased erosion rates and subsequently increased sediment supply, and the increase in flood frequency and intensity provides more stream power for moving sediment through the system and subsequently the reworking of the braidplain (Fookes et al., 2007). Stream power is a term used to define the total energy available in a river to erode and rework sediment, and is calculated by multiplying the volume of water (discharge) with the channel slope and the specific weight of water (Fryirs & Brierley, 2013).

For the early 20th century positive IPO phases (between 1900 and 1907, and 1925 and 1944) which are pre aerial imagery and flow data, we rely on documented records like J.L. Benn's "Chronology of Flooding on the West Coast" to testify how active the Wanganui River was. He records that in the early 1900's flooding of the Hari Hari flat when the Wanganui River broke its banks and flowed into La Fontaine Ck was a regular occurrence, as was the Poerua River breaking its banks and also flowing into La Fontaine Ck with flooding in the Hari Hari flats area as well (Benn, 1990).

When flow data is available, another indicator of this increased frequency of flooding is the duration of time a river spends annually above its 2-year annual return interval flow, otherwise known as bankfull discharge (1 – 2 years; Knighton, 1998). Extended years of annual high durations in five West Coast rivers including the Hokitika and Whataroa Rivers which are immediately to the north and south of the Wanganui River, tend to correspond with the positive IPO phases; between 1976/77 and 1998, and most recently beginning around 2020 (Figure 3-13).

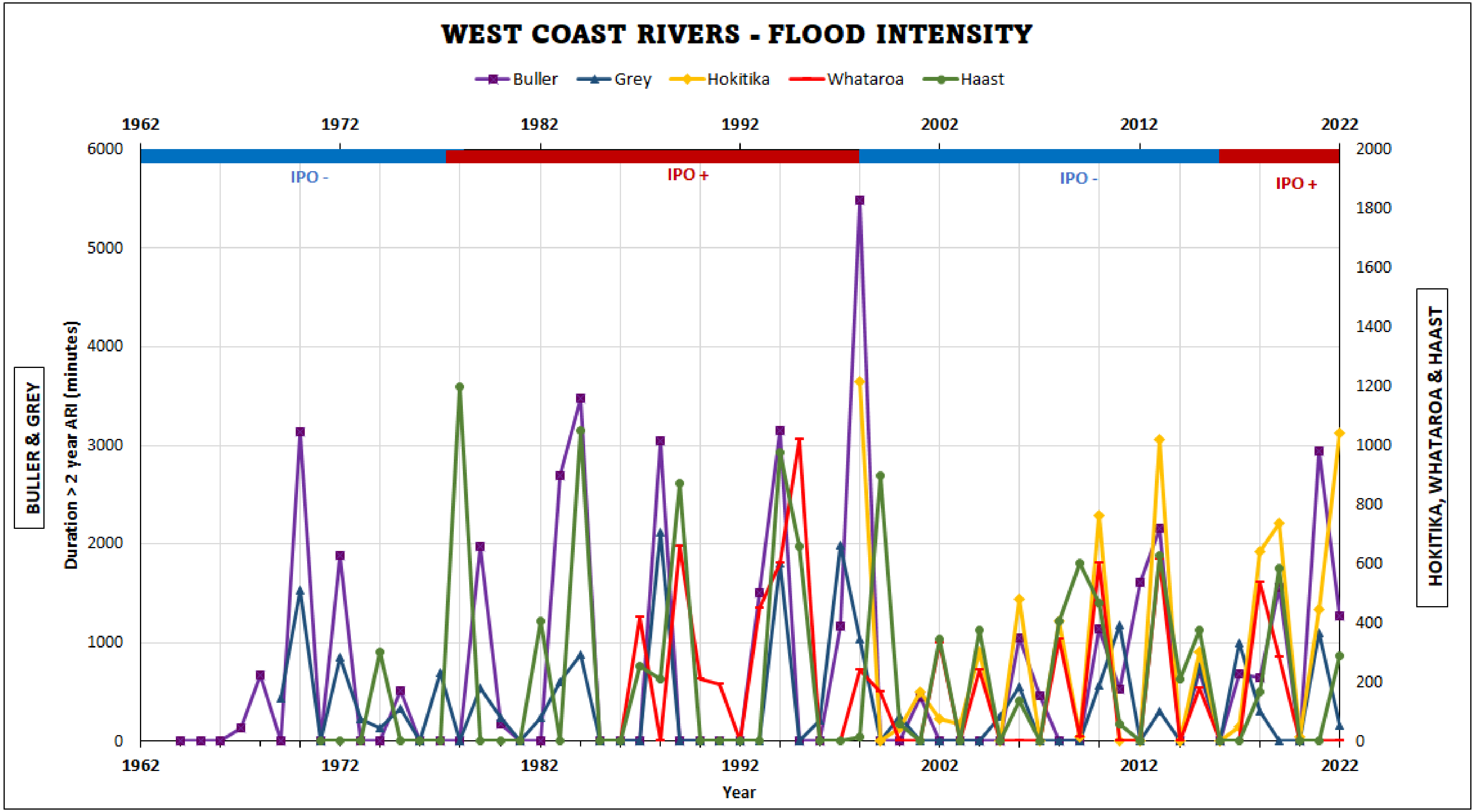

Figure 3-13: duration (minutes) per year that five West Coast rivers (Buller, Grey, Hokitika, Whataroa and Haast) spend above their 2-year ARI flows (Gumbel distribution).

Finally, when comparing the aerial imagery, in 1981 (positive IPO) there is clearly more erosion throughout the catchment, and therefore more sediment available to the Wanganui River compared to in 1964 (negative IPO) (Figure 3-13). This is likely due to more frequent higher intensity rainfall events and periods like the prolonged rainfall experienced in Westland during September 1980 (the Hokitika gauge recorded rainfall every single day except one during September, with a total rainfall 161% above its average), with many Westland gauges also recording above normal for the months preceding and succeeding September (Hessell, 1982).

As a result of the increased sediment supply, in the 1981 imagery we see a much more active braidplain through increased channel complexity and braidplain width, as the river tries to work the excess sediment through its system (Figure 3-14). It was around this time that the records report more frequent damage to the Wanganui protective network due to floods in 1980, 1982, 1985, and 1994 (West Coast Regional Council, 2022). In comparison, in 1964, the Wanganui River appears to be in a much more quiescent phase, with simpler braid patterns and more vegetated islands.

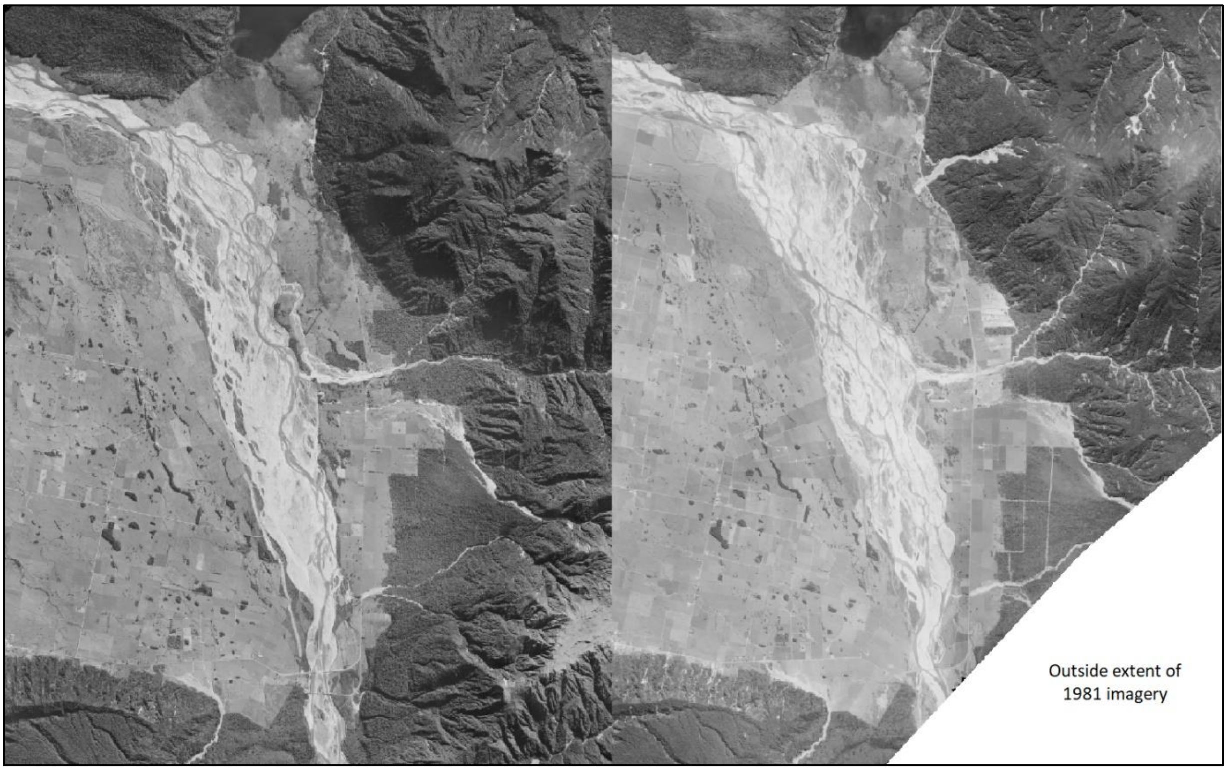

Figure 3-14: increased erosion about the Wanganui catchment in the 1981 (positive IPO) imagery compared to the 1964 (negative IPO). As a result, the 1981 imagery shows a more complex and expanded braid network compared to the 1964 which has a simpler braid pattern and more vegetated islands.

Summary

In summary, the changes to the Wanganui River channel behaviour and its braidplain appear to have been the result of both natural and human influence. Climatic cycles such as the Interdecadal Pacific Oscillation (IPO) influence frequency and intensity of rainfall, and therefore sediment supply and flood event frequency, with increases in both tending to occur during positive phases. As flood event frequency and size increases, often so too does the damage to surrounding farmland and the protective works. During the 1980s and 1990s as the true right protective scheme grew, it was also repeatedly damage by large floods (positive IPO) which prompted further works. Comparatively, the bulk of the true left scheme was constructed in the 1950s to 1970s, and at the time fared better as the river was in a quiescent phase (negative IPO).

Looking to the future, climate change projections are forecasting a wetter West Coast (Mullan et al., 2001; Rutledge et al., 2017), and the IPO is thought to have entered a positive phase around 2020, indicating that flood event frequency and intensity is likely to continue a similar trend as the last few years in addition to continued high inputs of sediment to river systems. However, the Wanganui River is now rigidly restricted by a narrow protective scheme on both sides that runs much of the length of the valley. In a forecast of increased sediment supply, and more frequent and intense flood events, this means that the river has very little braidplain to rework sediment in and to absorb flood waters. This can only result in continued pressure on the protective scheme.

Conclusions

- The Wanganui River behaves like a typical braided river, shifting back and forth across the active braidplain as it moves its high volume of sediment and water from source to sea.
- The protective network constructed largely during the 20th century has affected the natural behaviour of the river by reducing the braidplain significantly resulting in less space to deposit sediment and absorb floodwaters, as well as narrowing the corridor the river has access to and so changing the behaviour of the main channel of flow. This has exacerbated river bed aggradation resulting in a decreased level of service from the existing stopbanks.
- In addition to human influence, the Wanganui River appears to be influenced by the positive and negative phases of the Interdecadal Pacific Oscillation (IPO) which result in active and quiescent phases, respectively. The bulk of the true left side of the scheme was built in a quiescent phase (1950s to 1970s), whilst the true right side was constructed in a more active phase (1980s to 1990s) and as such experienced repeated damage at the time, due to large and more frequent flood events.
- The IPO is believed to have switched to a positive phase around 2020, and climate change projections forecast a wetter West Coast, which will result in an increased sediment supply from greater amounts of catchment erosion, and increased flood event frequency and intensity.
- The combination of increased sediment supply and flow variability, as well as the potential for further additions to the network seems likely to exacerbate the current situation, resulting in continued network damage and chances of breach or overtopping.

4. INPUT DATA

4.1. LIDAR

LiDAR was flown by New Zealand Aerial Surveys as part of the regional PGF LiDAR programme. The LiDAR for the Wanganui River was flown in June 2020, and has been supplied in the New Zealand Vertical Datum (NZVD) 2016.

The LiDAR has been interrogated over the entire area and appears to be of high quality, however unfortunately the extent does not cover all the way up to the SH6 bridge (Figure 4-1). A colourised hillshade visualisation of a section of the LiDAR is also presented in Figure 4-1.

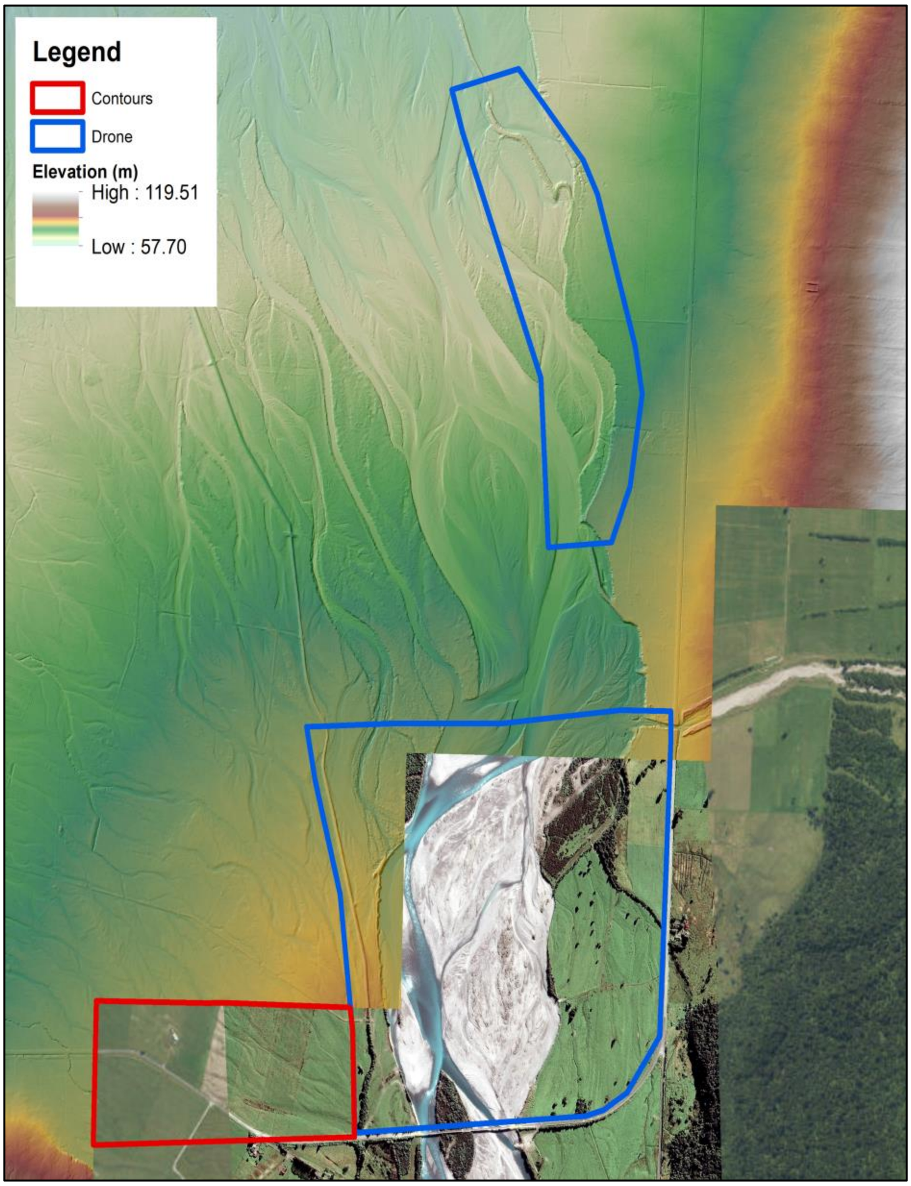

Figure 4-1: Colourised hillshade visualisation of the 2020 LiDAR imagery, with the areas missing in outlined.

4.2. DRONE SURVEY

In order to allow the model to be extended up to the SH6 Bridge; where the 2020 LiDAR extent stopped, a detailed drone survey was completed to capture the area immediately downstream of the SH6 bridge as well as the area of recent erosion near Raymond's stopbank (stopbank 1), and one section of stopbank crest on the true left (Figure 4-2).

A basic survey report for the drone survey is included in Appendix D.

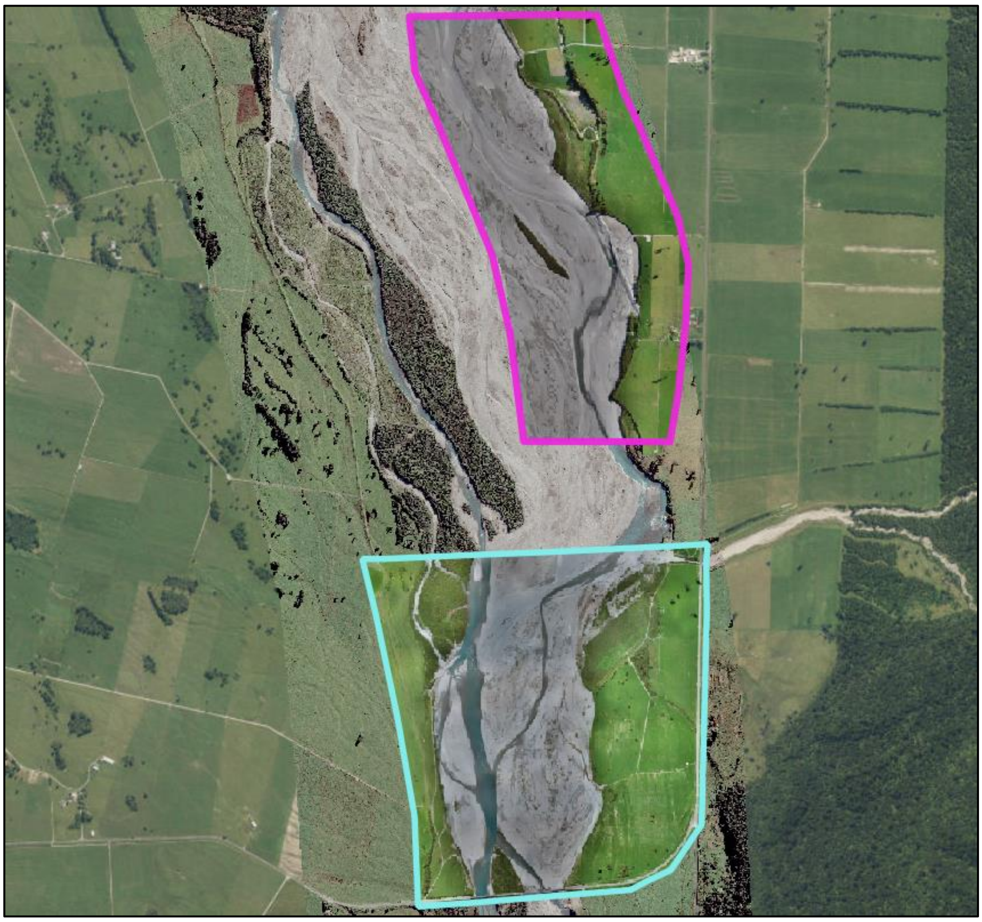

Figure 4-2: imagery from the 2022 drone survey with the area downstream of the SH6 bridge outlined in blue, and the area of erosion in pink.

4.3. IMAGERY

The most recent high resolution aerial imagery of the West Coast was captured in the 2016/17 summer. However, as there have been several large floods since 2016/17, high resolution (0.5m GSD) satellite ortho imagery from April 2022 was purchased to allow us to visualise the significant changes in the braid network, channel vegetation and damage to the stopbanks caused by the floods.

Additionally, Sentinel satellite imagery was downloaded from June 2020 to help us better identify the braid network which coincides with the June 2020 LiDAR allowing us to represent the braid network more accurately in the model.

5. HYDROLOGY

The Wanganui (Whakanui) River is located approximately 70km south of Hokitika and just north of Hari Hari on the West Coast of the South Island of New Zealand where it flows from the steep mountains west of the Southern Alps onto and across a foreland plain to the Tasman Sea (Figure 5-1).

The river is primarily fed by a 344 km^2 catchment upstream of the SH6 bridge, and frequently experiences intense storm events as a result of its exposure to the 'roaring forties', a prevailing moist westerly airflow (Davies, 1997). Sediment supply is also high, with large amounts of metamorphosed schist/gneisses, and greywacke entering the system via subaerial erosion (i.e., rockfalls and landslides). As a result, this steep, high energy, gravel bed river, has the potential to transport and deposit large amounts of sediment on the alluvial fan that extends as an elongated braidplain between the mountains and the sea.

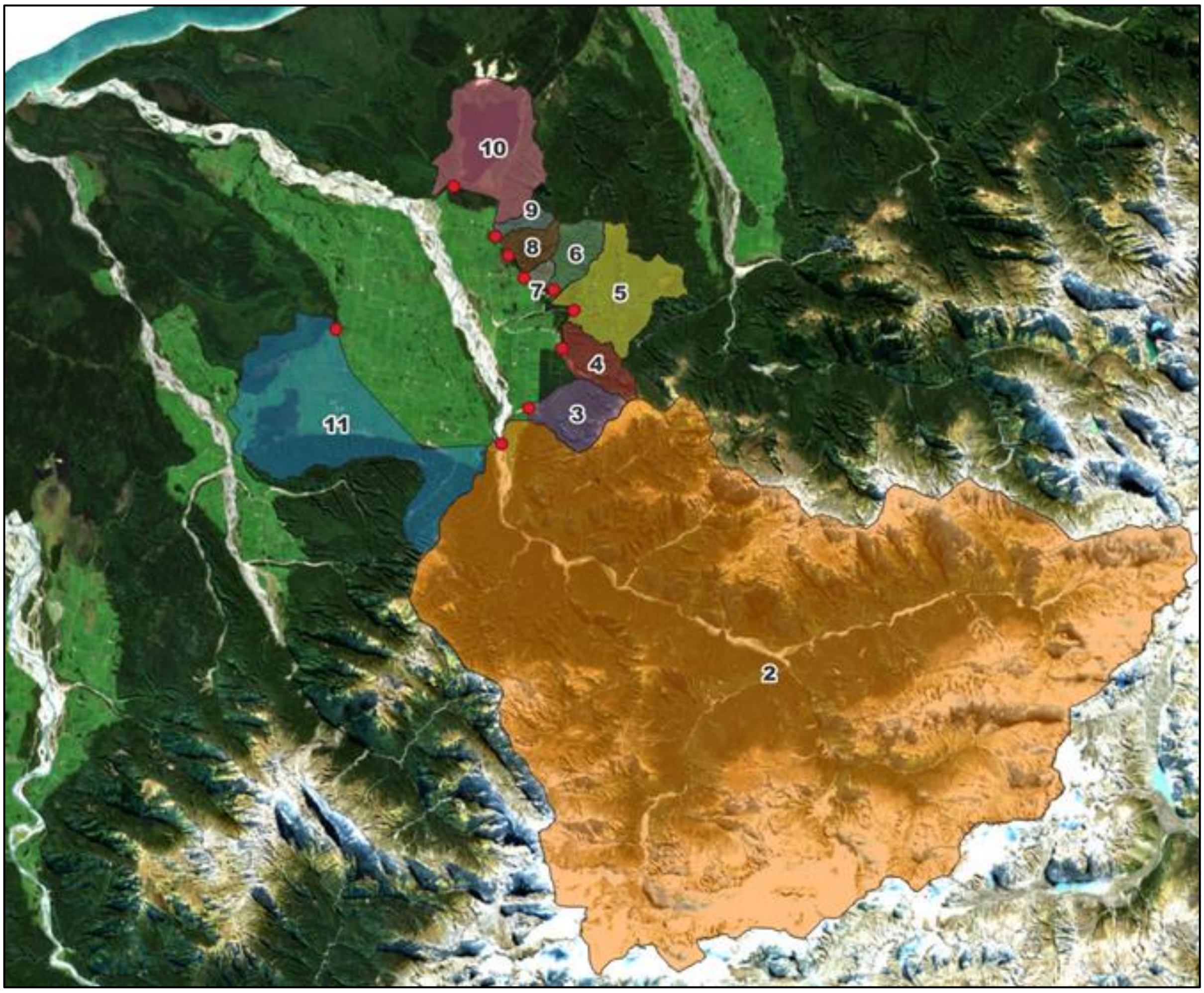

Figure 5-1: Wanganui catchment map with the ten sub-catchments and their input points used in the model; 2) Wanganui Rv, 3) Hurleys Ck, 4) Cowhide Ck, 5) Evans Ck, 6) Haro Ck, 7) Unnamed, 8) Adamson Ck, 9) Bonar CK, 10) Ianthe Ck, and 11) La Fontaine Stm.

5.1. DESIGN FLOWS – HISTORIC CLIMATE

No recorded hydrological information is available for the Wanganui River catchment. Inflow hydrology assumptions for modelling have been based on consideration of at-site records from the nearby Whataroa and Hokitika catchments, and the online NIWA tool for flood statistics (Table 5-1).

Table 5-1: 1% AEP (100-year ARI) flows at the Hokitika Rv at Gorge and Whataroa Rv at SH6 monitoring sites.

Site	At-site flow (m^3/s)	NIWA estimated flow (m^3/s)	Difference (%)
Hokitika Rv @ Gorge	3,400	2,600	23.5
Whataroa Rv @ SH6	5,200	4,700	9.4

The magnitude of the Wanganui River 1% AEP design hydrograph has been calculated using the online NIWA tool for flood statistics (regional flood estimation method) and provides a peak flow of 3,300 m3/s (Table 5-2). However, as the at-site flows at both the Hokitika River and Whataroa River monitoring sites differed to the NIWA flood statistics estimated flows, we have also included two sensitivity runs with an additional 10% and 20% to the 1% AEP peak flow (Table 5-2).

Table 5-2: 1% AEP (100-year ARI) flow at the Wanganui River using the regional flood estimation method.

Site	NIWA estimated flow (m^3/s)	+10% (m^3/s)	+ 20% (m^3/s)
Wanganui River	3,300	3,600	3,900

The shape of the Wanganui River design hydrograph has been taken from consideration of the flow hydrographs of five of the largest events recorded at the Whataroa Rv @ SH6 monitoring site. These events have been normalised to the same peak and similar time of occurrence, and assessed. For this modelling exercise, the 2010 shape has been used (Figure 5-2). However, there is little storage in the model and peak water level predictions will be largely unaffected by the particular shape chosen.

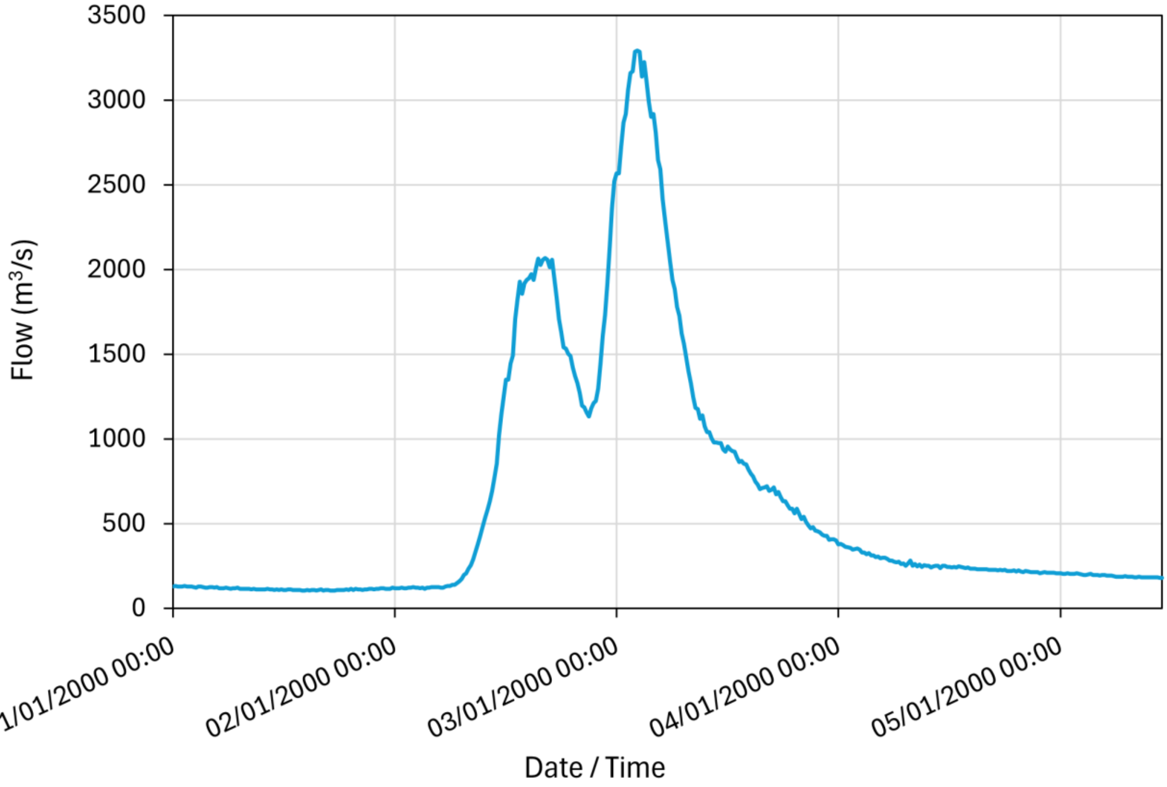

Figure 5-2 - Wanganui River 1% AEP design hydrograph.

The primary model inflow location for the catchment is upstream of SH6 bridge, with other sub-catchments contributing to the river flow downstream (Figure 5-1). The sub-catchment information has been derived from NIWAs REC-2 database.

5.2. DESIGN FLOWS – RCP8.5

The 1% AEP (100-year ARI) flow under the representative concentration pathway (RCP) 8.5 has been calculated by multiplying the 1% AEP historic climate (estimated) flow by the same scaling factor (1.24) used for the Hokitika River (Gardner, 2020) which is in line with a recent climate change impact study on peak discharge completed by NIWA for the Buller River (Zammit, 2022).

This has resulted in a flow of 4,092 m^3/s. Given the high uncertainty in the design flows due to lack of recorded flow data, we have rounded this RCP8.5 – 1%AEP flow to 4,100 m^3/s.

6. MIKE21 FM MODEL BUILD

6.1. MESH GENERATION / INTERPOLATION

The MIKE 21 model has been set up using the Flexible Mesh module and used a variable mesh size allowing varying degrees of resolution over the floodplain. The model has been split into sub areas and assigned a maximum mesh element resolution ranging from 15 m^2 to 1000 m^2. Areas such as the Wanganui River corridor, tributaries, and a band of farmland to the true left of the river have been assigned the finest resolution, with areas such as the ocean, coastline, swamp, and lake being assigned a coarser resolution.

In essence, each mesh element is assigned an elevation, hence the finer the mesh, the greater definition of the underlying topography is able to be represented. There is a trade-off required however between model stability, model runtime and file size that needs to be made. The final model has been designed so that it can run within a day on a high spec computer with multiple GPUs. A summary of the final mesh resolution is presented in Figure 6-1. It should be highlighted that the mesh sizes stated below are the maximum element size within that area and that the majority of the mesh elements are significantly less than the maximum resolution.

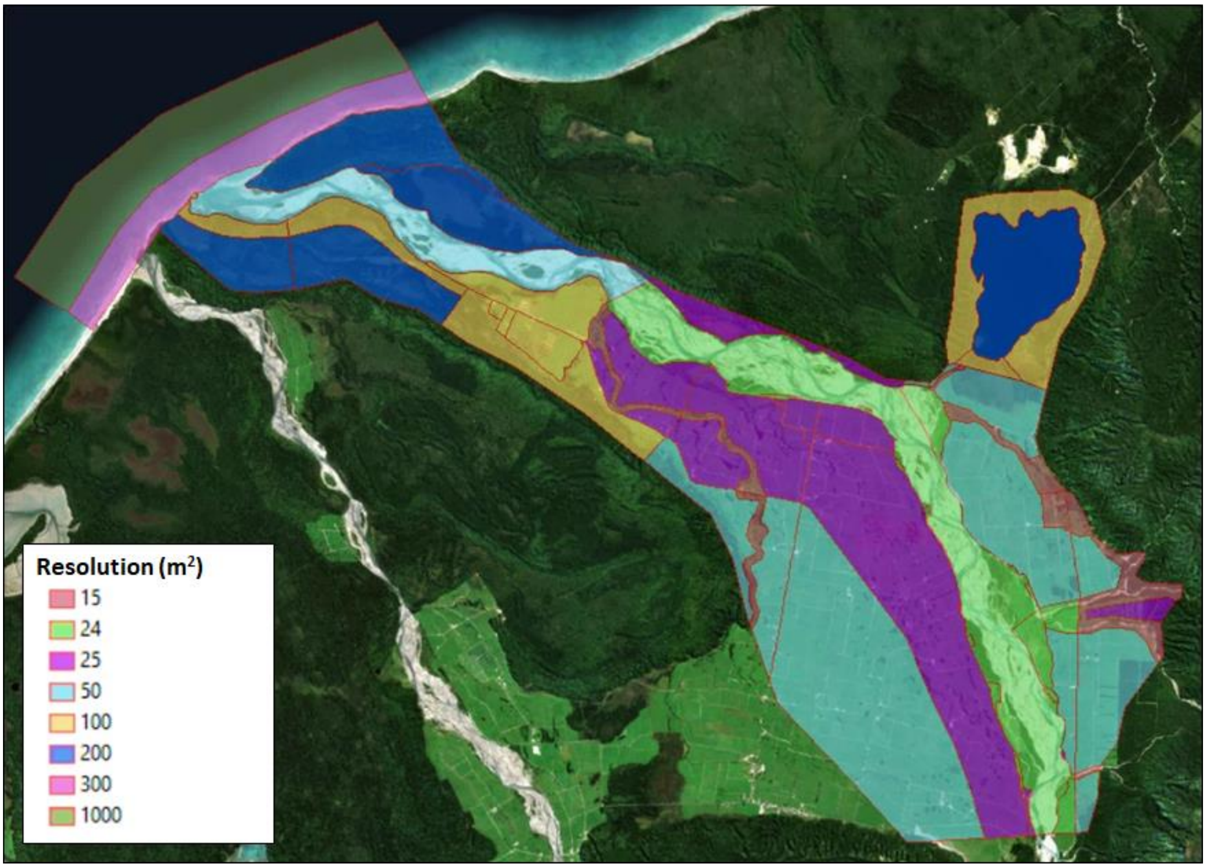

Figure 6-1: Summary of assigned maximum mesh resolution.

The underlying topography has been based on the 2020 LiDAR supplied by the WCRC and supplemented with the 2022 drone data for the area immediately downstream of the SH6 bridge and an area of recent erosion on the true right by Raymond's stopbank (stopbank 1; Figure 4-2).

The area to the immediate true left (west) of the SH6 bridge was not captured in the LiDAR or drone surveys, therefore, it had to be generated manually. Simplified contours were drawn across the area which tied into the LiDAR contours at the edges and a DEM was interpolated based on these contours (Figure 6-2). This simply allows the water to flow in a natural direction across the floodplain, should it spill immediately downstream of the SH6 Bridge. LiDAR is scheduled to be flown in this area in the next 2 to 3 years and this area can be replaced with actual LiDAR data once data has been collected.

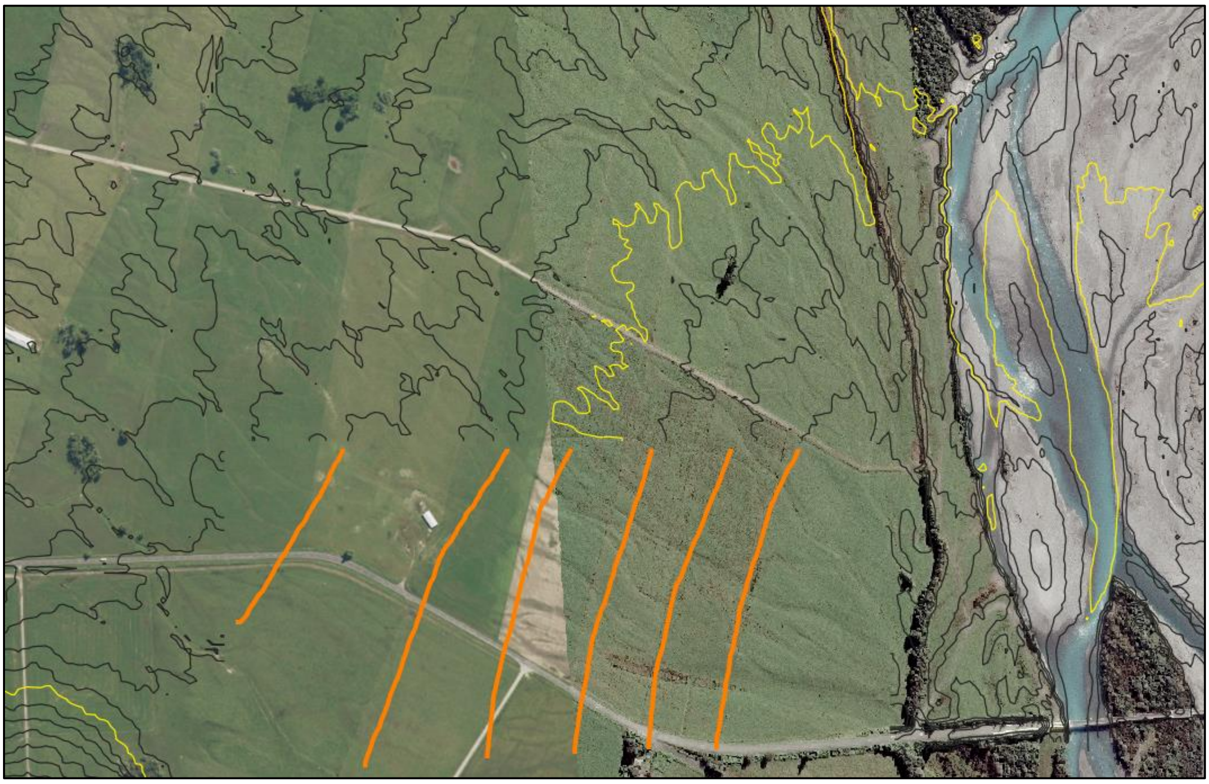

Figure 6-2: Manually generated contours (orange) for the area downstream and to the immediate true left of the SH6 bridge.

6.1.1. BATHYMETRY INTERPOLATION

In order to allow the full river to be modelled in 2D, it has been necessary to interpolate a detailed river bathymetry. To do this, we have interpolated the bathymetry using points generated at a 1.0 m grid resolution from the LiDAR DEM. However, because the river channel changed after the LiDAR image was captured, it became necessary to burn in a 1.0 m trapezoidal main channel and two 0.5 m rectangular subsidiary channels (La Fontaine Stm and Adamson Ck) (Figure 6-3, Figure 6-4). The channel edges were designed to tie in with the DEM elevations. The model was then run with the inserted channel for all the design and sensitivity runs.

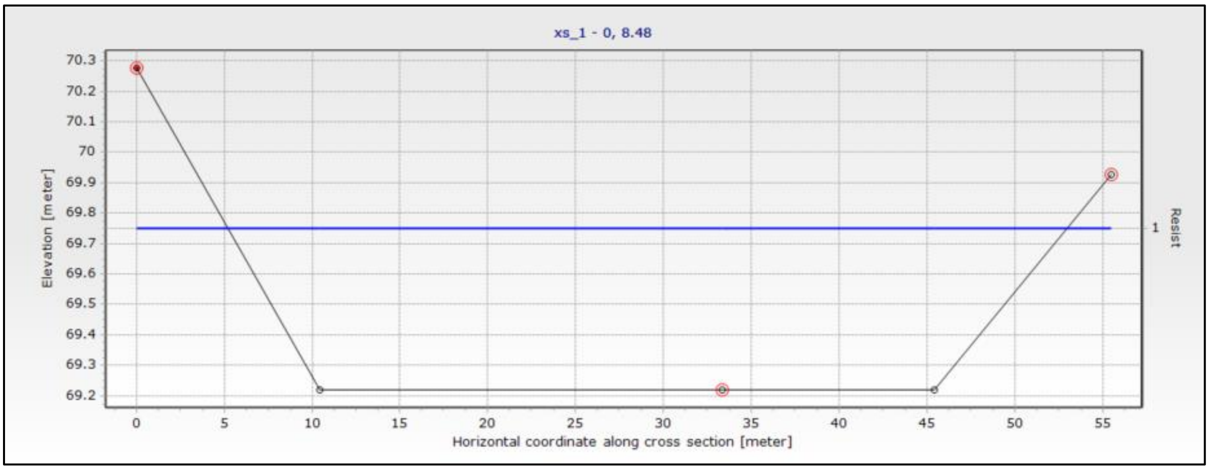

Figure 6-3: Example of the typical trapezoidal channel shape in MIKE Hydro River.

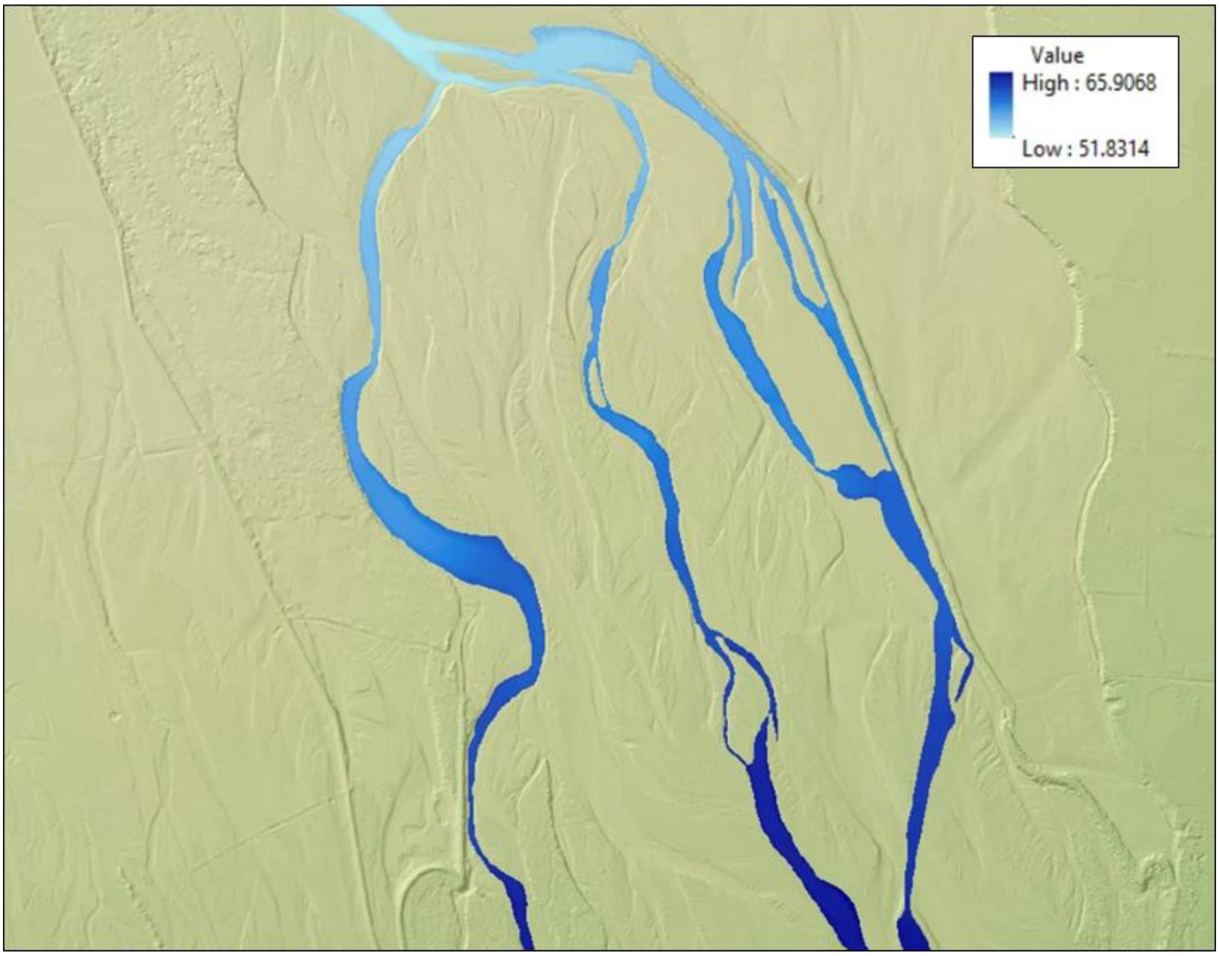

Figure 6-4: Visualisation of interpolated 2D bathymetry

6.2. FLOODPLAIN RESISTANCE

Floodplain resistance has been represented in the model using a spatially varying Manning's 'n' coefficient.

For the river channel, it was difficult to accurately assess a manning's 'n' value without sediment grading information or calibration information. Therefore, we determined sediment grading based on scaled photographs at a range of locations in the river (Figure 6-5).

- Calculations using two different formulae for gravel river systems developed by George Griffiths have been used as well as the Strickler Formula. Results indicate a Manning's range in the order of 0.03 to 0.05.
- Therefore, a roughness value of 0.04 has been applied to the 10% and 5% AEP (10 and 20-year ARI) design runs, and 0.05 to the 2% and 1% AEP (50 and 100-year ARI) design runs, for the active channel width.

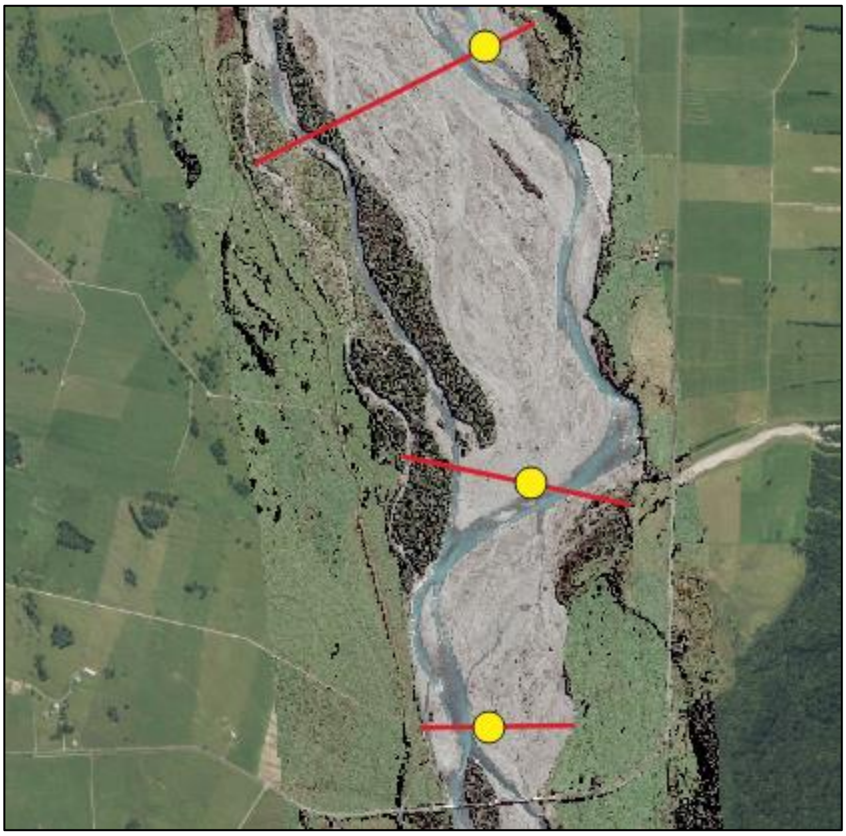

Figure 6-5: the locations of the three photos used to grade the sediment for the Wanganui River channel.

To account for varying roughness values on the floodplain, a raster of roughness values with a grid size of 1m has been created where each cell has been assigned a Manning's 'n' value based on the land use visible in the latest aerial imagery.

This task has been carried out using a combination of manual and automatic image classification techniques to ensure the most accurate classification of land uses. Buildings have been located based on a digitised building footprint shapefile supplied by Land Information New Zealand (LINZ).

The adopted Manning's 'n' values are summarised in Table 6-1 with a visual representation of the final Manning's values presented in Figure 6-6.

The 2021 high resolution satellite ortho image was used for the river channel roughness delineation, whilst the 2016/17 satellite imagery was used for the farmland roughness.

Table 6-1: Floodplain Manning's 'n' values

Land Use	Manning's 'n'
Buildings	2.0
Grass – pasture	0.035
Lake	0.06
River (2% and 1% AEP)	0.05
River (10% and 5% AEP)	0.04
Tributaries	0.05
Roads	0.025
Vegetation – dense	0.15
Vegetation – medium	0.12
Vegetation – light	0.09
Swamp	0.06
Ocean	0.02

Figure 6-6 – Visualisation of Manning's 'n' roughness representation

6.3. ENFORCEMENT OF STOPBANK / ROAD CRESTS

Several important floodplain features have been represented as dikes within MIKE 21 to ensure that the maximum level which will control the flow in this location is picked up. These features are generally stopbanks, natural bunds and key roads. To accurately represent these features, the maximum crest levels have been extracted from the LiDAR data and applied as a 1-dimensional weir within the software, rather than relying on the sampled value (based on the mesh size) applied in the MIKE21 mesh. Each crest level has been plotted manually within excel and any unnatural gaps in the crest level due to heavy vegetation blocking the crest etc has been removed manually. This ensures that the model doesn't show water overtopping a bank due to an unnatural gap in the LiDAR data. The location of modelled DIKES is presented in Figure 6-7.

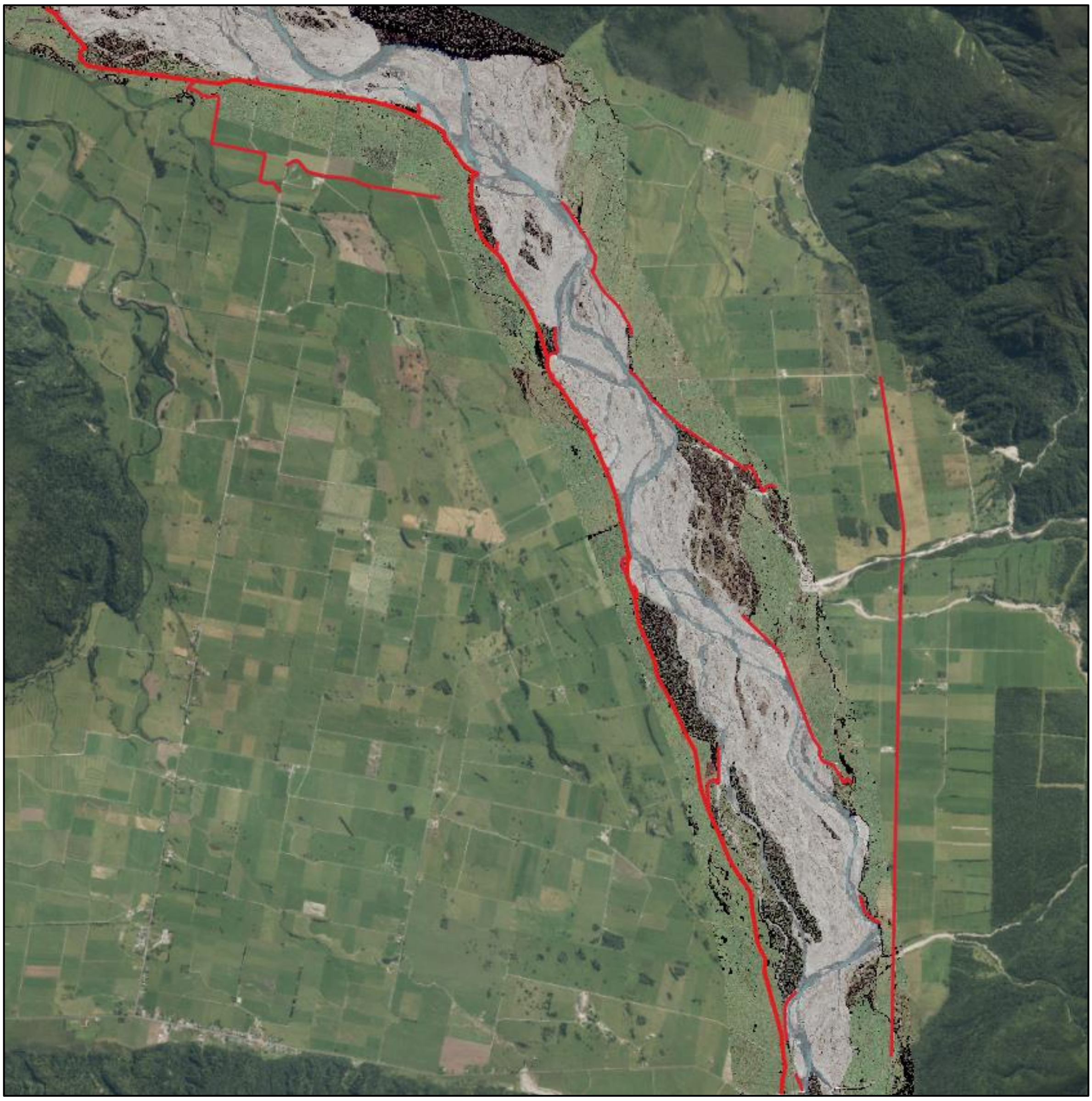

Figure 6-7: Location of features where crest levels have been enforced.

7. MODEL RESULTS

Three categories of runs have been simulated:

- **Design (Table 7-1):** 10, 5, 2 and 1% annual exceedance probability (AEP; 10, 20, 50 and 100-year ARI) flows under the historic climate, and a 1% AEP flow under an approximated RCP 8.5 scenario.
- **Sensitivity (Table 7-2):** two hydrology scenarios with increases to the 1% AEP flow by 10 and 20 percent, and a roughness scenario with a decrease in the river channel manning's 'n'.
- **Residual hazard (Table 7-3):** four types of runs were simulated to demonstrate the residual risk to the local community and surrounding farmland. These included all stopbanks down, right stopbanks down, overtopping breach and scour breach scenarios. Given the number of residual hazard runs completed, only those with notable results have been discussed, with the remainder provided as maps electronically.

Level of service simulations have also been completed for the historic and RCP8.5 1% AEP design flow scenarios, and for the two hydrology sensitivity scenarios. In these simulations, each stopbank has been made infinitely high to prevent overtopping (referred to as glass walled) in order to show the maximum level required to contain such a flow should the upstream or downstream stopbanks be raised in the future.

The water level from these level of service simulations have been plotted with the crest level (extracted from the LiDAR) and a freeboard allowance of 0.5 m for each stopbank.

'Freeboard' is a term used to describe a factor of safety above a design flood level for flood mitigation works. Freeboard allows for the uncertainties in hydrological predictions, wave action, modelling accuracy, topographical accuracy, final flood defence levels and the quality of the digital elevation models (King, 2010).

Table 7-1: Design run scenarios for 10, 5, 2 and 1% AEP (10, 20, 50 and 100 year ARI) flows. *MAF - mean annual flood.

Run name	Wanganui River		Sub catchments ARI (year)	Climate change
	AEP (%)	ARI (year)		
WANGANUI_D_10PC-AEP_F	10	10	MAF*	Historic
WANGANUI_D_5PC-AEP_F	5	20	5	Historic
WANGANUI_D_2PC-AEP_F	2	50	10	Historic
WANGANUI_D_1PC-AEP_F	1	100	20	Historic
WANGANUI_D_1PC-AEP-CC_F	1	100	20	~RCP8.5

Table 7-2: Sensitivity run scenarios.

Run name	Wanganui River		Sub catchments ARI (year)	Comments
	AEP (%)	ARI (year)		
WANGANUI_S-HYD01_1PC-AEP_F	1	100	20	3,600m3/s flow (+10%)
WANGANUI_S-HYD02_1PC-AEP_F	1	100	20	3,900m3/s flow (+20%)
WANGANUI_S-RGH01_1PC-AEP_F	1	100	20	River manning's 'n' of 0.04

Table 7-3: Residual hazard run scenarios.

Run name	Wanganui River		Sub catchments ARI (year)	Stopbank
	AEP (%)	ARI (year)		
WANGANUI_R-DWN-01_5PC-AEP_F	5	20	5	All stopbanks down
WANGANUI_R-DWN-01_2PC-AEP_F	2	50	10	All stopbanks down
WANGANUI_R-DWN-01_1PC-AEP_F	1	100	20	All stopbanks down
WANGANUI_R-DEF-01_2PC-AEP_F	2	50	10	Right stopbanks down
WANGANUI_R-DEF-01_1PC-AEP_F	1	100	20	Right stopbanks down
WANGANUI_R-OBRE-RB-01_1PC-AEP_F	1	100	20	Overtopping breach, RB1
WANGANUI_R-OBRE-RB-02_1PC-AEP_F	1	100	20	Overtopping breach, RB2
WANGANUI_R-SBRE-LB-01_5PC-AEP_F	5	20	5	Scour breach, LB1
WANGANUI_R-SBRE-LB-02_5PC-AEP_F	5	20	5	Scour breach, LB2
WANGANUI_R-SBRE-LB-03_5PC-AEP_F	5	20	5	Scour breach, LB3
WANGANUI_R-SBRE-RB-01_5PC-AEP_F	5	20	5	Scour breach, RB1
WANGANUI_R-SBRE-RB-02_5PC-AEP_F	5	20	5	Scour breach, RB2
WANGANUI_R-SBRE-RB-03_5PC-AEP_F	5	20	5	Scour breach, RB3
WANGANUI_R-SBRE-LB-01_2PC-AEP_F	2	50	10	Scour breach, LB1
WANGANUI_R-SBRE-LB-02_2PC-AEP_F	2	50	10	Scour breach, LB2
WANGANUI_R-SBRE-LB-03_2PC-AEP_F	2	50	10	Scour breach, LB3
WANGANUI_R-SBRE-RB-01_2PC-AEP_F	2	50	10	Scour breach, RB1
WANGANUI_R-SBRE-RB-02_2PC-AEP_F	2	50	10	Scour breach, RB2
WANGANUI_R-SBRE-RB-03_2PC-AEP_F	2	50	10	Scour breach, RB3
WANGANUI_R-SBRE-LB-01_1PC-AEP_F	1	100	20	Scour breach, LB1
WANGANUI_R-SBRE-LB-02_1PC-AEP_F	1	100	20	Scour breach, LB2

WANGANUI_R-SBRE-LB-03_1PC-AEP_F	1	100	20	Scour breach, LB3
WANGANUI_R-SBRE-RB-01_1PC-AEP_F	1	100	20	Scour breach, RB1
WANGANUI_R-SBRE-RB-02_1PC-AEP_F	1	100	20	Scour breach, RB2
WANGANUI_R-SBRE-RB-03_1PC-AEP_F	1	100	20	Scour breach, RB3

The results have been discussed in the following sections (7.1, 7.2 and 7.3) and presented in the form of:

- Peak Depth Maps (Appendix E)
- Peak Speed Maps (Appendix F)
- Hazard Maps (Appendix G)

There are a large number of potential hazard categorisations to use. For this report, hazard categories have been presented based on the general guidelines from the Australian Rainfall and Runoff Guidelines (Cox, 2016) and are based on a combination of depth and velocity. The hazard categories are summarised in Table 7-4 and presented graphically in Figure 7-1.

Table 7-4: Description of Hazard Categories.

Hazard Classification	***Vulnerability***	***Description***
H1		Generally safe for vehicles, people and buildings.
H2		Unsafe for small vehicles.
H3		Unsafe for vehicles, children and the elderly.
H4		Unsafe for vehicles and people.
H5		Unsafe for vehicles and people. All buildings vulnerable to structural damage. Some less robust buildings subject to failure.
H6		Unsafe for vehicles and people. All building types considered vulnerable to failure.

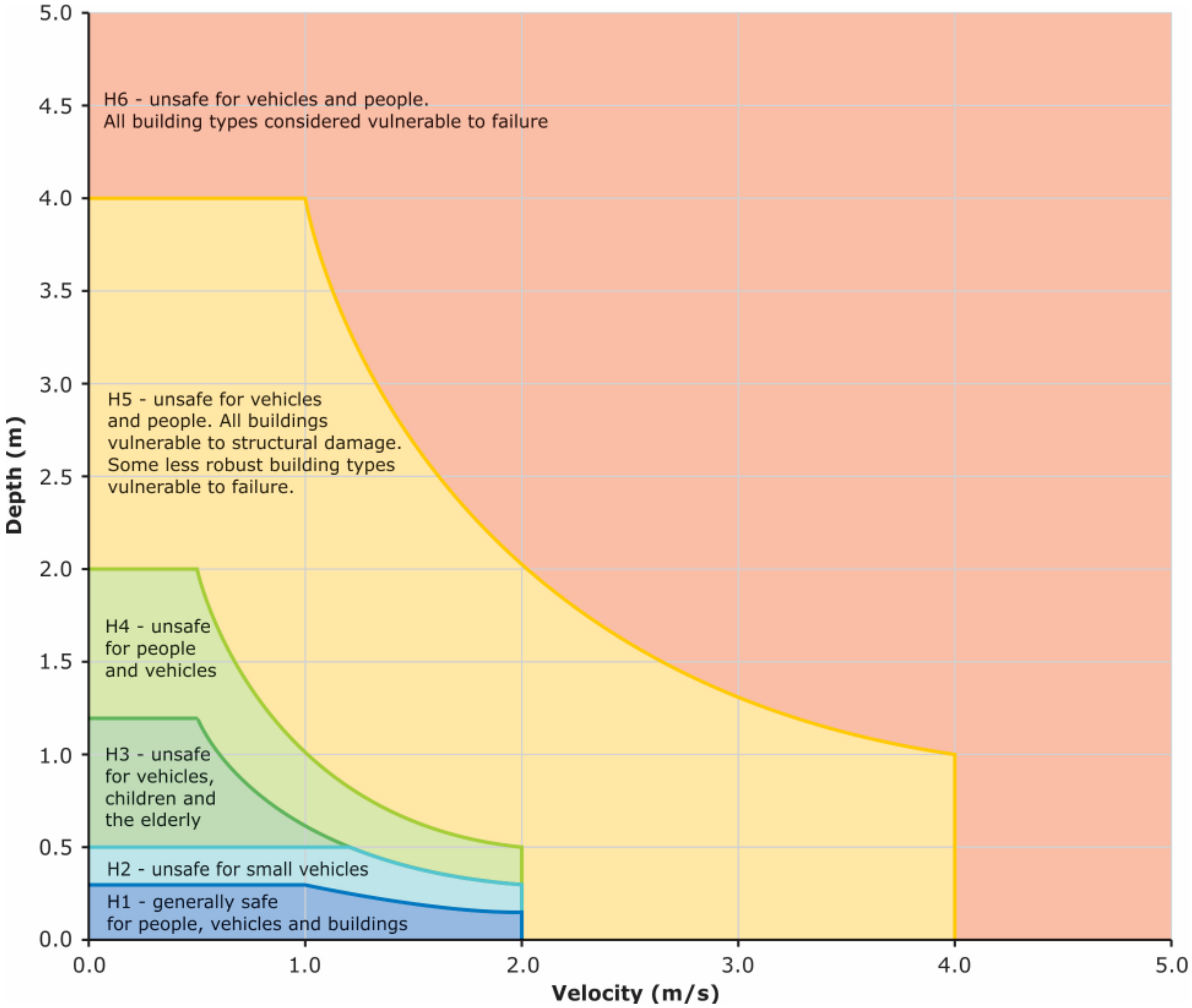

Figure 7-1: Graphical representation of the Hazard Categories

More detailed information on the derivation of the Hazard Categories can be found in the Australian Rainfall and Runoff guidelines which can be accessed online at http://arr.ga.gov.au/arr-guideline (NB. hazard categories are discussed in Chapter 7 of Book 6 – Hydraulics).

There are a range of more specific hazard categorisations available which are more specific for evacuation planning etc, however the categories adopted for these maps are the most general and suitable for a wide range of purposes.

7.1. RESULTS ANALYSIS – DESIGN RUNS

7.1.1. 10% AEP – HISTORIC CLIMATE

The 10% AEP (10-year ARI) event with a mean annual flow in all the tributaries was the smallest of the simulated events. The true left stopbank network performs well, with no overtopping.

On the true right floodwater spills out between the gaps in the stopbanks, as well as overtops parts of both stopbanks 2 and 3. This leads to inundation of the farmland on the true right between stopbank 3 and Lake Ianthe (Figure 7-2).

- For the most part the flow appears to follow paleochannels with depths averaging around 0.5 m, however where it nears the unnamed creek there are places where depths exceed 1.0 m.
- Velocities are also highest in the larger of these paleochannels, around 1.0 m/s, and in the smaller, around 0.5 m/s.

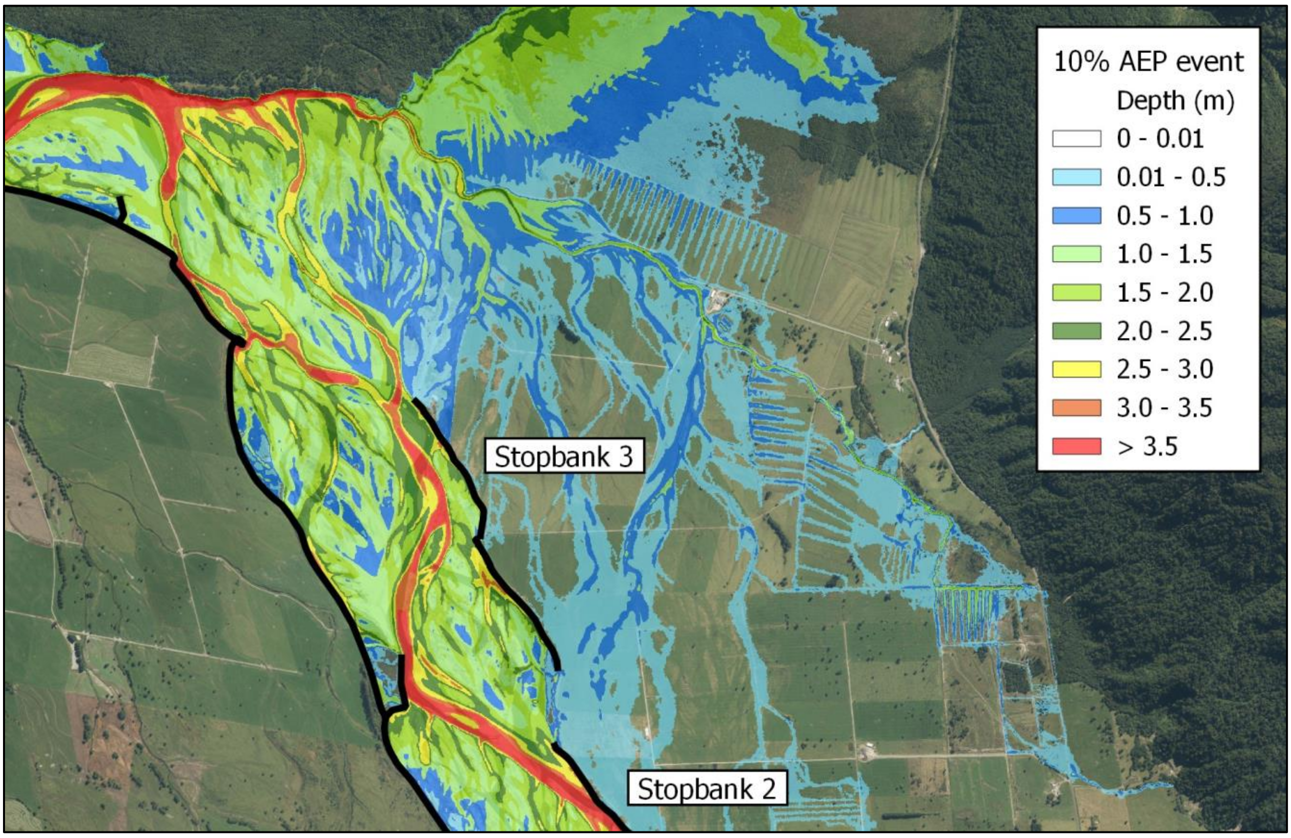

Figure 7-2: Peak depth (m) of the inundation of the true right farmland during the 10% AEP event.

7.1.2. 5% AEP – HISTORIC CLIMATE

The 5% AEP (20-year ARI) event with 20% AEP (5-year ARI) flows in the tributaries, performed similarly to the 10% AEP (10-year ARI) event.

Flood waters inundate the true right farmland to a slightly greater extent than the smaller 10% AEP event, with minor increases in depth. However, velocities in the larger of the flow paths across the farmland increase more significantly, now averaging between 1.0 and 1.5 m/s, with peaks of up to 2.0 m/s (Figure 7-3).

It is also worth noting, that breakouts from the tributaries on both sides of the Wanganui River continue to cause localized inundation with depths of up to 0.5 m and speeds around 0.5 to 1.0 m/s, with peaks as high as 2.0 m/s (Figure 7-3).

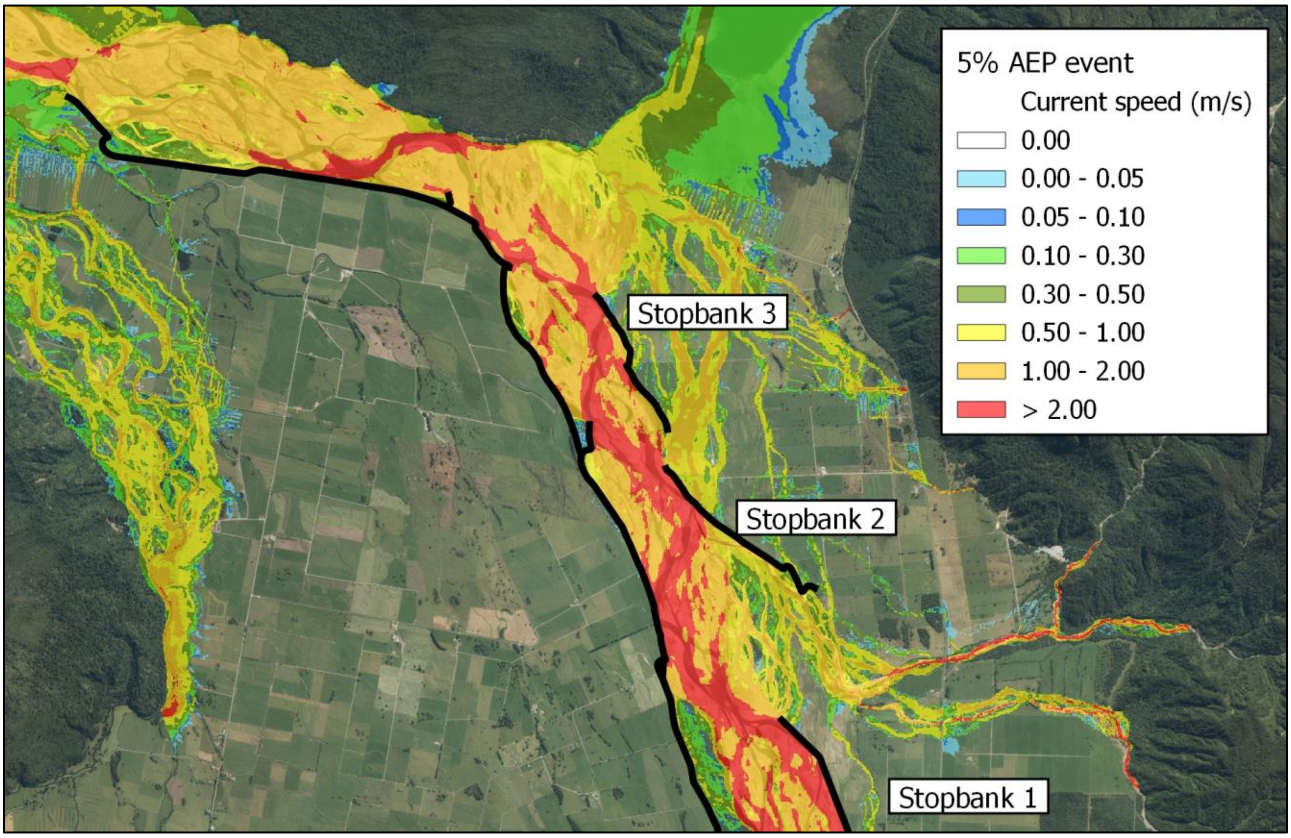

Figure 7-3: Peak current speed for the 5% AEP event.

7.1.3. 2% AEP – HISTORIC CLIMATE

The 2% AEP (50 year ARI) event with 10% AEP (10 year ARI) flows in the tributaries performed similarly to both the 10 and 5% AEP (10 and 20-year ARI) events. Notable changes include:

- The extent of flooding of the farmland on the true right downstream of Evans Ck increases, as does the average depth and velocities.
- In several places on the true right, floodwaters overtop stopbank 1 (Figure 7-4).
- Floodwaters almost entirely overtop the small section of true right stopbank immediately downstream of Hurleys Ck (Figure 7-4).
- On the true left between 5.4 km and 5.7 km downstream of the SH6 bridge, three sections of stopbank overtop (Figure 7-4), though for the most part depths and velocities remain below 0.5 m and 0.4 m/s.
- Inundation from the tributaries also increases, with an additional flood path developing from Haro Ck across the farmland and down to SH6.

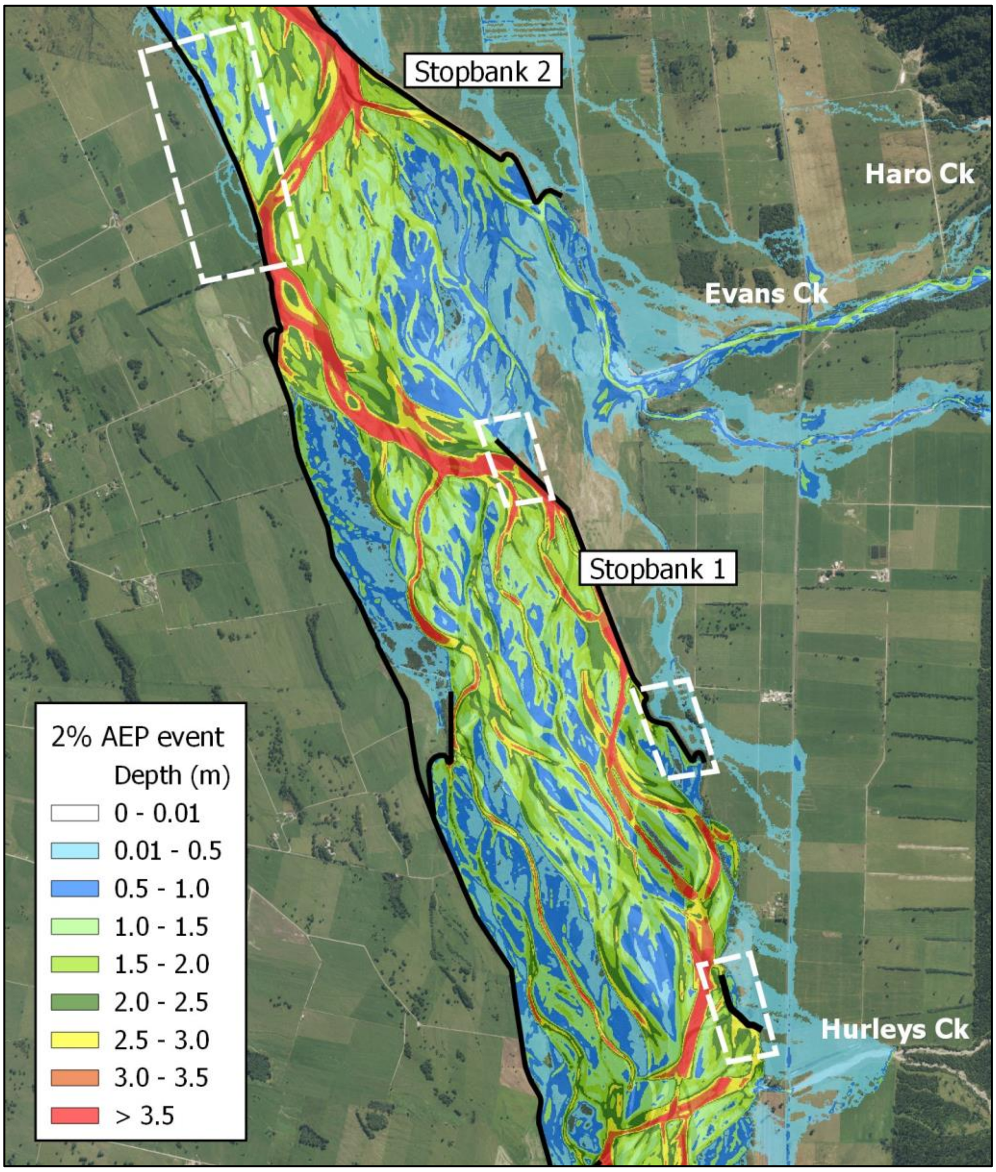

Figure 7-4: 2% AEP peak depth (m) showing where the stopbank network over tops (white dashed rectangles) on the TL stopbank in two of the three places, TR stopbank 1, and the stopbank downstream of Hurleys Ck.

7.1.4. 1% AEP – HISTORIC CLIMATE

On the true left, the small sections of overtopping shown in the 2% AEP flood continue to overtop with the majority of the flow following the existing channel across farmland to where it joins La Fontaine Stream, whilst the remainder results in localized flooding near the stopbank (Figure 7-5).

On the true right, inundation increases in extent, depth and velocity from the smaller modelled events in the historically active and depositional area between the Wanganui River and Lake Ianthe (Figure 7-5). This is largely due to the true left side of the stopbank network holding up well against the flows (and without any simulated breaches).

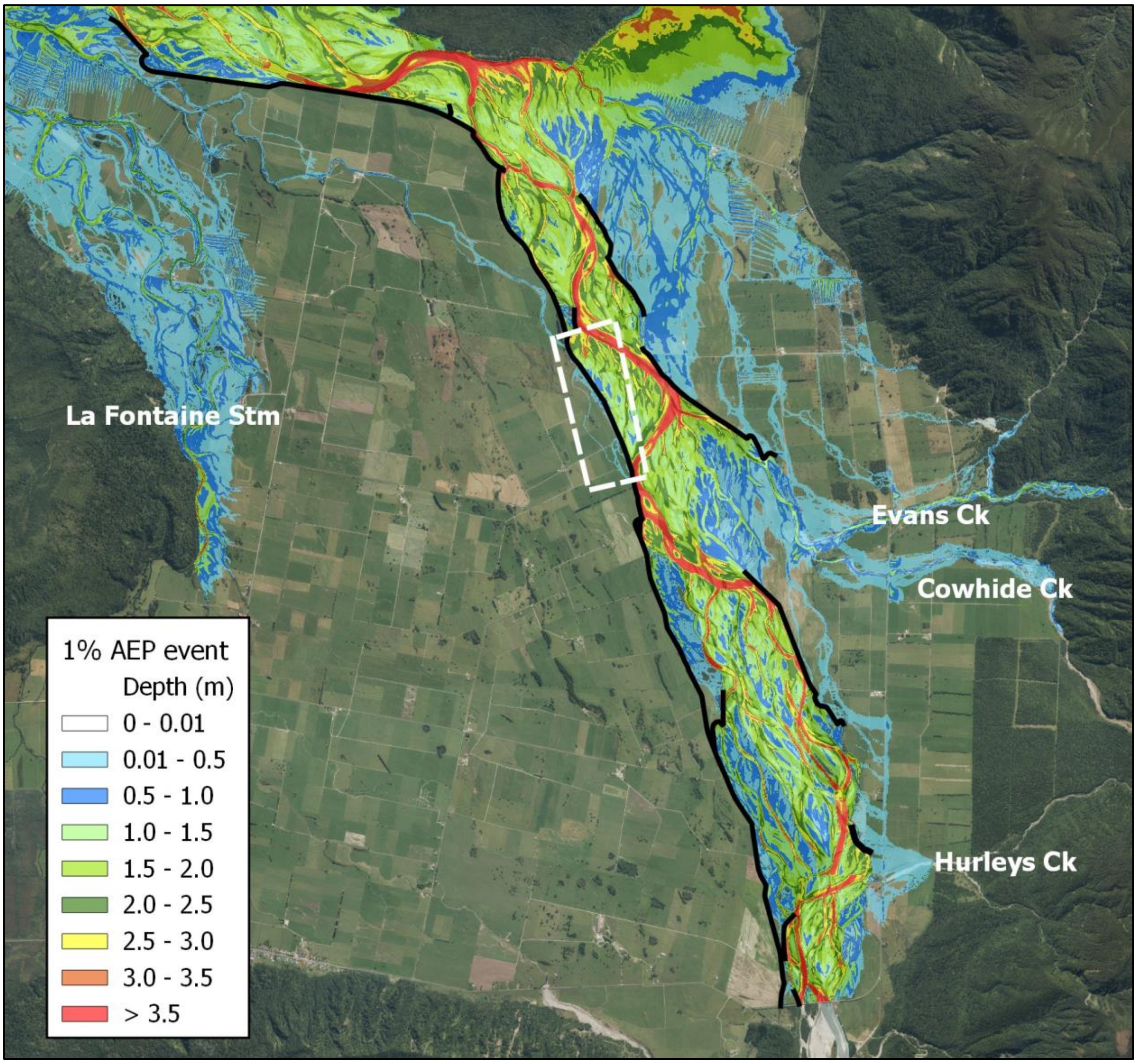

Figure 7-5: 1% AEP (100-year ARI) peak depth (m) map with stopbanks overlaid in black, and the overtopping on the TL stopbank shown by the white dashed rectangle.

The right stopbanks also continue to overtop, however these areas are already inundated from floodwaters coming through gaps in the network which are causing substantial surface flooding of the farmland. There is however significant risk that if the banks were overtopping substantially in a major flood event, that they could fail. The impacts of potential overtopping and scour failures are investigated in Section 7.3 Results Analysis – Residual Hazard Runs.

Additionally, floodwaters from the tributaries on both sides of the valley result in considerable surface flooding. The Hurleys, Cowhide, and Evans creeks contribute to extensive surface flooding on the true right side of the Wanganui River, as well as overtopping SH6 and flowing behind the true right stopbanks. Additionally on the true left, La Fontaine Stream begins to overtop its banks early in the modelled flood run before spreading across much of the farmed area where the valley narrows up again.

7.1.5. 1% AEP – APPROXIMATED RCP8.5

The 1% AEP (100-year ARI) approximated RCP8.5 scenario shows a notable increase in inundation compared with the historic climate scenario.

- On the true left, multiple sections of stopbank now overtop from about 4.4 km downstream of the SH6 bridge (Figure 7-6; white dashed rectangle). These sections result in multichannel inundation across the true left farmland, until they meet the floodwaters spreading out from where the protective network ends around 13.0 km downstream of the SH6 bridge.
- On the true right side, stopbank 3 is almost entirely underwater, with the area between Lake Ianthe and the downstream end of stopbank 2 also completely underwater. This inundated farmland on the true right is covered on average by at least 0.5 m of water with the channelized flow peaking at depths as high as 2.0 m, and velocities on average between 1.0 and 2.0 m/s with small areas peaking higher at ~2.5 m/s (Figure 7-7).

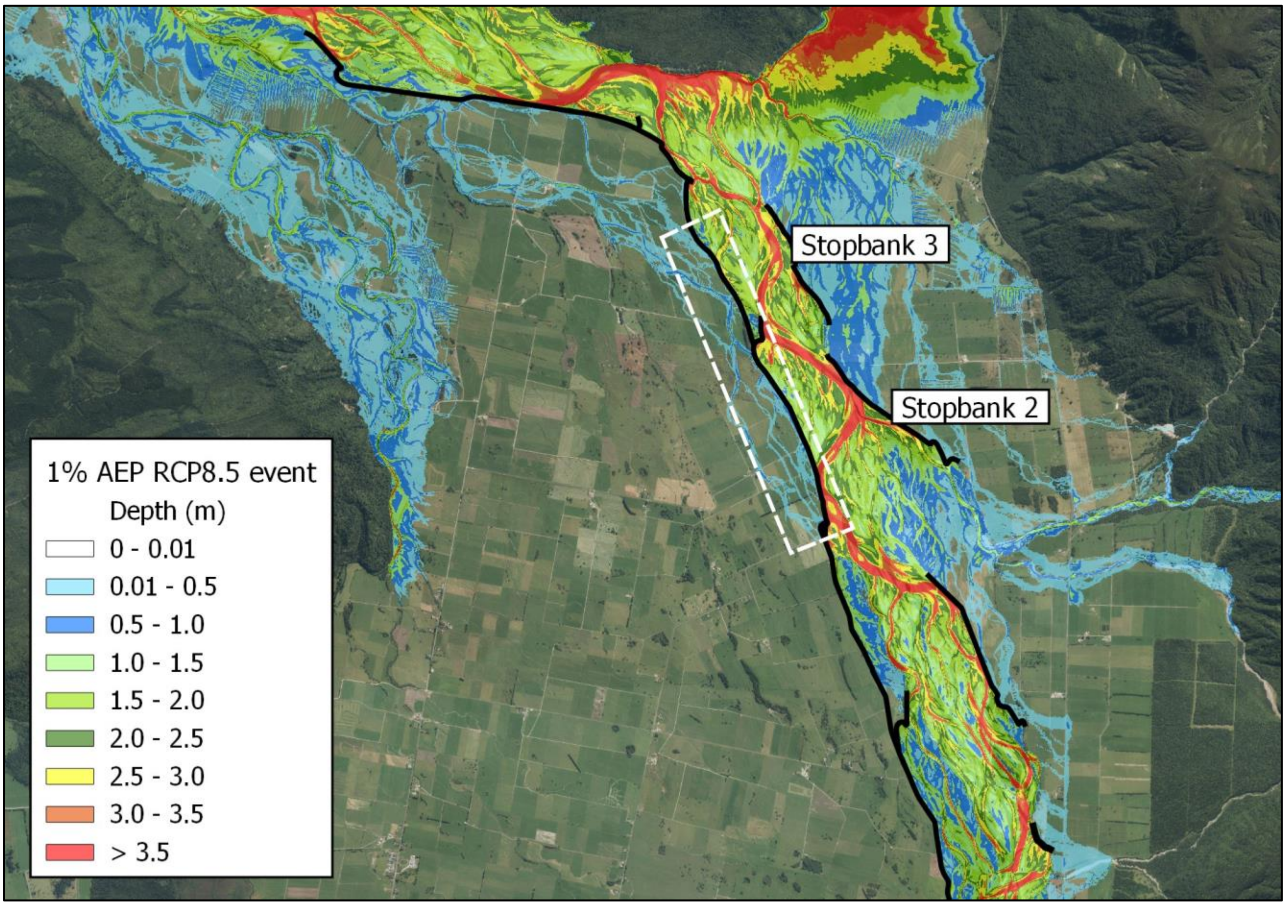

Figure 7-6: peak depth (m) for the 1% AEP (100-year ARI) approximated climate change RCP8.5 event.

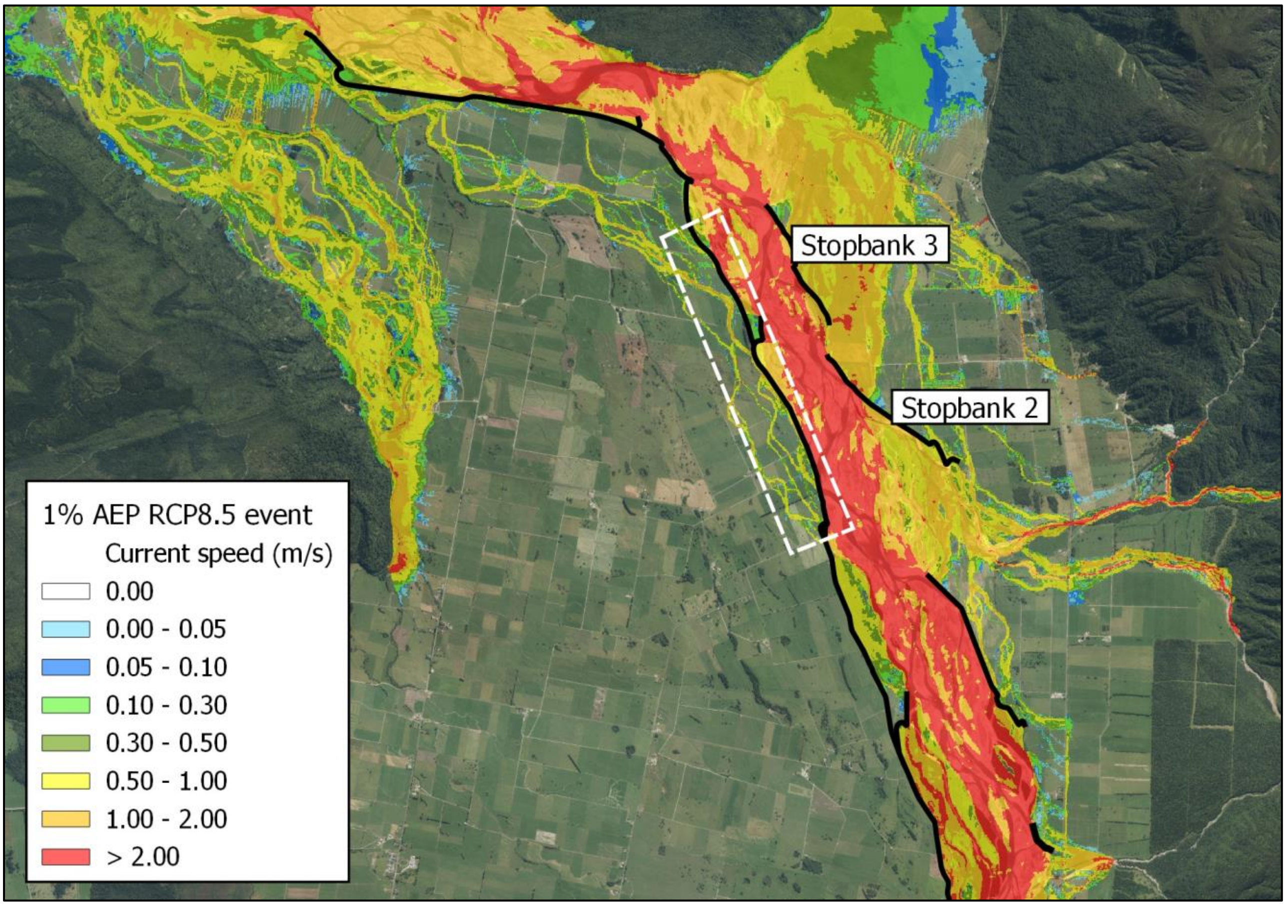

Figure 7-7: peak current speed (m/s) for the 1% AEP (100-year ARI) approximated climate change RCP8.5 event.

7.2. RESULTS ANALYSIS – SENSITIVITY RUNS

7.2.1. HYDROLOGY SCENARIOS – S-HYD01 AND S-HYD02 – HISTORIC CLIMATE

The at-site calculated 1% AEP (100-year ARI) flows at both the Hokitika Rv @ Gorge and Whataroa Rv @ SH6 differ to the flows estimated by the NIWA online flood statistics tool. For the former it's by about 24% and the later 10%. Given that there is no at-site data for the Wanganui River, the NIWA estimated 1% AEP flow has been used, with additional model runs completed to test for sensitivity to a 1% AEP flow with an extra 10% and 20% of flow.

Results show that there is minimal difference in flood extent between the three 1% AEP flows (3,300 m^3/s, 3,600 m^3/s and 3,900 m^3/s) as much of the flow remains confined by the protective network and major breakouts continue to be through the gaps in the stopbanks on the true right.

The few key differences between the estimated 3,300m^3/s flow and the two sensitivity runs include:

- Areas already flooding fill out more, with increased flooding on both sides of the river where the flow wraps around the start/end of a stopbank.
- On the true left, several more sections of stopbank overtop, however flow from these tend to occupy paleochannels which carry the water across the farmland to join La Fontaine Stream. A comparison of peak water levels where the difference is most notable along the true left stopbank (3 to 9 km downstream of the SH6 bridge) has been presented in Figure 7-8 and Figure 7-9.
- The groyne on the true left just downstream of the SH6 bridge built to protect the main true left stopbank from erosion, overtops, but the flow is still confined by the main true left stopbank.
- On the true right, sections of stopbank overtopping increase in length.

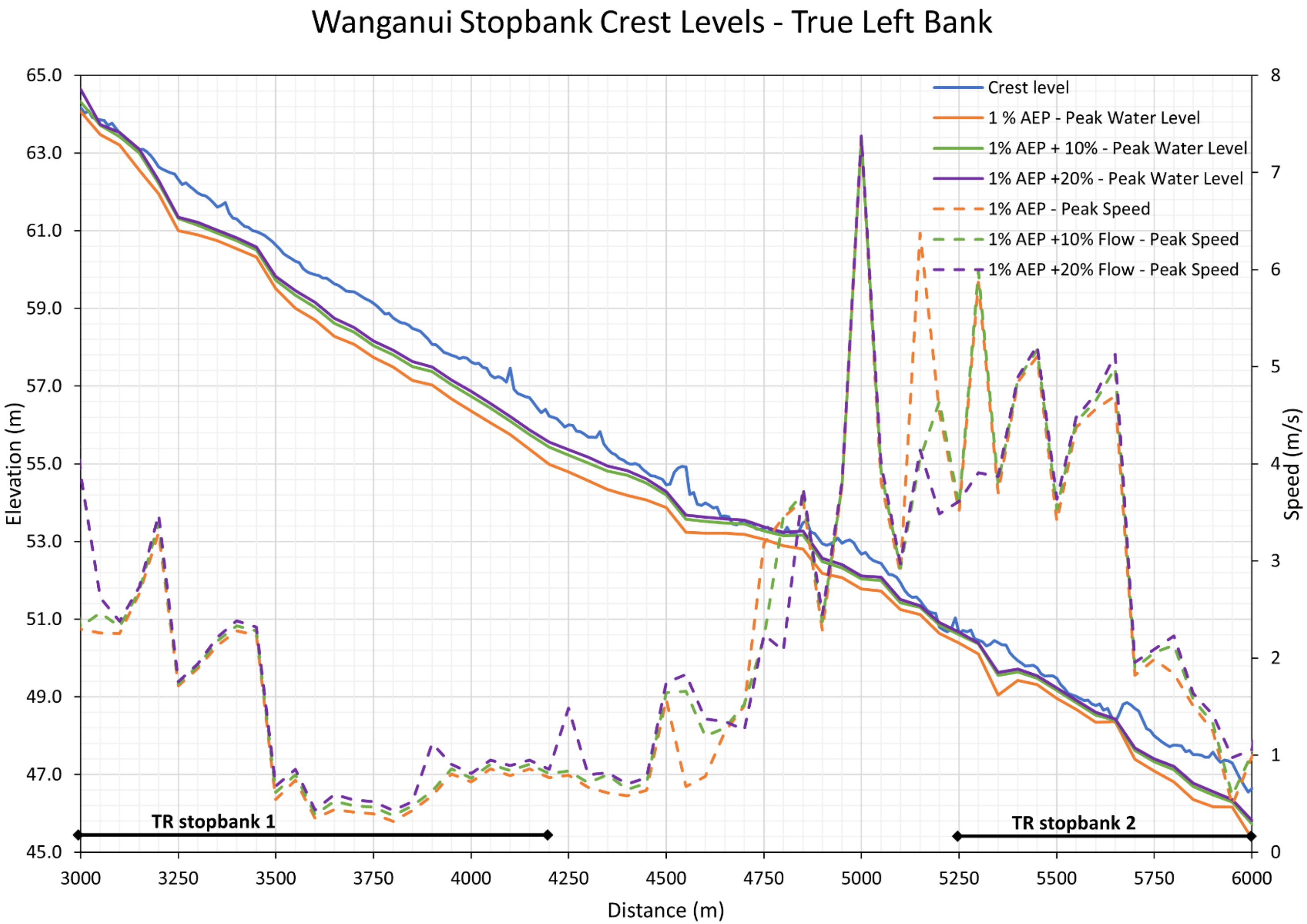

Figure 7-8: Peak water level and speed comparisons along the true left stopbank (3 km to 6 km) between the 1% AEP flow with the two sensitivity runs (1% AEP flow +10% and +20%).

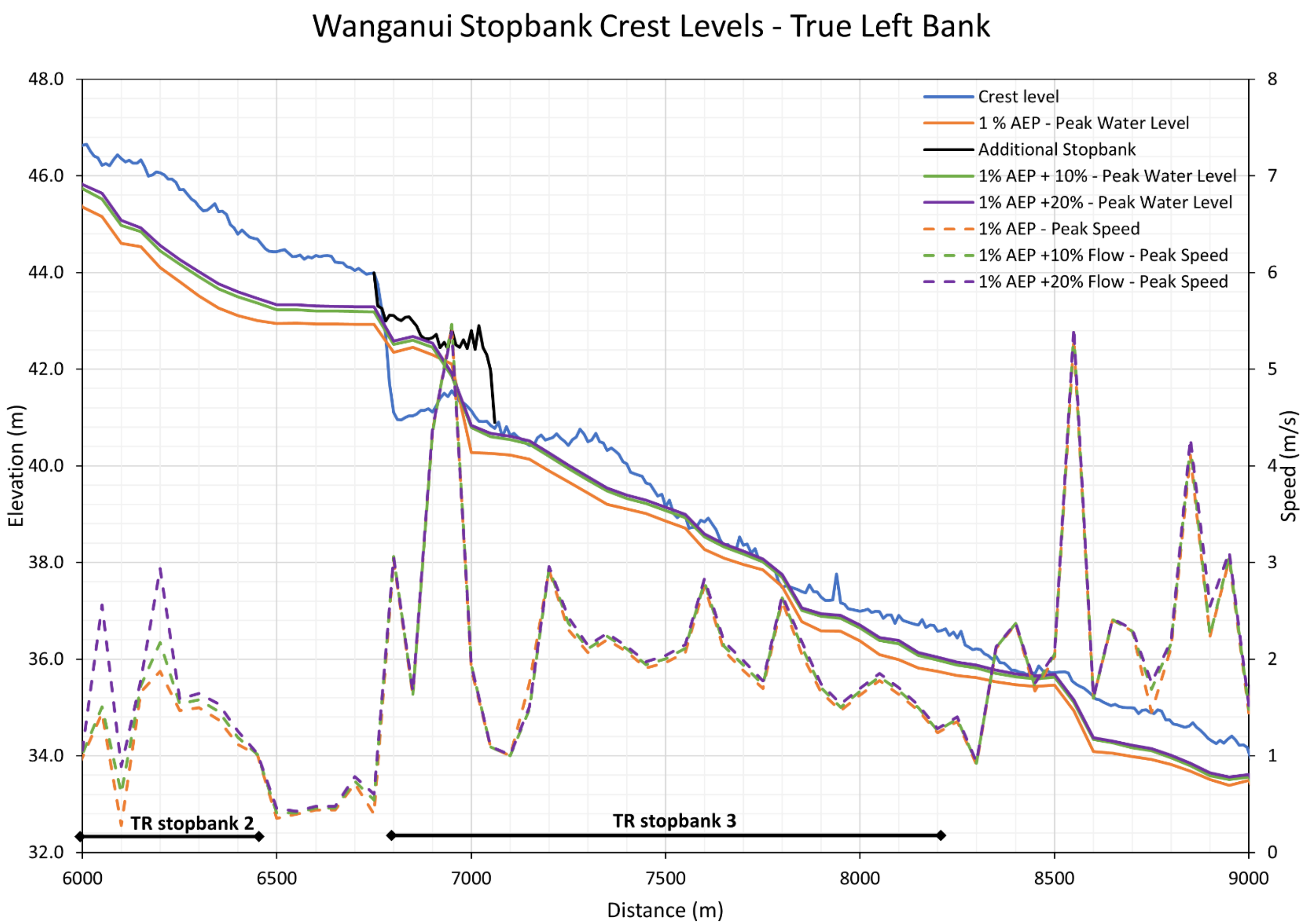

Figure 7-9: Peak water level and speed comparisons along the true left stopbank (6 km to 9 km) between the 1% AEP flow with the two sensitivity runs (+10% and +20%). The additional stopbank (black) represents the hook groyne which protects the main true left stopbank between 6.75 km and 7.05 km.

7.2.2. ROUGHNESS SCENARIO – S-RGH01 – HISTORIC CLIMATE

As the roughness values for the river channel were estimated, a test for sensitivity to roughness was run for the 1% AEP (100-year ARI) design flow using a Manning's 'n' value of 0.04 – the design run used 0.05.

The lower manning's 'n' resulted in the following differences:

- Slightly smaller flood extent.
- Slightly reduced depths with minimal difference in peak water level along the true left stopbank (Figure 7-10).
- Due to the smoother bed in the main channel, velocities are in places slightly higher along the true left stopbank (Figure 7-10). However, velocities are slightly reduced in the floodplain as it is inundated by less flow.
- The true right stopbank 1 doesn't overtop (Figure 7-11).
- Fewer overflow paths across the true left farmland as more water remains in the main channel.

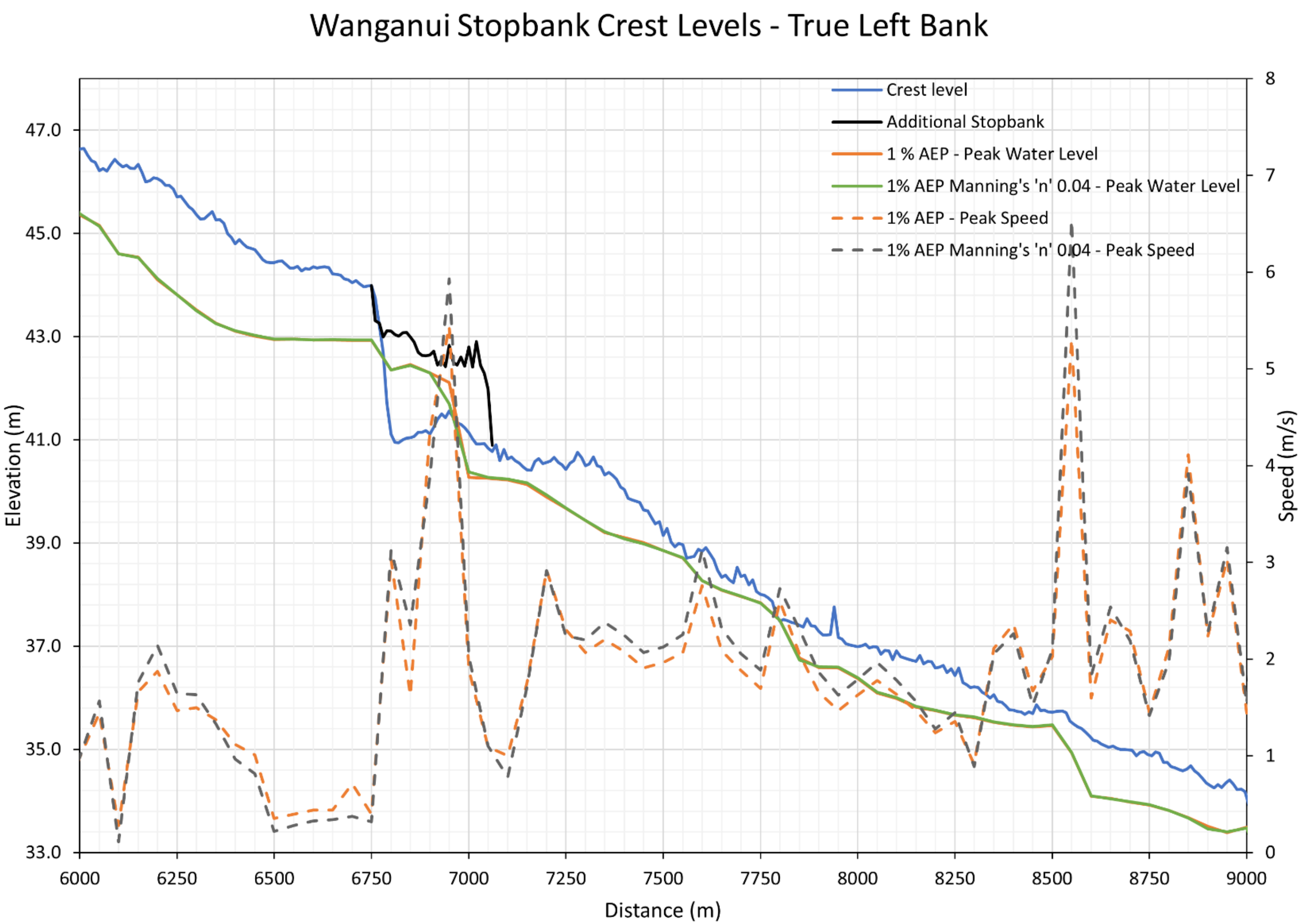

Figure 7-10: Peak water level and speed comparisons along the true left stopbank (6 to 9km) between the 1% AEP flow and the 1% roughness sensitivity run (lower manning's 'n').

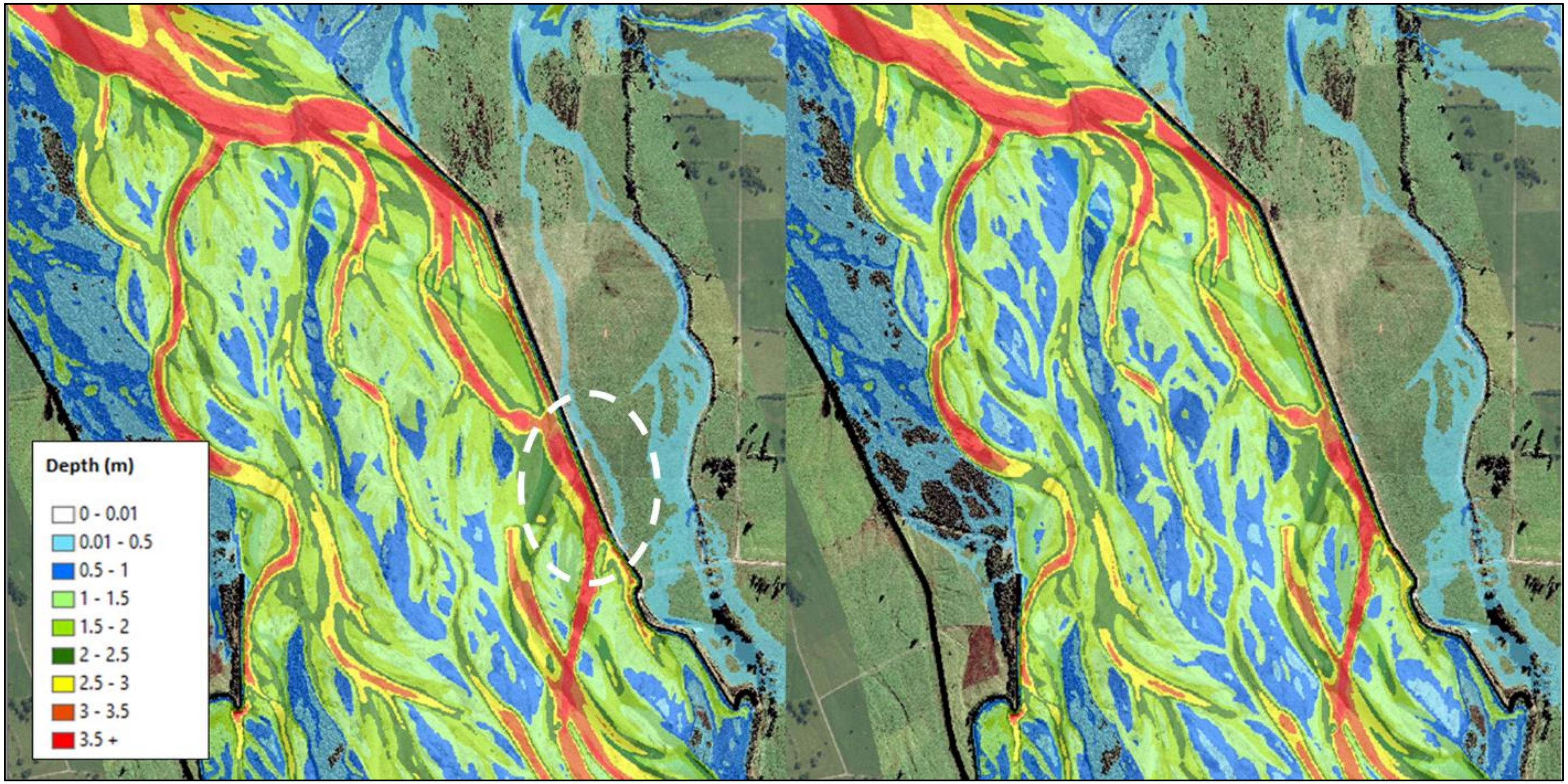

Figure 7-11: Peak depth (m) at the true right stopbank 1 where the 1% AEP flow overtops but the 1% AEP RGH01 sensitivity run (lower manning's 'n') does not.

7.3. RESULTS ANALYSIS – RESIDUAL HAZARD RUNS

The residual hazard runs include two different stopbank down scenarios (Figure 7-12) each simulated with both the 1% and 2% AEP (100 and 50-year ARI) flows, and six scour breach and two overtop breach scenarios all simulated with the 5%, 2% and 1% AEP (20, 50 and 100-year ARI) flows (Figure 7-13).

The most upstream breach scenario occurs on the true right at the first of the long sections of stopbank. Breaches have not been simulated further upstream of this for several reasons:

- The model begins just downstream of the current SH6 bridge, and therefore cannot be used to replicate the breach that occurred upstream of this in the early 1900's.
- At the time of writing, the river alignment meant that the true left stopbank was not affected by the main channel or the higher instream peaks and velocities when in flood, therefore a simulated breach in the network at this most upstream end would have little to show. However, the alignment does change, and this true left bank has become an area of concern. A breach could be modelled in future if the DEM were extended upstream with additional survey (LiDAR or drone) data.

Overtop breach scenarios were only simulated for the true right side as the stopbanks on this side already overtop under the design runs, whilst there is still freeboard on the true left stopbanks in the design runs.

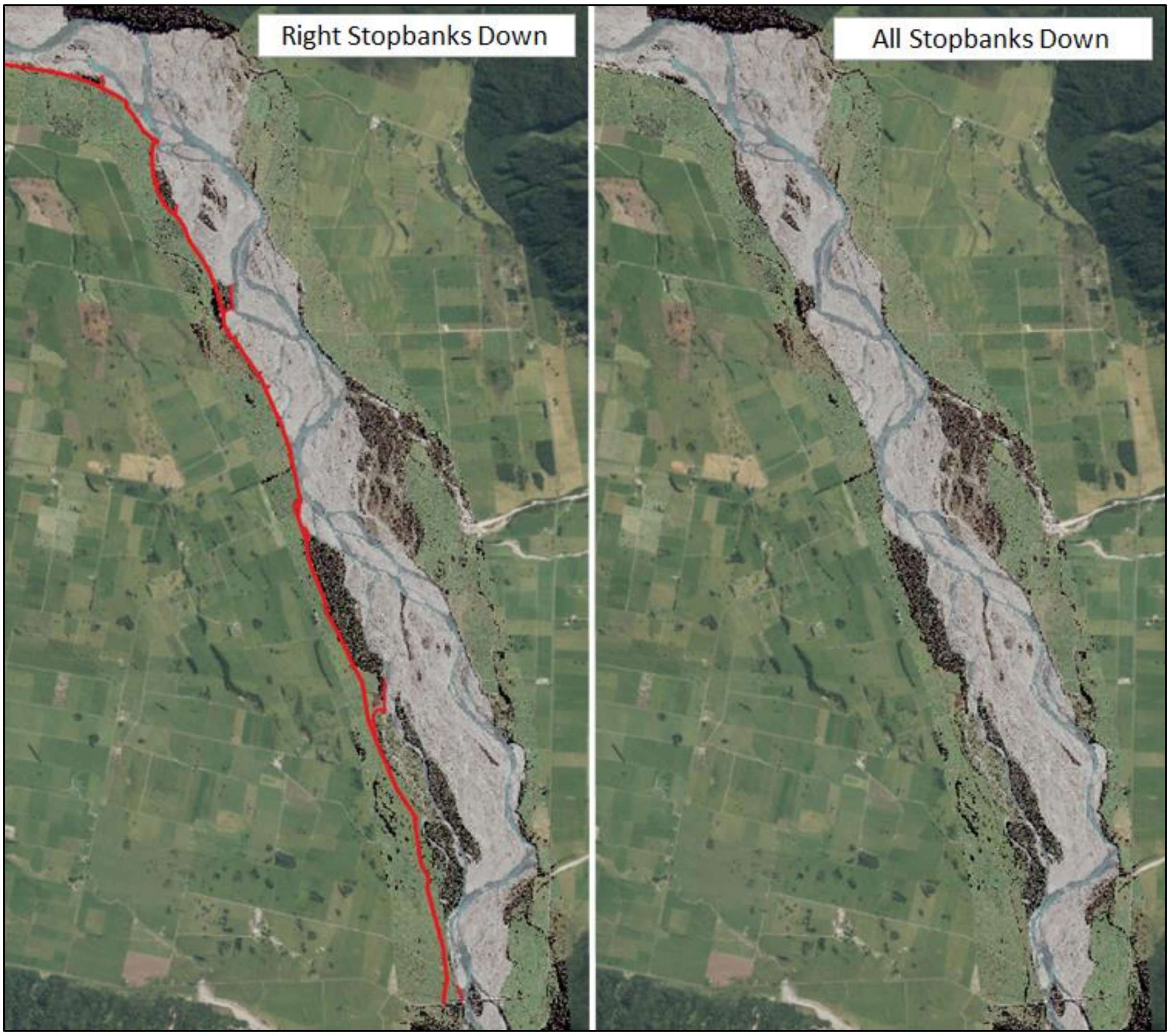

Figure 7-12: Right stopbanks down and all stopbanks down scenarios.

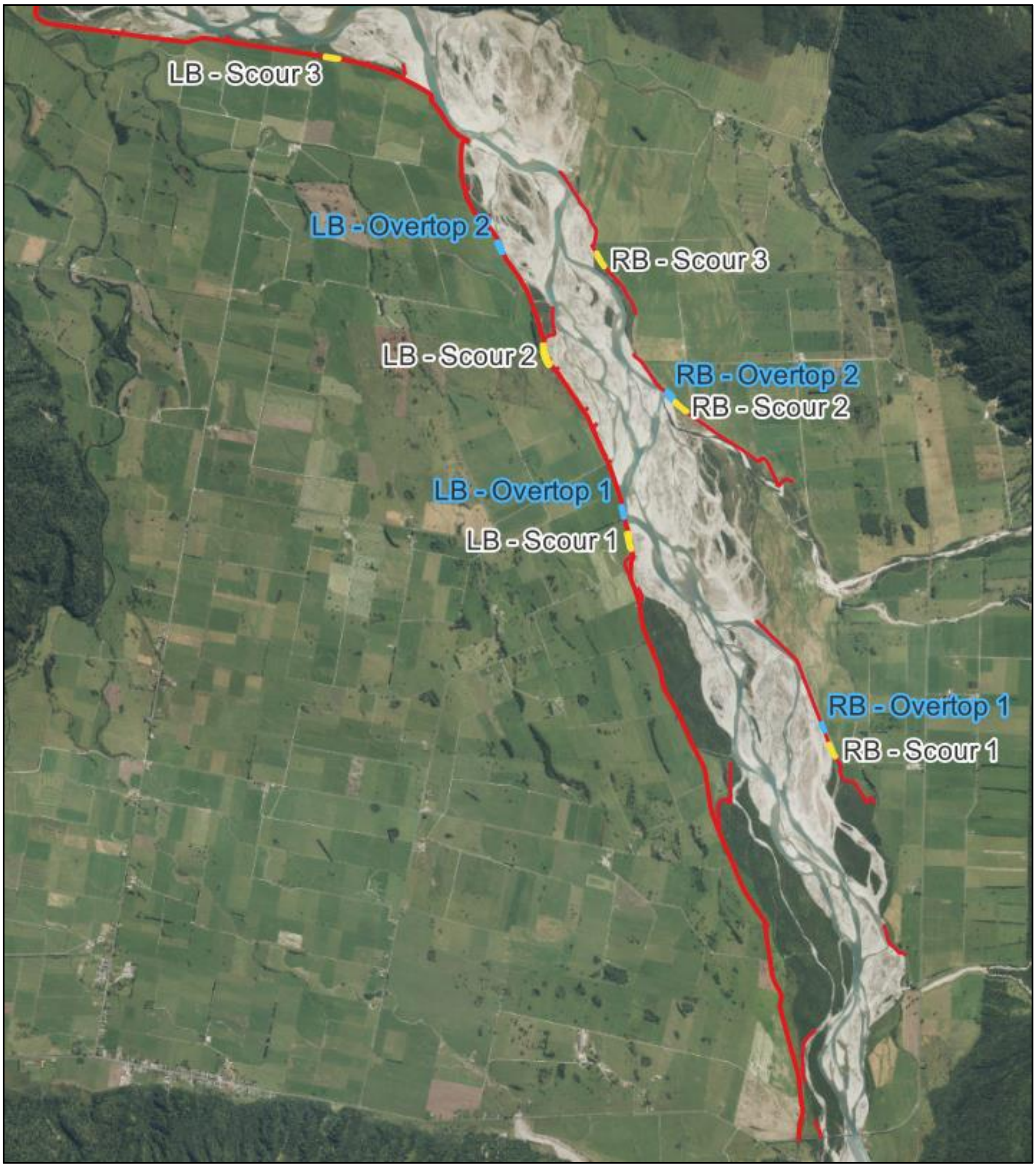

Figure 7-13: Modelled scour and overtop breach locations.

7.3.1. RIGHT STOPBANKS DOWN - 2% AND 1% AEP – HISTORIC CLIMATE

To investigate what the true right stopbanks are protecting and the impact of their removal, a scenario with the right stopbanks removed was simulated with both the 1% and 2% AEP (100 and 50-year ARI) flows. Both right stopbank down runs were very similar with only minor increases in extent and depth in the 1% scenario compared to the 2%, for this reason, the discussion below applies to both.

The results show that on the true right:

- The floodwaters inundate the area between the river and Lake Ianthe. This area was once active braidplain but is currently only accessible to the river through the gaps between the three true right stopbanks.
- Compared to the equivalent design runs (both 1% and 2% AEP) depths increase by 0.5 to 1.5 m (Figure 7-14) and velocities also show a significant increase (Figure 7-15).
- These increases in depth and speed, as well as extent of flooding on the true right would have considerable impact on the farmland as a result of sediment deposition, scouring of the land to form flow channels and general churning up of the paddocks.

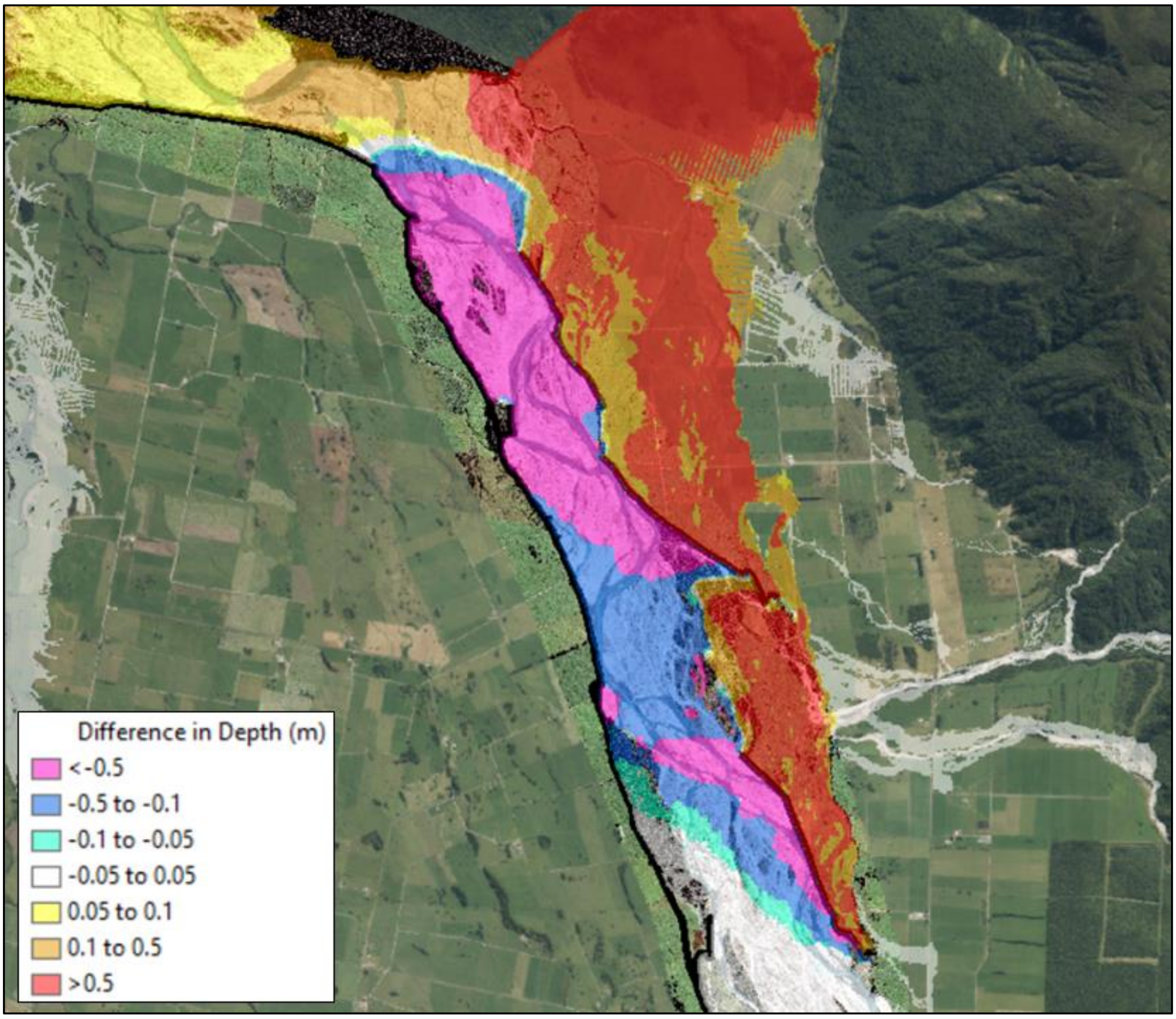

Figure 7-14: Depth difference map between the 2% AEP design run and the 2% AEP right stopbanks down run.

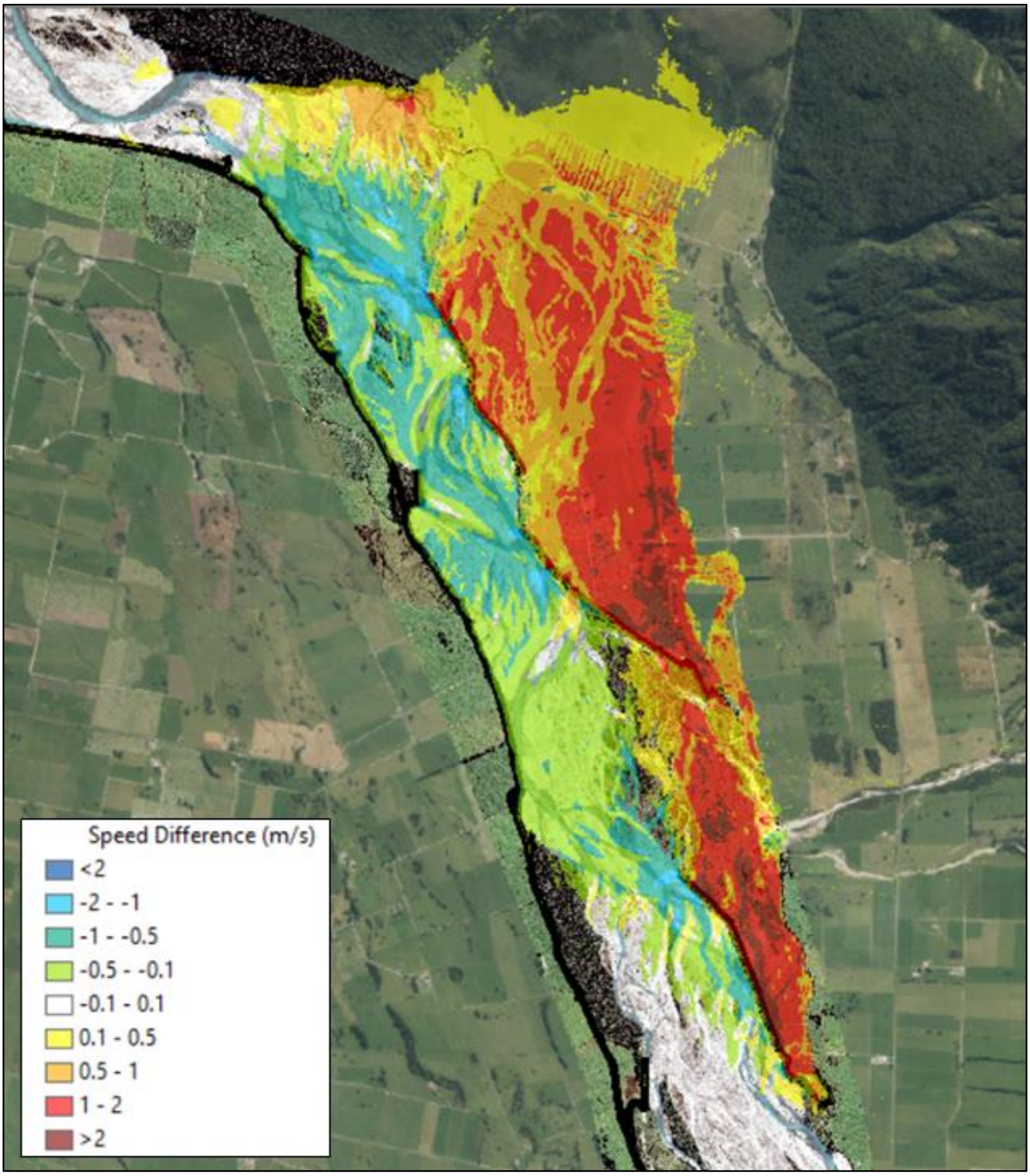

Figure 7-15: Speed difference map between the 2% AEP design run and the 2% AEP right stopbanks down run.

The removal of the true right stopbanks also a has notably positive impact along the true left side of the network. The results show:

- The true left bank no longer overtops (Figure 7-16).
- Along the true left bank in the section between the 6 km and 9 km distance markers (Figure 7-17), both peak water depths and velocities are significantly reduced, by up to 1.1 m and 3.0 m/s, respectively (Figure 7-18).

Land River Sea
CONSULTING

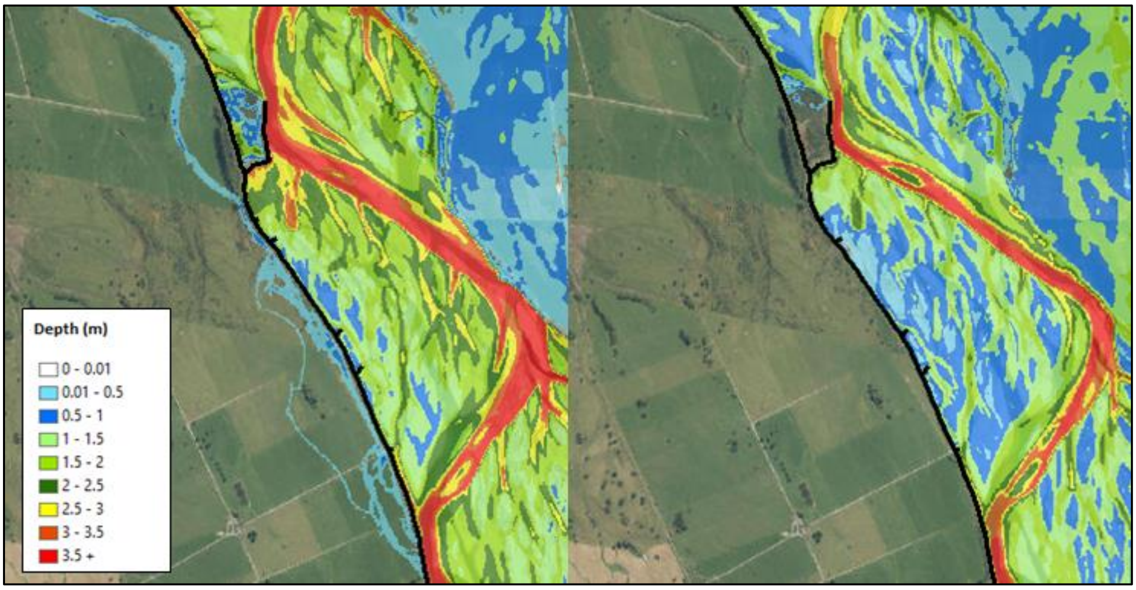

Figure 7-16: Comparison between the 1% AEP design and no right stopbank runs. The design run has several points of overtopping along the left back, this doesn't occur in the no right stopbank run.

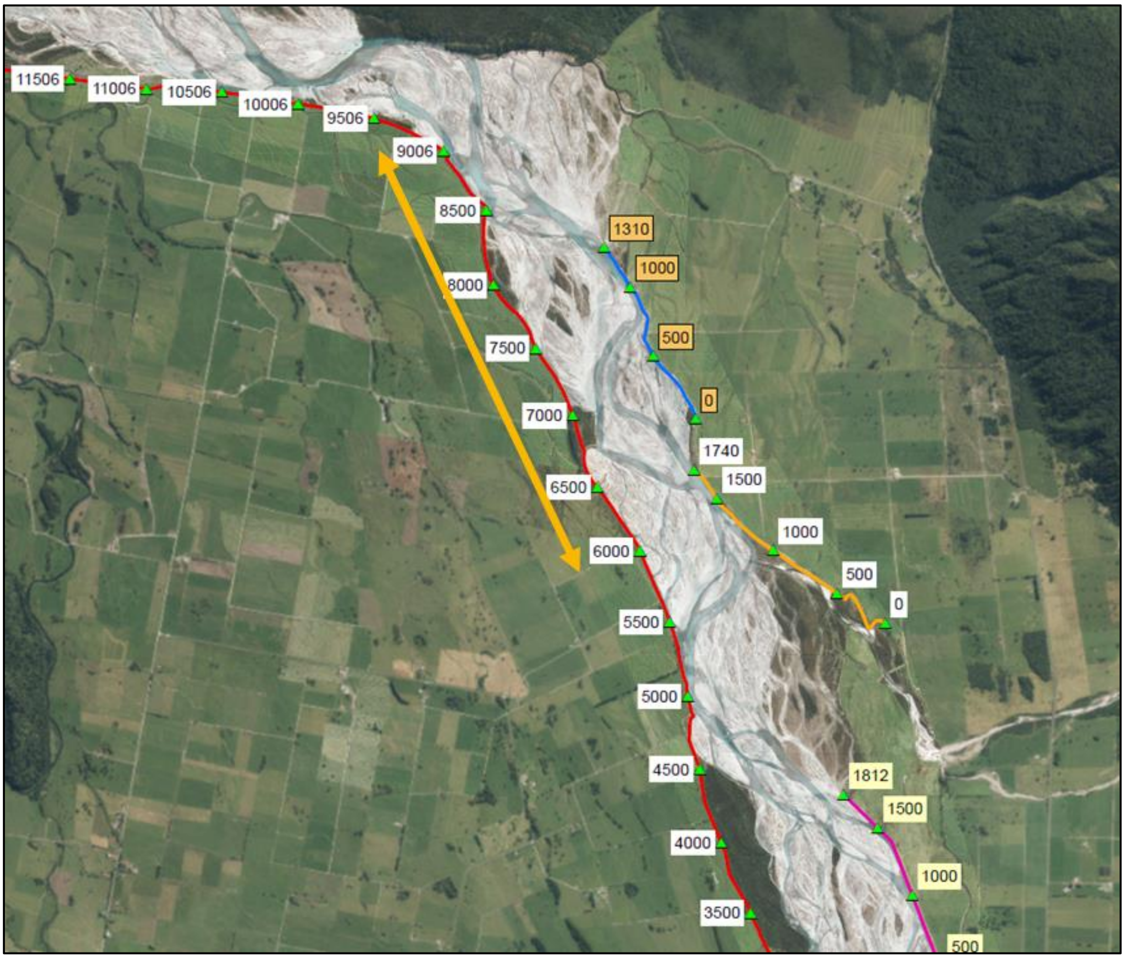

Figure 7-17: Distance markers on both sides of the Wanganui River, with the 6 to 9 km indicated by the orange arrows.

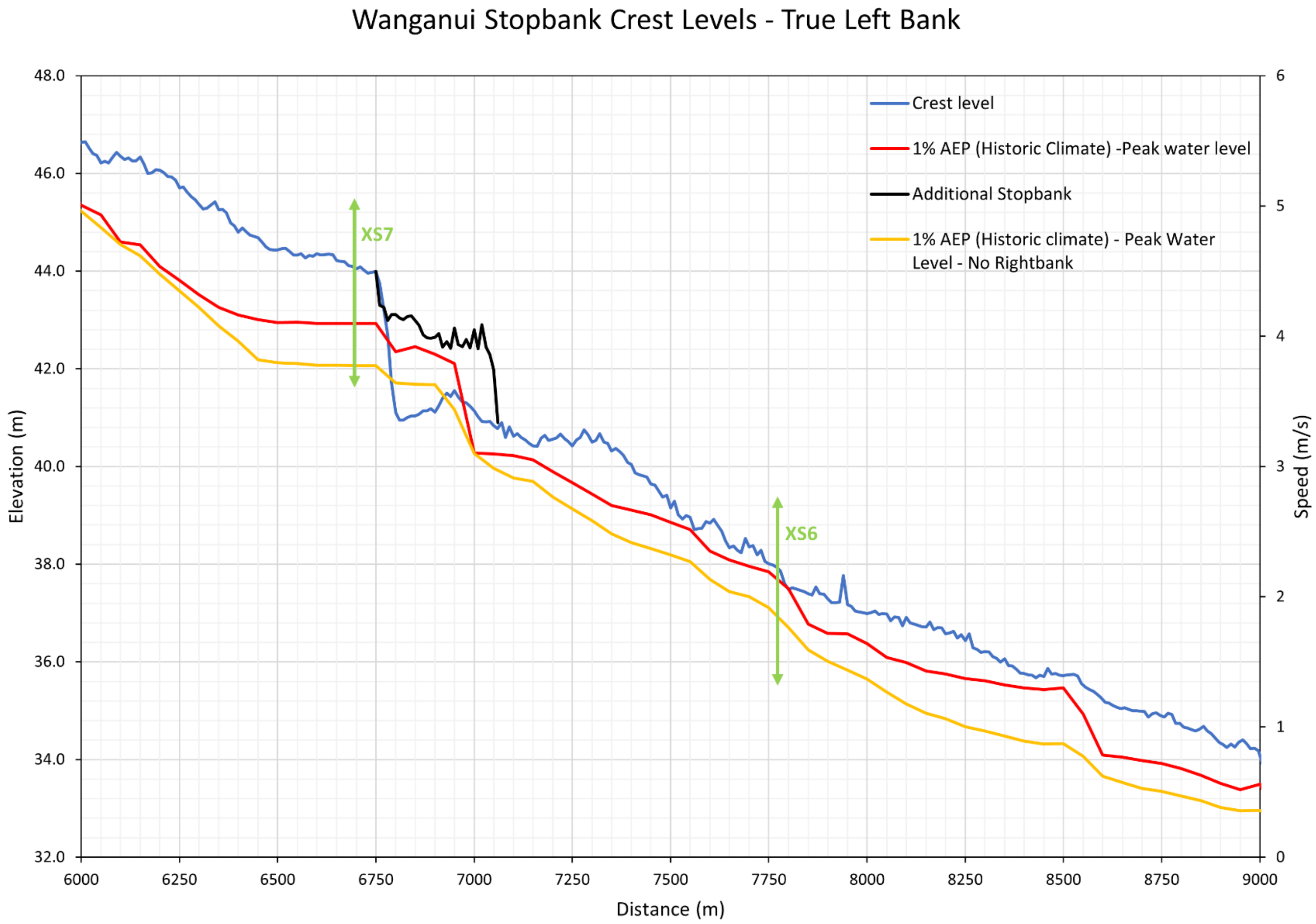

Figure 7-18: Long profile of the section between 6 and 9 km downstream of the SH6 bridge comparing the depth along the true left stopbank, between the 1% AEP deign run and the 1% AEP no right stopbanks run. Cross sections (XS) 6 and 7 have been denoted by the green arrows.

Land River Sea
CONSULTING

7.3.2. ALL STOPBANKS DOWN - 2% AND 1% AEP – HISTORIC CLIMATE

The all stopbanks down scenario was simulated to show the area the river would naturally occupy during large flood events.

- In both the 2% and 1% runs, the flood extent increased significantly, with the most notable change being the inundation of the farmland to the true left of the river (Figure 7-19).

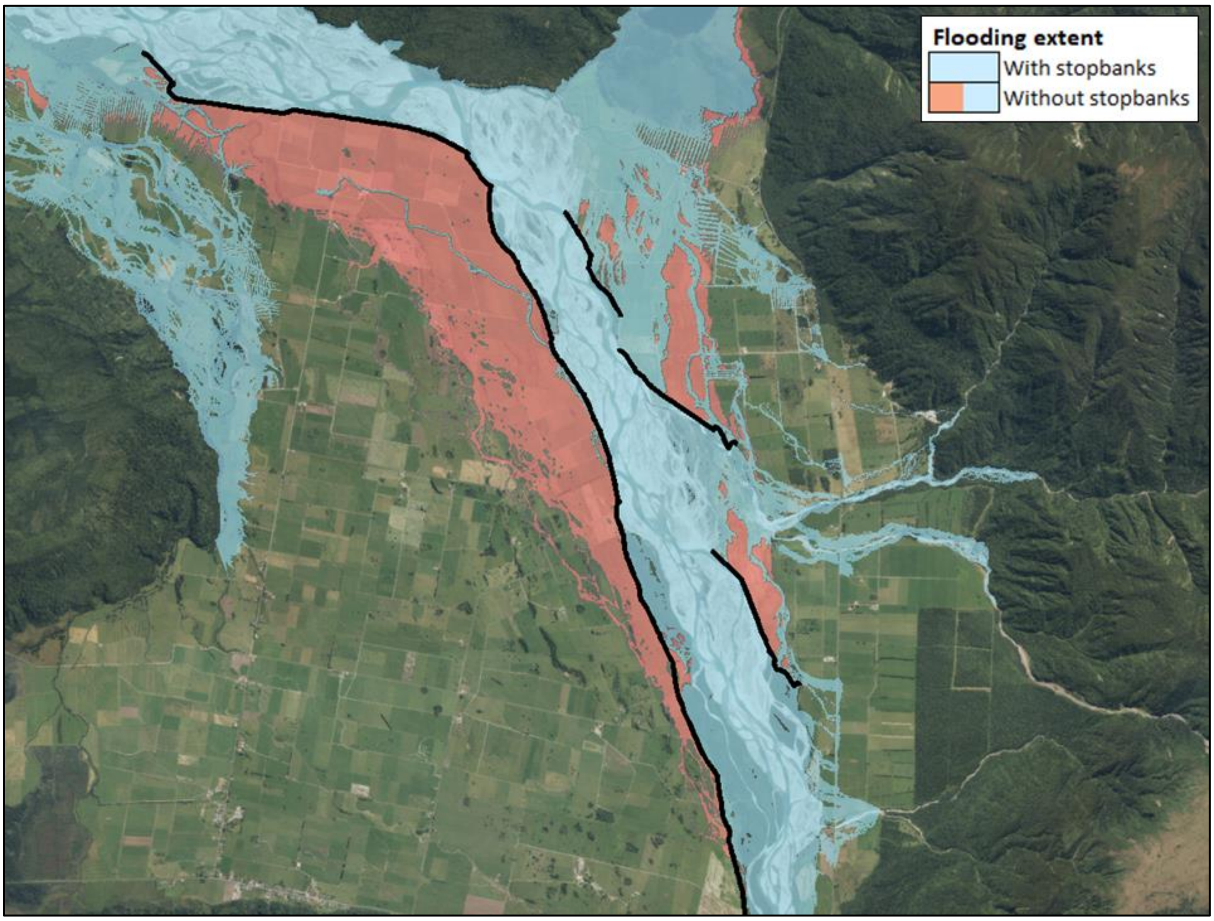

Figure 7-19: Flooding extents for a 2% AEP flow with and without stopbanks. The orange shaded area shows the additional inundation that would occur if the stopbanks weren't there.

Depths and velocities are also similar between the 2% and 1% AEP runs. The results show that:

- Depths on both sides of the river are between 0 and 1.0m, however channelised flow peaks as high as 2.5m. The deepest areas of flow remain within the current braid corridor.
- Velocities across the farmland are significant on both sides of the river, reaching damaging speeds of up to 3.0m/s but on average between 1.0 and 2.0m/s (Figure 7-20).

Additionally, in the 1% AEP run, a small shallow and slow moving flow path breaks out on the true left immediately downstream of the SH6 bridge (Figure 7-21).

Further, as the model starts at the bridge, we cannot provide advice regarding flood threat to the Hari Hari flats as a result of flood waters breaking out at or upstream of the bridge on the true left. With future surveys (LiDAR or drone) the model extent could be extended upstream so that this scenario could be addressed.

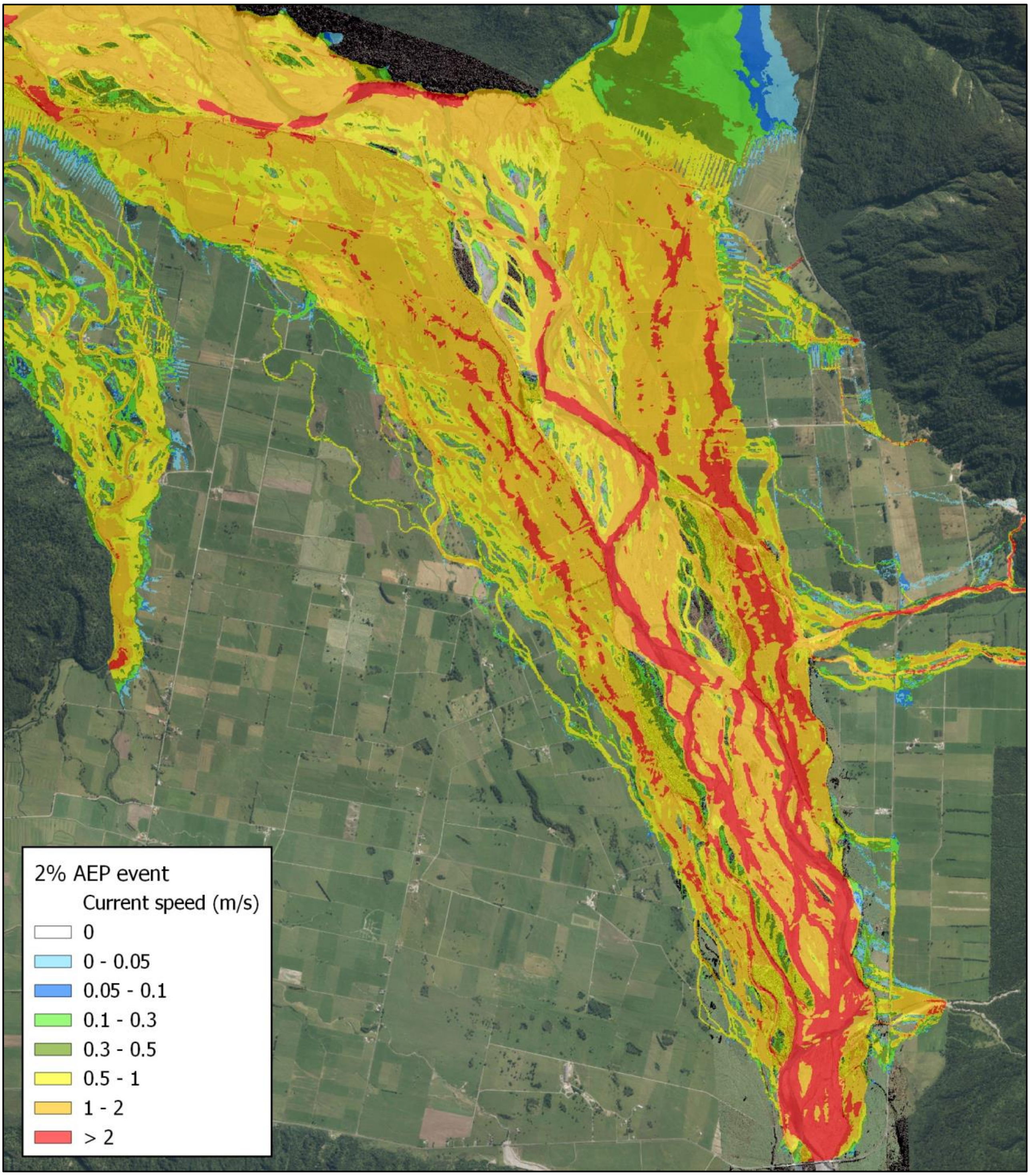

Figure 7-20: 2% AEP (50-year ARI) all stopbanks down peak speed (m/s) map to show surface flooding extent.

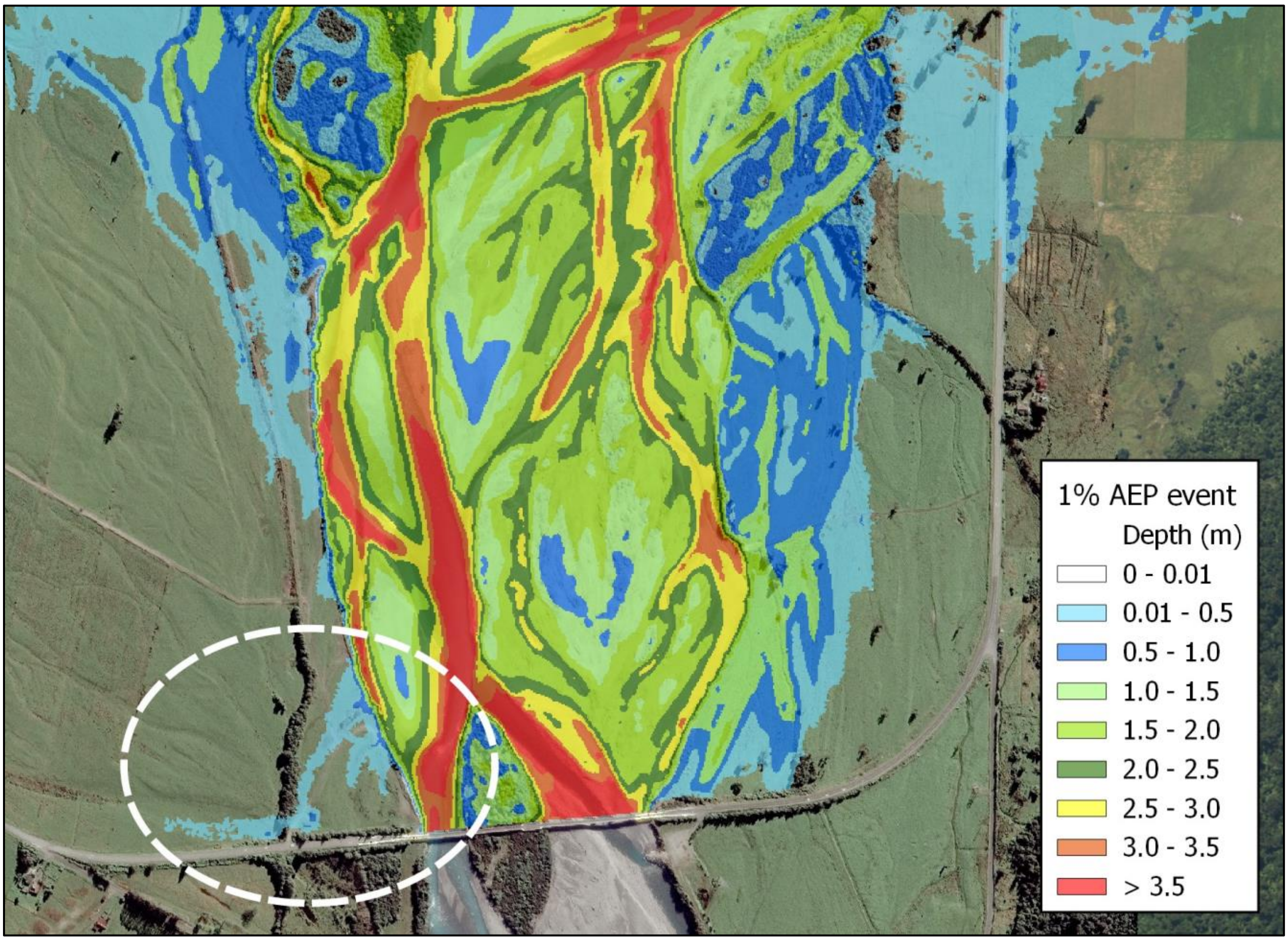

Figure 7-21: 1% AEP (100-year ARI) without stopbanks peak depth (m) map zoomed in to show small flow path just downstream of the SH6 bridge (white dashed ellipsoid).

7.3.3. LEFT BANK – BREACHES – HISTORIC CLIMATE

The results of the three scour breaches on the true left indicate that the location of the breach impacts on severity, with the further upstream the breach, the more severe the inundation of the true left farmland.

Flood extent:

- In scour breaches 1 and 2, for all three event sizes there is significant increases in flood extent compared to the design runs which only contain small (if any) flow paths across the TL farmland.
- Breaches 1 and 2, in all three event sizes inundate a ~3.0 km^2 area of farmland on the TL. Comparatively, breach 3, located much further downstream, has a smaller flood extent across the farmland (Figure 7-22).
- Additionally, in all three runs, with more water spilling out to the left, there's a reduction in the flooding extent on the true right of the river.

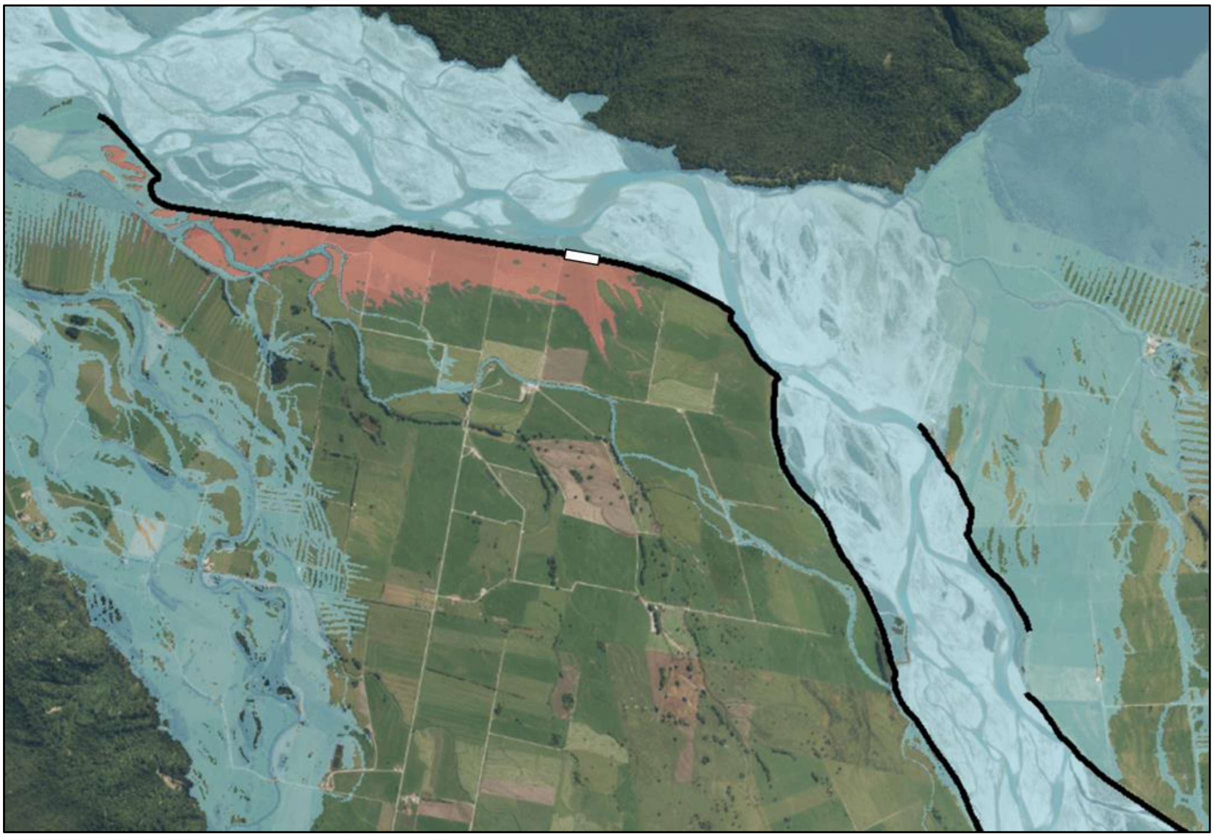

Figure 7-22: Flood extents for a 1% AEP flow with and without the left bank scour breach 3. The orange shaded area shows the additional flood extent with breach 3.

For all three breaches, depths and velocities across the true left farmland are similar.

- Depths are largely under 0.5 m, but in the channelised flow can be up to 2.0 m;
- Velocities peak between 1.0 and 2.0 m/s, with outliers of up to 3.0 m/s (Figure 7-23).

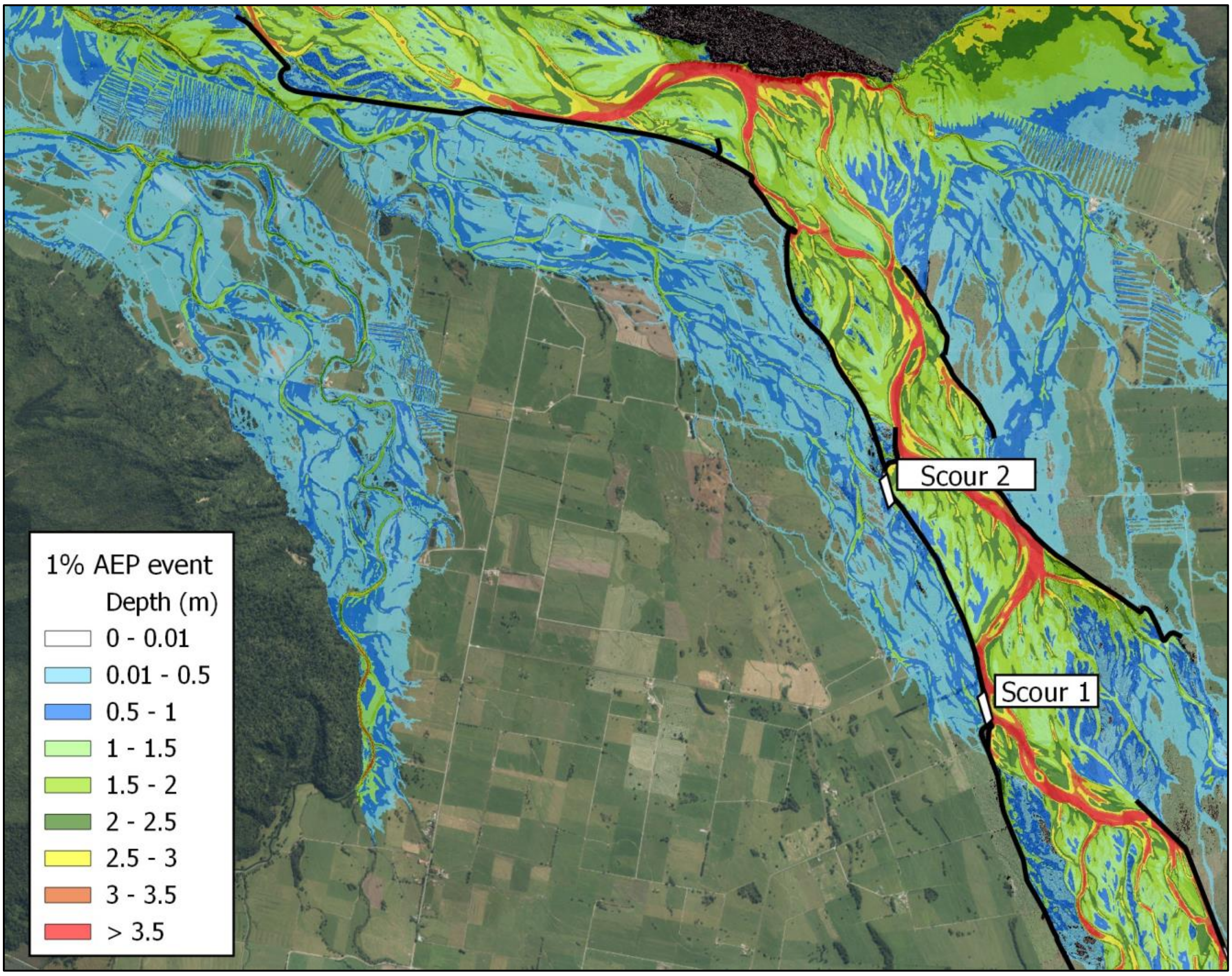

Figure 7-23: peak depth (m) of the LB scour breach 1 - 1% AEP (100-year ARI) scenario. The scour breach 2 scenario (location labelled) result was similar.

Both the overtopping and scour breaches on the true right of the river have more of an impact upon depths and velocities than extent compared to the breaches on the true left, as they contribute additional flow to areas that would already be flooded in the design runs.

Additionally, because more water spills out onto the true right farmland, there is less spill over on the true left.

Overtop 1 and scour 1:

- Both these breaches perform similarly for all three event sizes in that they show a notable increase in inundation behind stopbank 1 compared to the design runs which only have 2 small channels of flow (1 of which is from the upstream true right tributary).
- Depths are largely between 0.5 and 1.7 m, with velocities peaking as high as 3 m/s (Figure 7-24).
- They also result in additional flow paths across the TR farmland behind stopbank 2.

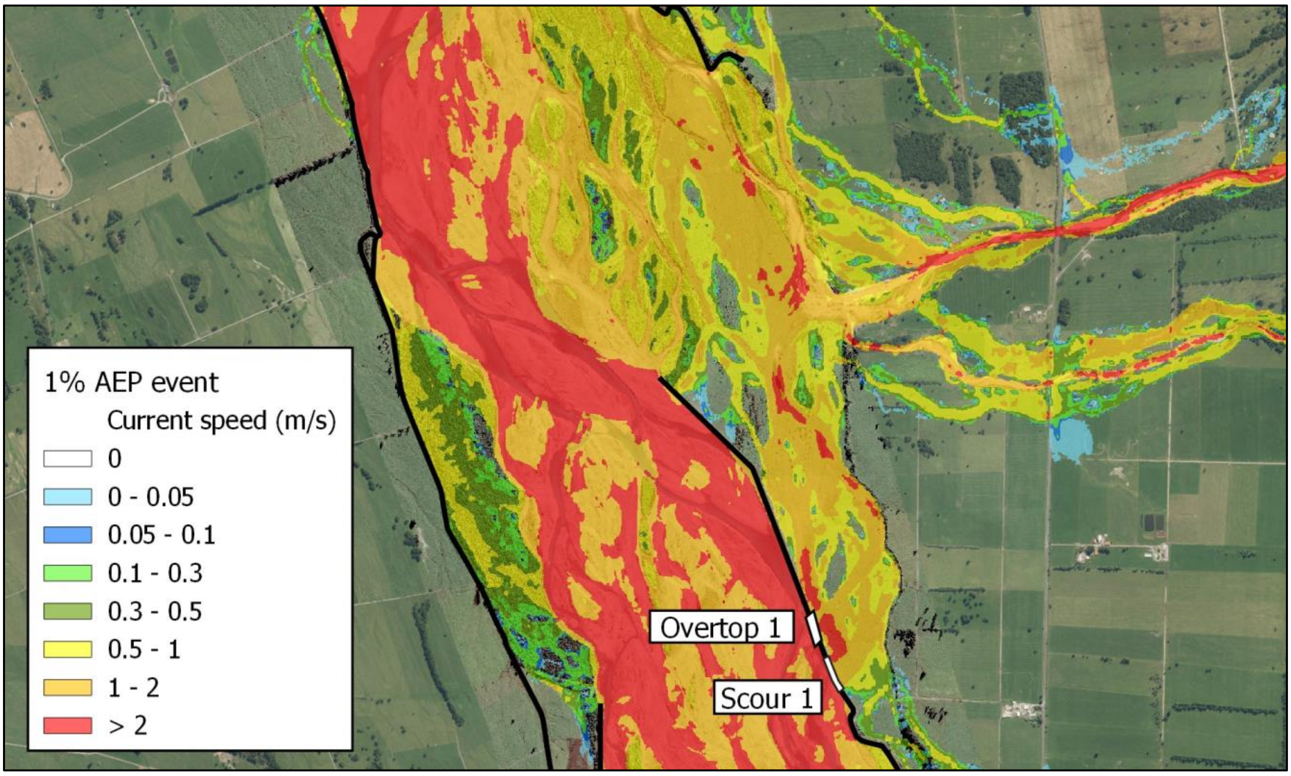

Figure 7-24: peak current speed (m/s) for the right stopbank scour breach 1 - 1% AEP (100-year ARI) scenario. The overtopping breach 1 scenario (location labelled) result was similar.

Scour 2 and 3:

- In these two scour breach scenarios, between 6 and 9 km downstream of the SH6 bridge, depths were between 0.1 and 1.0 m deeper across the farmland and 0.1 to 0.5 m shallower in the main channel compared to the design runs (Figure 7-25).
- When comparing the 2 scour scenarios against each other, depths and velocities are quite similar. Depths are largely under 1.0 m with velocities between 1.5 and 2.5 m/s and peaking higher for the 2 and 1% AEP (50 and 100-year ARI) runs (Figure 7-26).
- In terms of flood extent, both scenarios are larger than the design runs. Additionally, because it is located slightly further upstream, the scour 2 scenario has a greater inundation extent compared to scour 3.

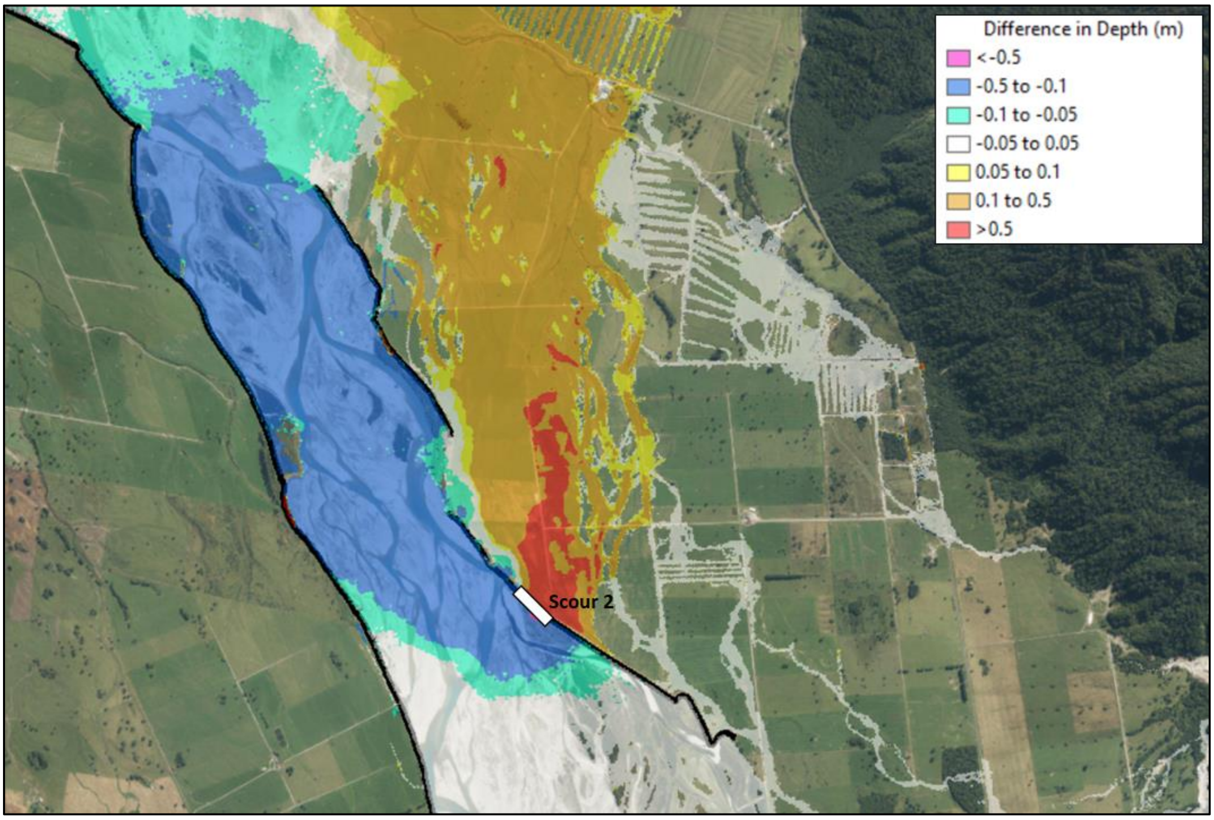

Figure 7-25: 1% AEP flow depth difference map between the design and RB scour breach 2 scenario.

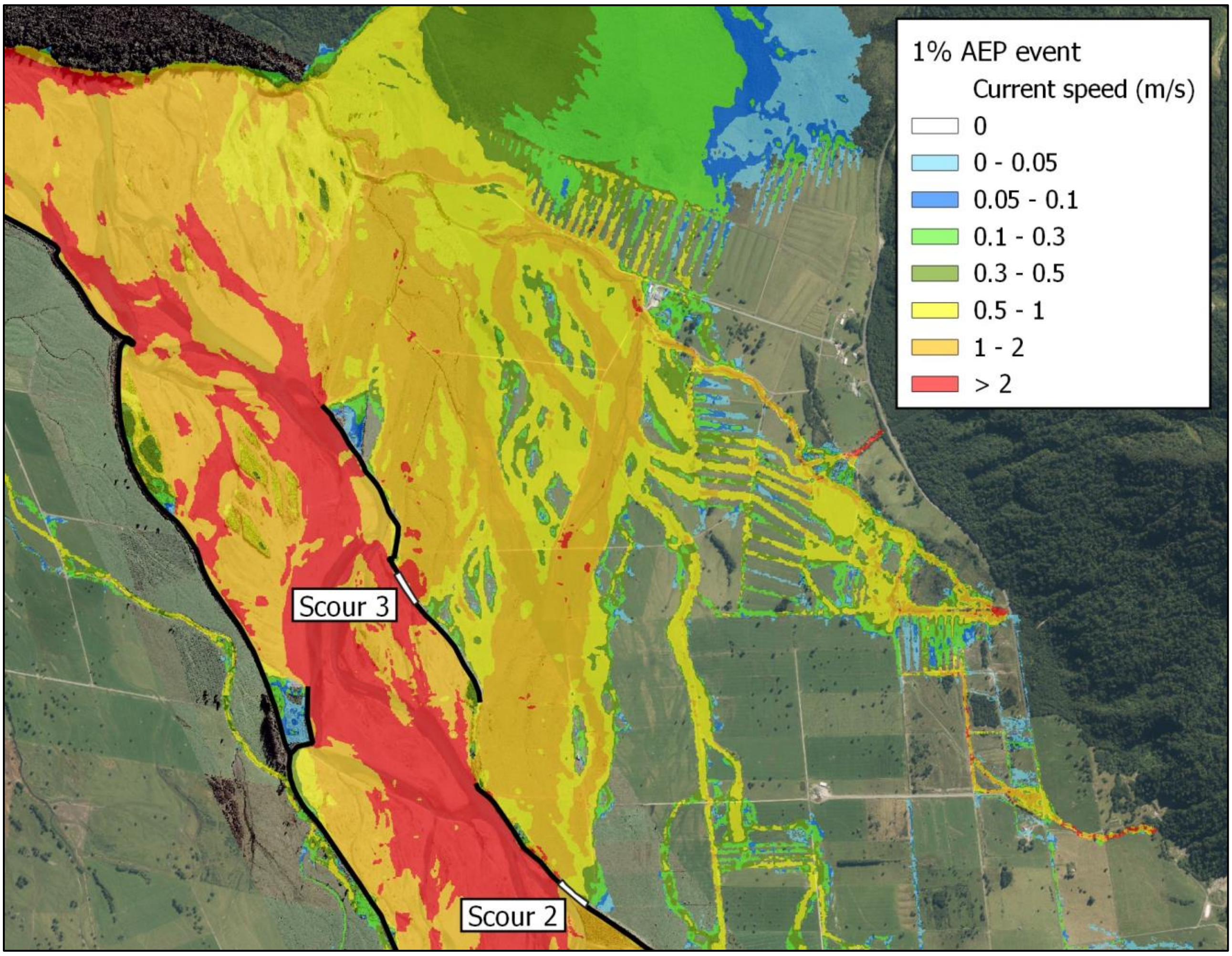

Figure 7-26: peak current speed (m/s) for the right scour breach 3 – 1% AEP (100 year ARI) scenario. The right scour breach 2 (location labelled) result was similar but with a channel of 2+m/s extending from the breach site.

Overtop 2

This overtopping scenario has less of an impact on the inundation than the more upstream scenario, likely because in the design runs, flow already spills out onto the farmland between the TR stopbanks as well as overtops stopbanks 2 and 3 (Figure 7-27).

As a result, depths, flood extent and velocities show only a small increase in comparison to the design runs.

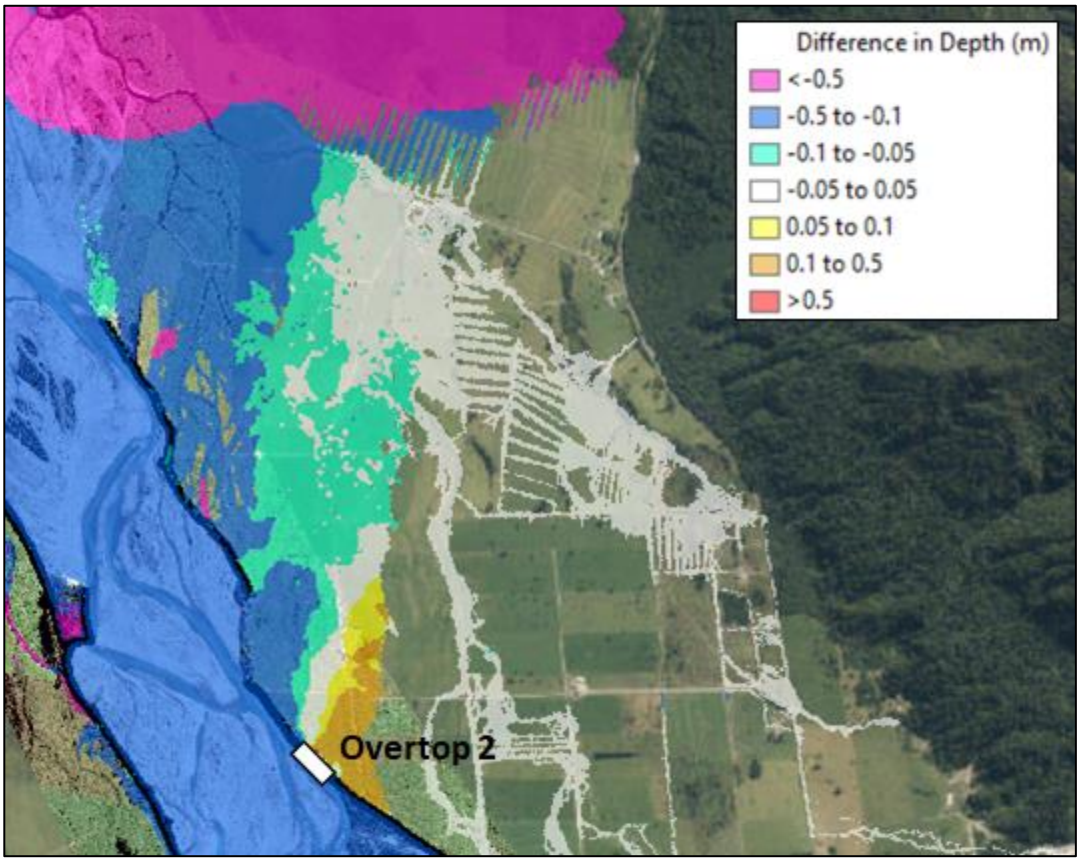

Figure 7-27: 1% AEP flow depth difference map between the design run and the right bank overtop 2 breach scenario.

Current level of service

- The modelling shows that the current protection scheme for the Wanganui River performs reasonably well during the 10, 5, 2 and 1% AEP (10, 20, 50 and 100 year ARI) design flows for the true left bank.

  The left side only overtops in events greater than a 2% AEP flow, and in these instances, the amount of flow is small, with the larger of these overtopped sections likely the result of a low point on the network where the river is accessed by vehicles and stock. A situation easily fixed.

  In general, the areas of inundation on the true left do not exceed 0.5 m in depth (except for the channelised flow in the 1% AEP RCP8.5 scenario), and do not reach damaging velocities, staying below 1.0 m/s. Therefore, there is unlikely to be significant damage to these areas as long as the stopbanks don't fail if (and where) they overtop.

  Comparatively, should the protection scheme (both left and right) not exist there would be considerable inundation of the adjacent farmland as the floodwaters would reoccupy the older braidplain and palaeochannels. Flows in this situation would on average be between 1.0 and 2.0 m/s which would cause significant damage to the land and threat to life.

- For the right side of the scheme, overtopping of the lower two stopbanks (stopbanks 2 and 3) and spillout through the gaps between them results in inundation of the adjacent farmland between Lake Ianthe and Evans Ck for all four design flows.

  In general, this inundation doesn't exceed depths of 0.5 m for surface flooding, however the channelised flow is on average up to 1.0 m deep, peaking at 2.0 m. Velocities are more concerning in the 5%, 2% and 1% AEP scenarios, as they surpass the damaging threshold of 1.0 m/s. Therefore, even without stopbank failure, there is likely to be considerable damage to this true right farmland during large flood events.

  However, these depths and velocities are significantly less than what they would be if the banks weren't there. The results from the runs where the true right stopbanks were removed, showed depths, flood extents and velocities increasing significantly as the floodwaters spill out onto the true right farmland. In these scenarios, whilst there would be considerable damage to the farmland and as a result a significant financial cost to the impacted landowners, there would also be a reduction in the depths and velocities in the main channel as well as up against the true left stopbanks by as much as 1.1m in depth and 3.0m/s in current speed compared with the design runs.

  It is also likely that the overtopping of the lower two stopbanks and the spillout through the gaps between them in the design runs reduces some of the pressure on the true left side of the scheme, therefore increasing the level of service the left side of the network provides, as well as perhaps reducing the frequency of damage and subsequent need for repairs to the true left stopbank.

Breach scenarios

- A number of overtopping and scour breach scenarios were simulated in different locations along both sides of the river. The results showed that a scour breach is likely to have more of an impact than an overtopping breach, with the location of the breach affecting the severity of the resulting inundation.

  On the left bank, breaches in the upper reaches will have the most significant consequences on the extent of flooding, with flow (largely under 1.0m deep) spreading out across the adjacent farmland.

  On the right bank, breaches will increase the severity of flooding in the area between Lake Ianthe and Evans Ck which already floods in the design scenarios. Most notable are the changes in velocities, which are expected to peak as high as 3.0 m/s.

- These breach and overtopping scenarios are not unrealistic. With the Interdecadal Pacific Oscillation (IPO) thought to have entered a positive phase in 2020, it is expected that storm intensities will remain high over at least one to two decades, with a continuation of the river behaviour seen in recent years. This will lead to increased sediment supply and risk of erosion and damage to the Wanganui flood protection network, and therefore an increased likelihood of breach or overtopping resulting in significant damage to the surrounding farmland.

9. CONCLUSIONS

The following conclusions can be drawn from this study:

- The true left bank has several low spots which are likely to begin to overtop in 2% AEP (50-year ARI) flow. Much of the bank has little to no freeboard available.
- The true right banks begin overtopping in relatively small events with overtopping apparent in limited locations in a 10% AEP (10-year ARI) event with more significant overtopping apparent in larger events. These banks would have a high probability of collapse should they overtop.
- The river is actively aggrading, and this is most likely due to artificial confinement with stopbanks. This is most notable between 7 km to 10 km downstream of the SH6 bridge where the main channel has become perched above the floodplain.
- The trend of increasing bed levels will further reduce the capacity of the flood protection network over time, increasing the chance of breach or overtopping during events.
- Due to the significant aggradation, historical behaviour of the river cannot be relied upon in order to predict future behaviour due to the nature of the changing climate as well as ongoing aggradation in the river.
- The current management regime for the river is likely to be financially unsustainable in the long term. The river has been severely constrained and whilst the bank network has survived until now, the climate appears to have been in a quiescent stage since the late 1990's. However, it seems reasonable that we can expect a continuation of the active river behaviour from the last few years in at least the coming decade.
- Expanding the protective network to fill in gaps may serve only to exacerbate the current situation, resulting in continued network damage and increasing the likelihood of breaches or overtopping.
- Removal of all or part of the right bank protection works may assist in slowing the rate of aggradation, reducing the pressure on the true left protection works, and decreasing the chance of breach or overtopping. This would have significant negative impact on the existing right bank land users and would require further study.

10. RECOMMENDATIONS

The following recommendations can be made from this study.

- Investigate installing a flow gauge in the catchment to allow an accurate estimate of flow at the State Highway 6 bridge to be determined.
- Collect peak water levels down the full length of the river immediately after a flood event to assist with calibration of the model and to improve our understanding of river behaviour.
- Keep detailed logs of recollections from local residents / flood photos on file.
- Overtopping and scour breach scenarios show very significant impacts. Geotechnical investigations to determine the condition of the existing banks and to better determine their likelihood of failure are recommended.
- Further investigations in order to better understand the long term aggradation trends as well as river characteristics would be worthwhile.
- Minor earthworks to raise low spots on the true left bank could add significant resilience to the scheme by reducing the risk of an overtopping failure.
- Regular inspections of the entire scheme are recommended after each high flow event in order to determine if there is any minor damage which could be further exacerbated in future events. Model results indicate that there are very high velocities in locations and potential for scour failure is high should any rockwork be damaged.
- Serious consideration needs to be made about realistic long-term management of the scheme. Consideration needs to be given to affordability / return on investment for long term protection. Trade-offs in regard to protection of the right / left bank may need to be made.
- Decisions around the desired level of service for the scheme will be necessary, with the scheme currently providing less than a 2% AEP (50-year ARI) of service based on the historic climate. This level of service is actively decreasing with ongoing aggradation as well as a warming climate bringing more intense and larger flood events.

11. REFERENCES

Benn, J. L. (1990). *A Chronology of Flooding on the West Coast, South Island, New Zealand. 1846 - 1990.*

Cox, S. (2016). *Australian Rainfall Runoff Guidelines: Flood Hydraulics - Chapter 7. Safety Design Criteria*.

Davies, T. (1997). Long-term management of facilities on an active alluvial fan - Waiho River fan, Westland, New Zealand. *Journal of Hydrology (NZ)*, *36*(1), 127–145.

Fookes, P. G., Lee, E. M., & Griffiths, J. S. (2007). *Engineering geomorphology: theory and practice*. Whittles Publishing.

Fryirs, K. A., & Brierley, G. J. (2013). *Geomorphic Analysis of River Systems: An Approach to Reading the Landscape*. Wiley-Blackwell.

Gardner, M. (2020). *Hokitika River Hydraulic Modelling and Flood Hazard Mapping*.

Gardner, M., & Wallace, P. (2013). *Wanganui River Stopbank Design Levels*.

Hessell, J. W. D. (1982). The Climate and Weather of Westland. *New Zealand Meteorological Service Miscellaneous Publication*, *115*(10).

King, J. (2010). *Preparing for future flooding: a guide for local government in New Zealand*.

Knighton, D. (1998). Fluvial Forms & Process A New Perspective. In *Fluvial Forms & Processes A New Perspective*. Hodder Education.

Mullan, A. B., Wratt, D. S., & Renwick, J. A. (2001). Transient model scenarios of climates for New Zealand. *Weather and Climate*, *21*, 3–34.

Rutledge, D. T., Ausseil, A.-G. E., Baisden, T., Bodeker, G., Booker, D., Cameron, M. P., Colins, D. B. G., Daigneault, A., Fernandez, M., Frame, B., Keller, E., Kremser, S., Kirschbaum, M. U. F., Lewis, J., Mullan, B., Reisinger, A., Sood, A., Stuart, S., Tait, A., … Zammit, C. (2017). Identifying Feedbacks, Understanding Cumulative Impacts and Recognising Limits: A National Integrated Assessment. Synthesis Report RA3. *Climate Changes, Impacts and Implications for New Zealand to 2100*.

West Coast Regional Council. (2022). *Wanganui Rating District 2021-2024 Asset Management Plan*.

Wratt, D., Salinger, J., Bell, R., Lorrey, D., & Mullan, B. (2022). *Past climate variations over New Zealand*. NIWA. https://niwa.co.nz/our-science/climate/information-and-resources/clivar/pastclimate

Zammit, C. (2022). *Climate change impact on peak discharge and bank-full flow duration at Te Kuha Stream: An analysis of Te Kuha streamflow gauging station under different warming scenarios and for different return periods and durations*.

APPENDIX A – SITE VISIT PHOTOS

Locations in latitude and longitude of the site visit photos have been provided in Table 0-1 below.


IMG_9534

IMG_9536

IMG_9538

IMG_9520

DJI_0509

DJI_0504

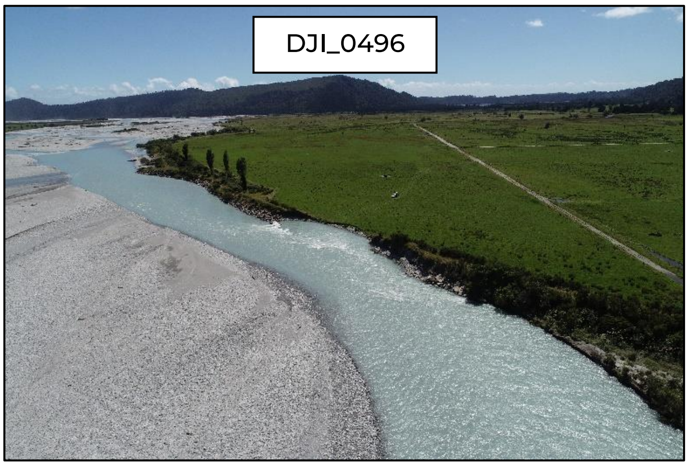

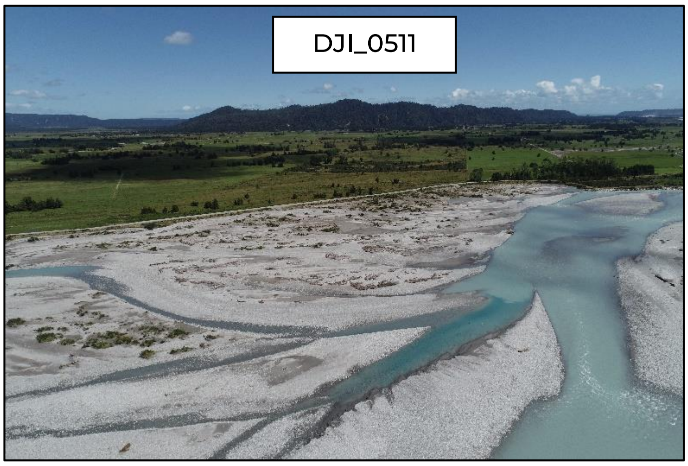

Table 0-1 - location of camera and drone photos.

File name	Longitude	Latitude
IMG_9464	170.625519	-43.145325
IMG_9466	170.622497	-43.145656
IMG_9497	170.624467	-43.154567
IMG_9518	170.620208	-43.148639
IMG_9520	170.618272	-43.147214
IMG_9527	170.627792	-43.161831
IMG_9532	170.629089	-43.134983
IMG_9534	170.629075	-43.134961
IMG_9536	170.628328	-43.135722
IMG_9538	170.628311	-43.135711
DJI_0496	170.610322	-43.104719
DJI_0504	170.606845	-43.101190
DJI_0509	170.606819	-43.101182
DJI_0511	170.606818	-43.101184

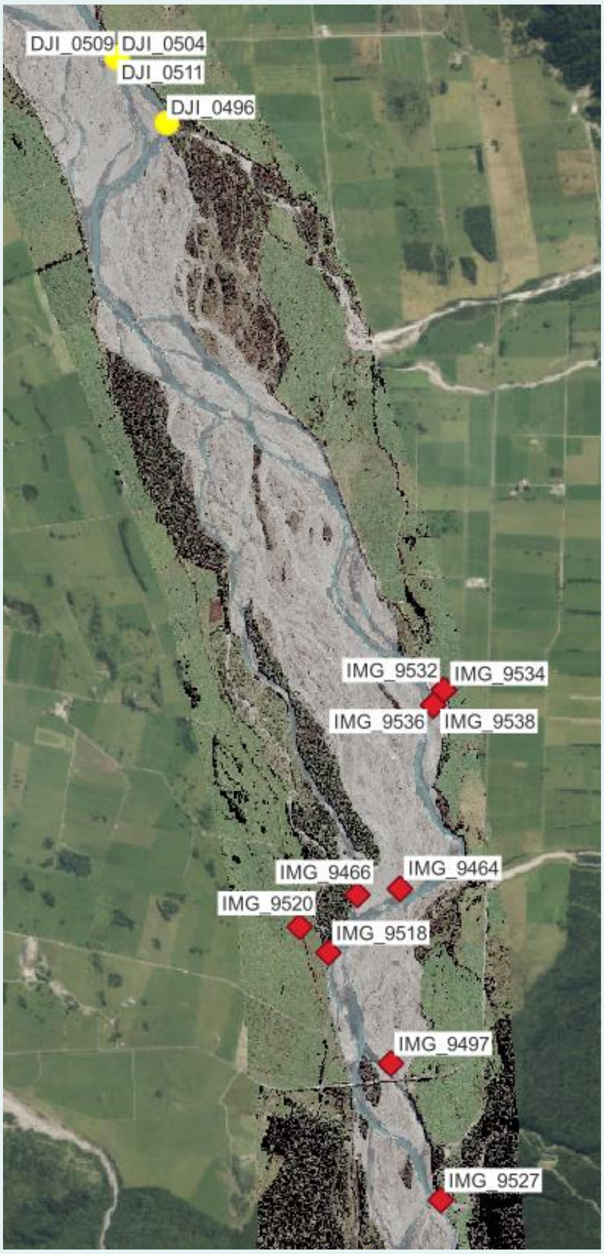

Land River Sea CONSULTING

APPENDIX B – AERIAL IMAGERY

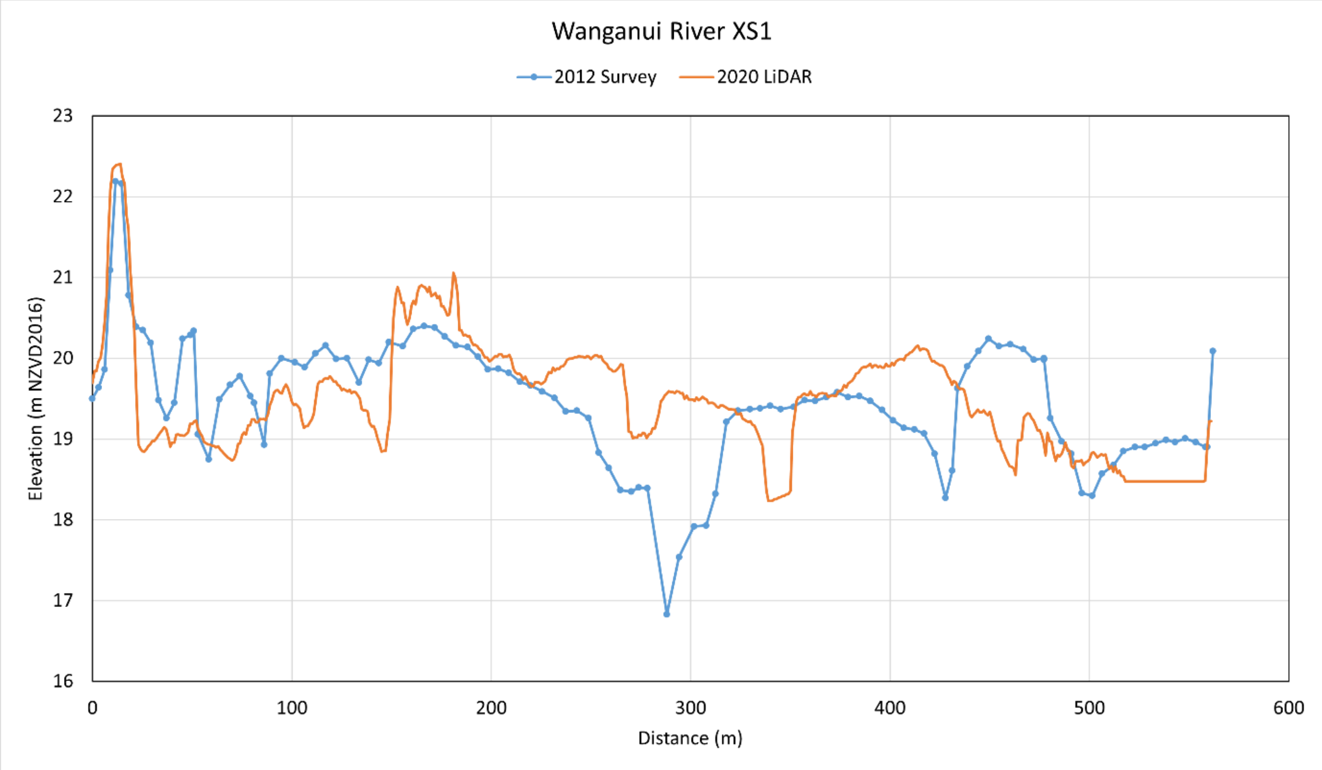

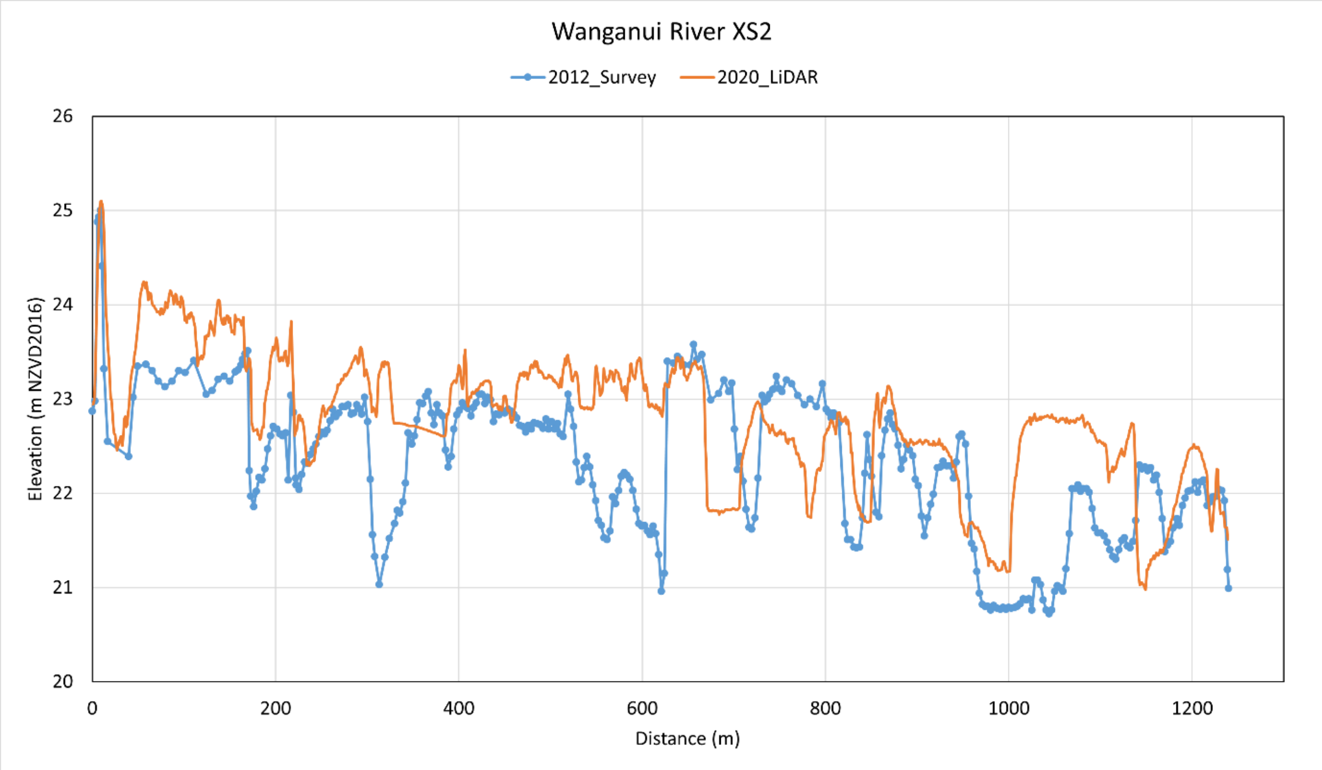

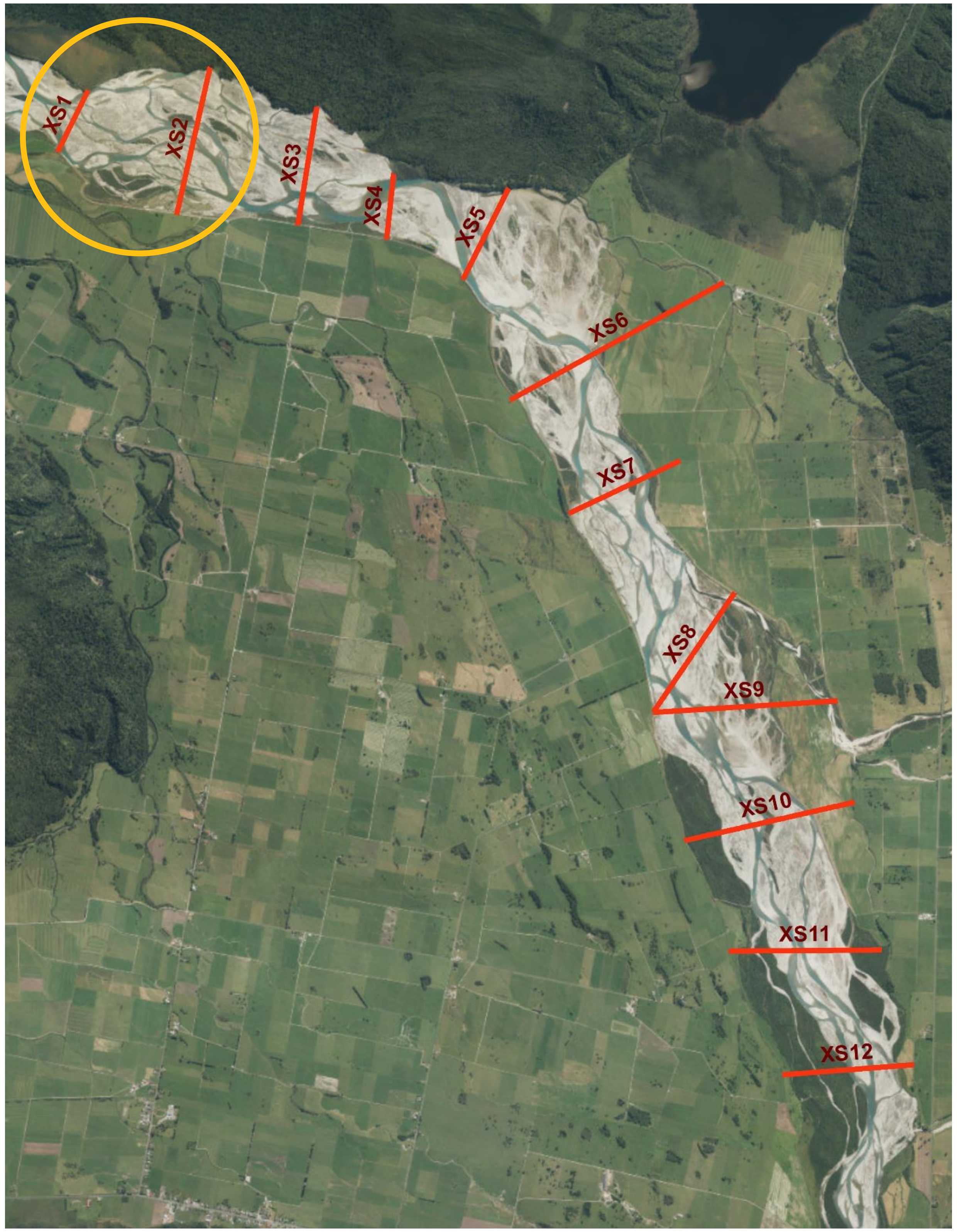

Land River Sea
CONSULTING

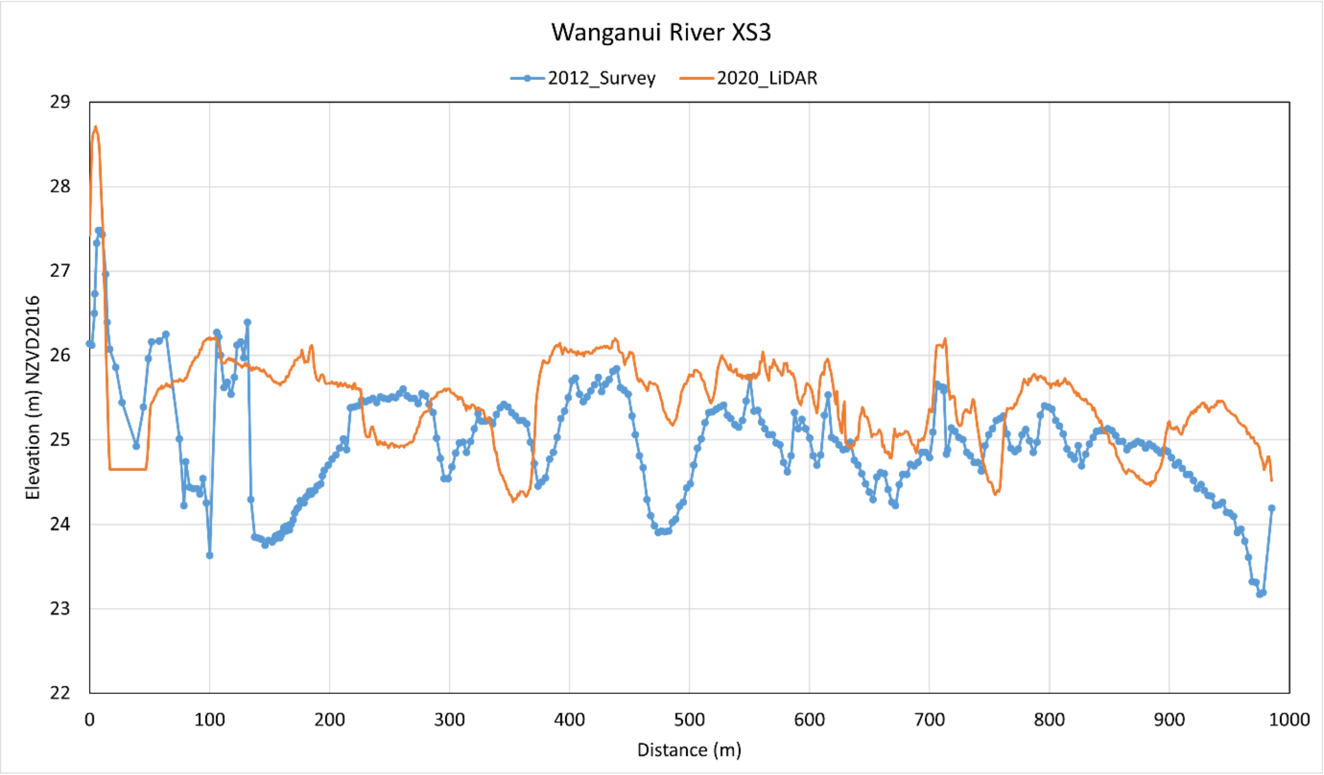

Wanganui River XS3
2012_Survey
2020_LiDAR
Elevation (m) NZVD2016
Distance (m)

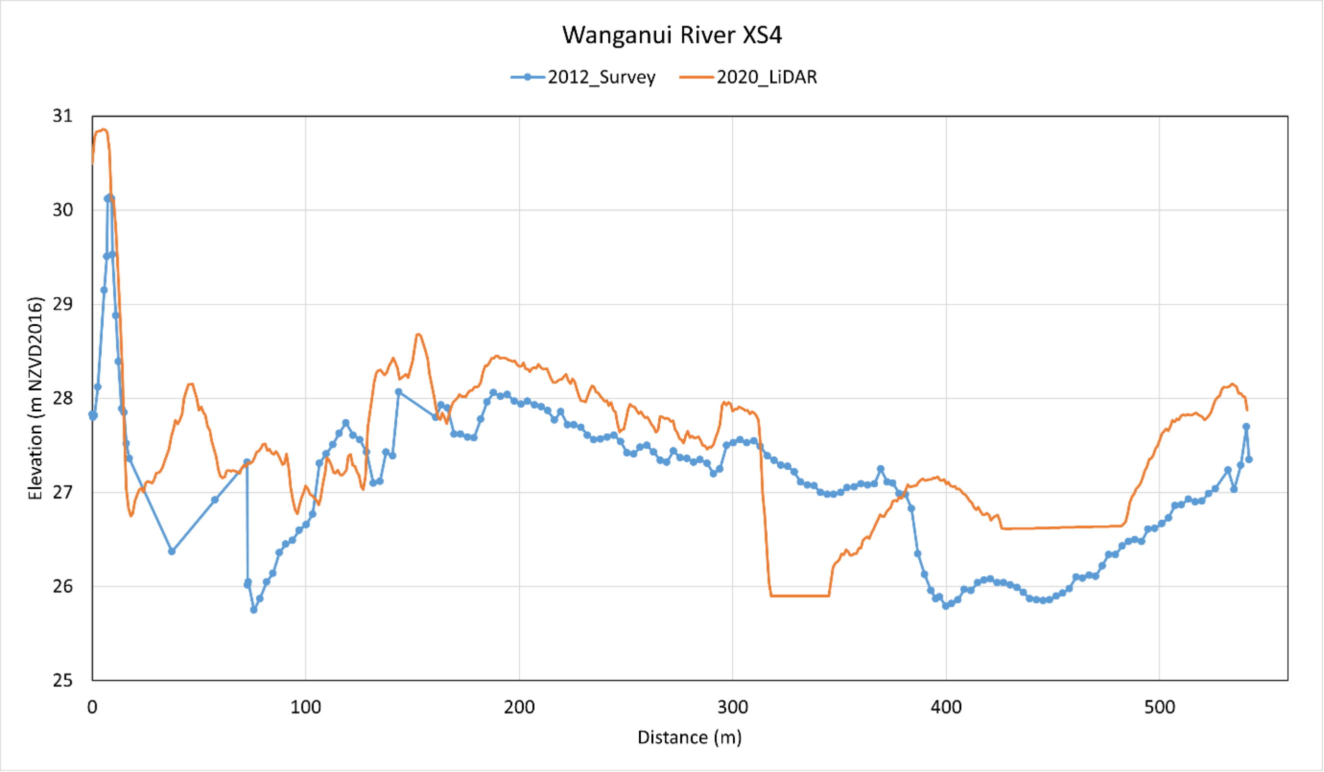

Wanganui River XS4
2012_Survey
2020_LiDAR
Elevation (m NZVD2016)
Distance (m)

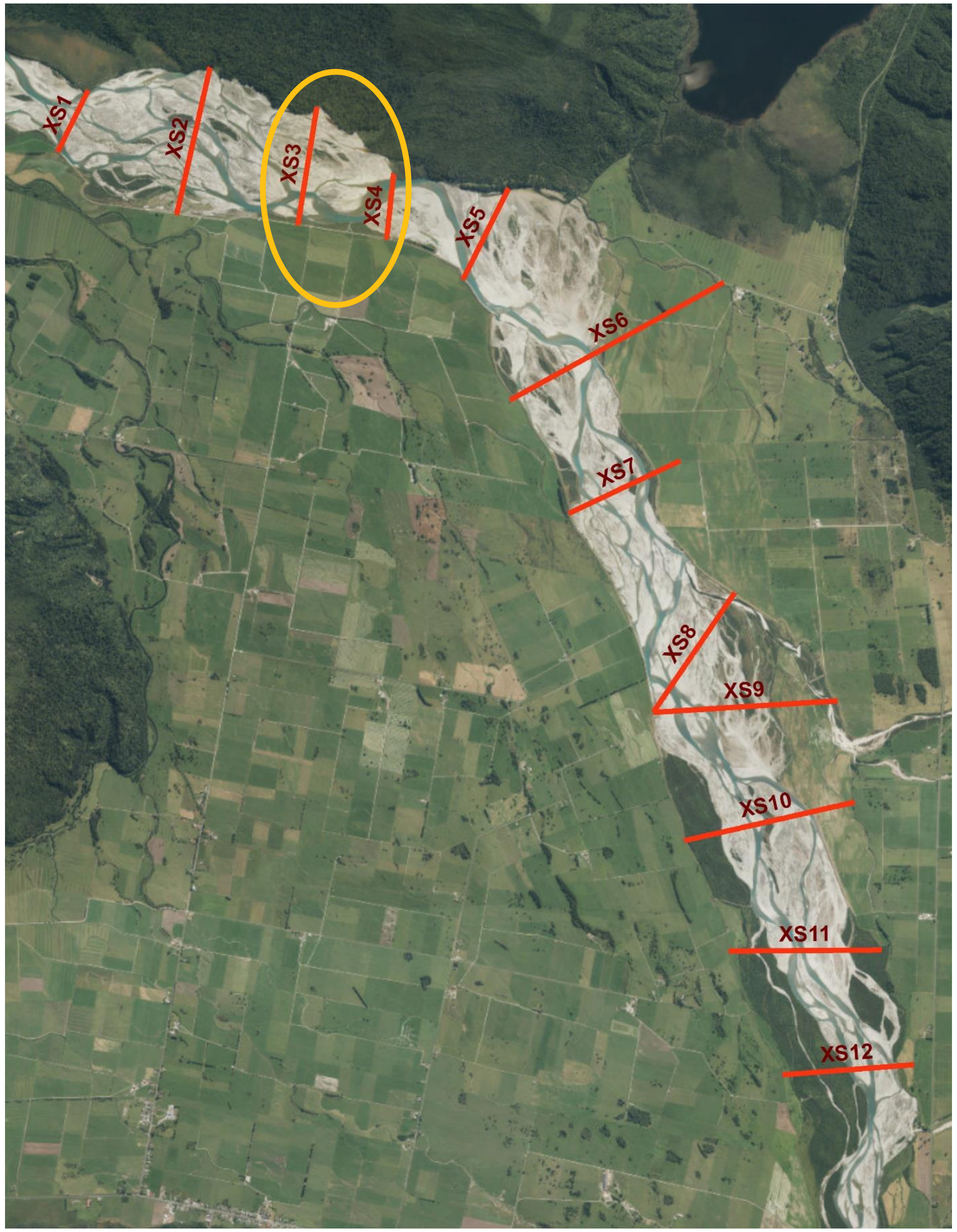

XS1
XS2
XS3
XS4
XS5
XS6
XS7
XS8
XS9
XS10
XS11
XS12


Wanganui River XS5
2012_Survey
2020_LiDAR
Elevation (m NZVD2016)
Distance (m)
35
34
33
32
31
30
29
28
27
0
100
200
300
400
500
600
700
800

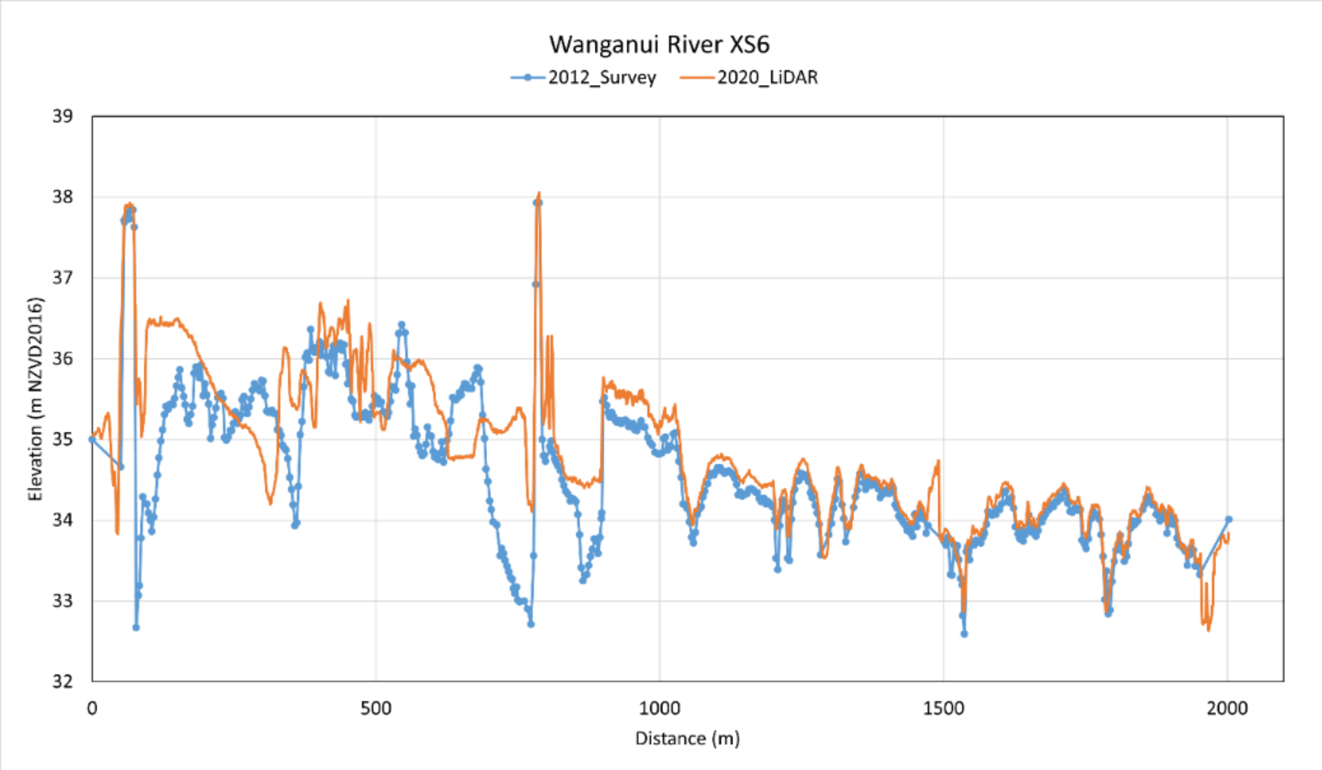
Wanganui River XS6
2012_Survey
2020_LiDAR
Elevation (m NZVD2016)
Distance (m)
39
38
37
36
35
34
33
32
0
500
1000
1500
2000

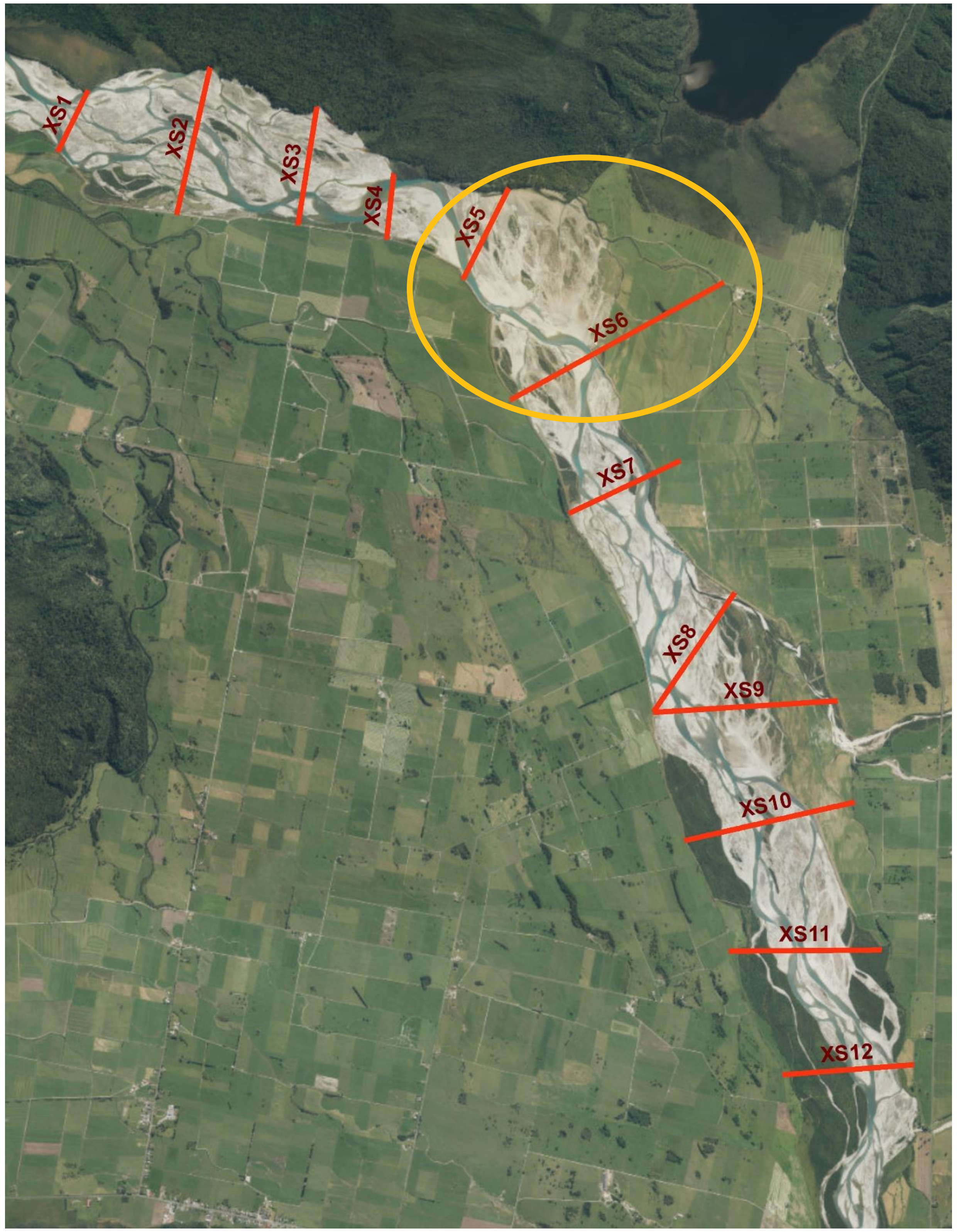
XS1
XS2
XS3
XS4
XS5
XS6
XS7
XS8
XS9
XS10
XS11
XS12

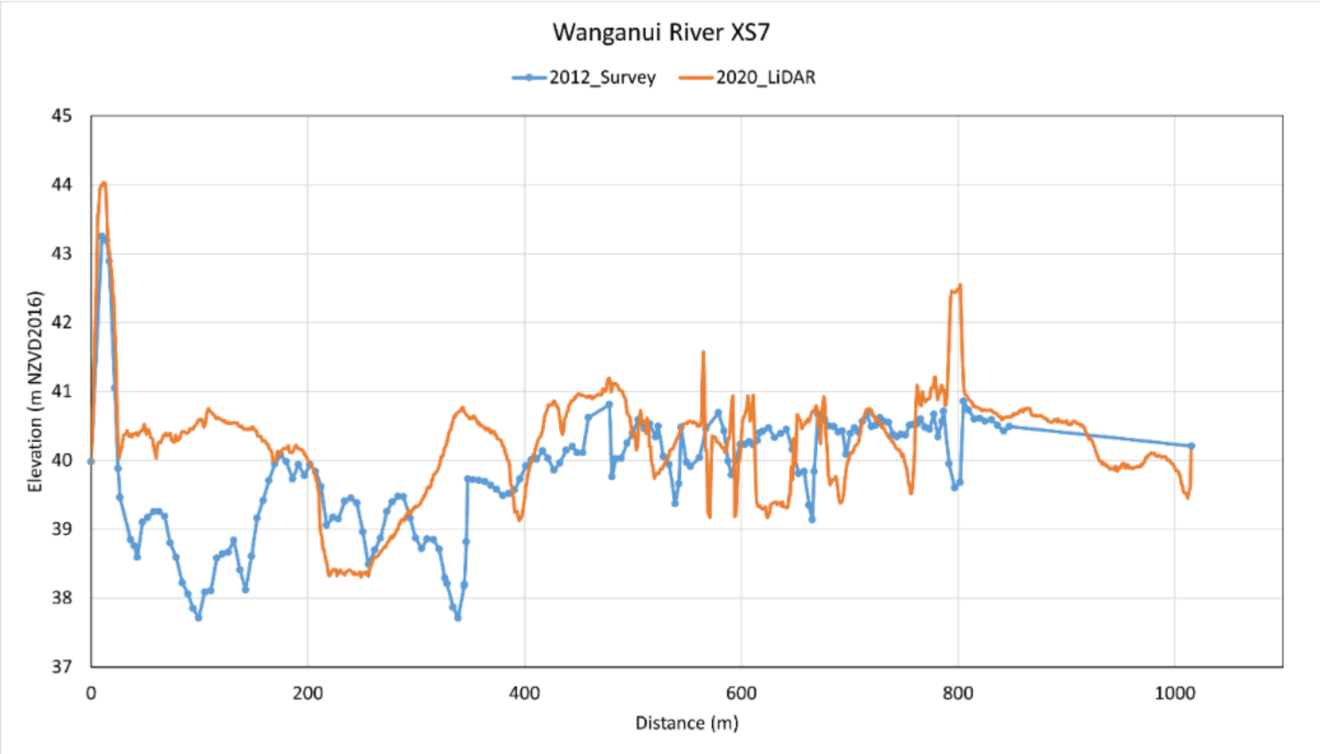
Wanganui River XS7
2012_Survey
2020_LiDAR
Elevation (m NZVD2016)
Distance (m)
45
44
43
42
41
40
39
38
37
0
200
400
600
800
1000

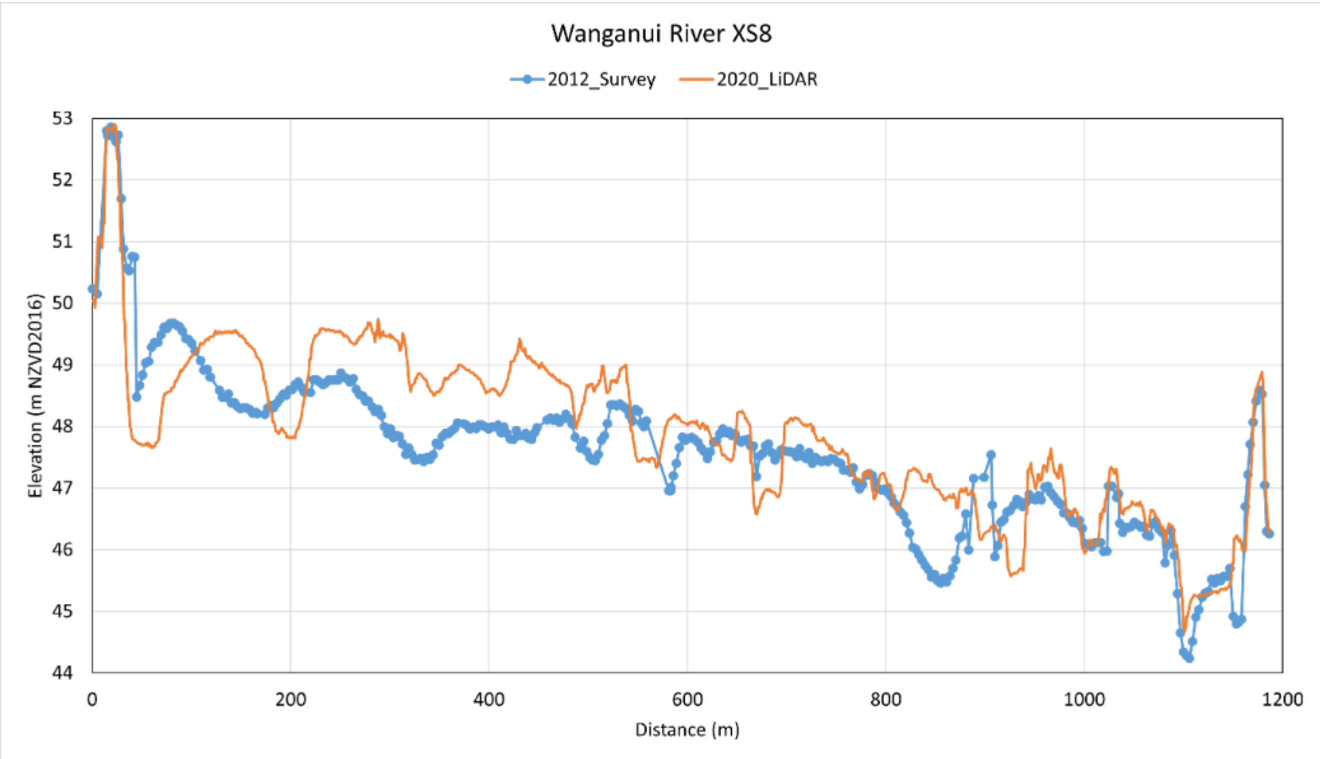
Wanganui River XS8
2012_Survey
2020_LiDAR
Elevation (m NZVD2016)
Distance (m)
53
52
51
50
49
48
47
46
45
44
0
200
400
600
800
1000
1200

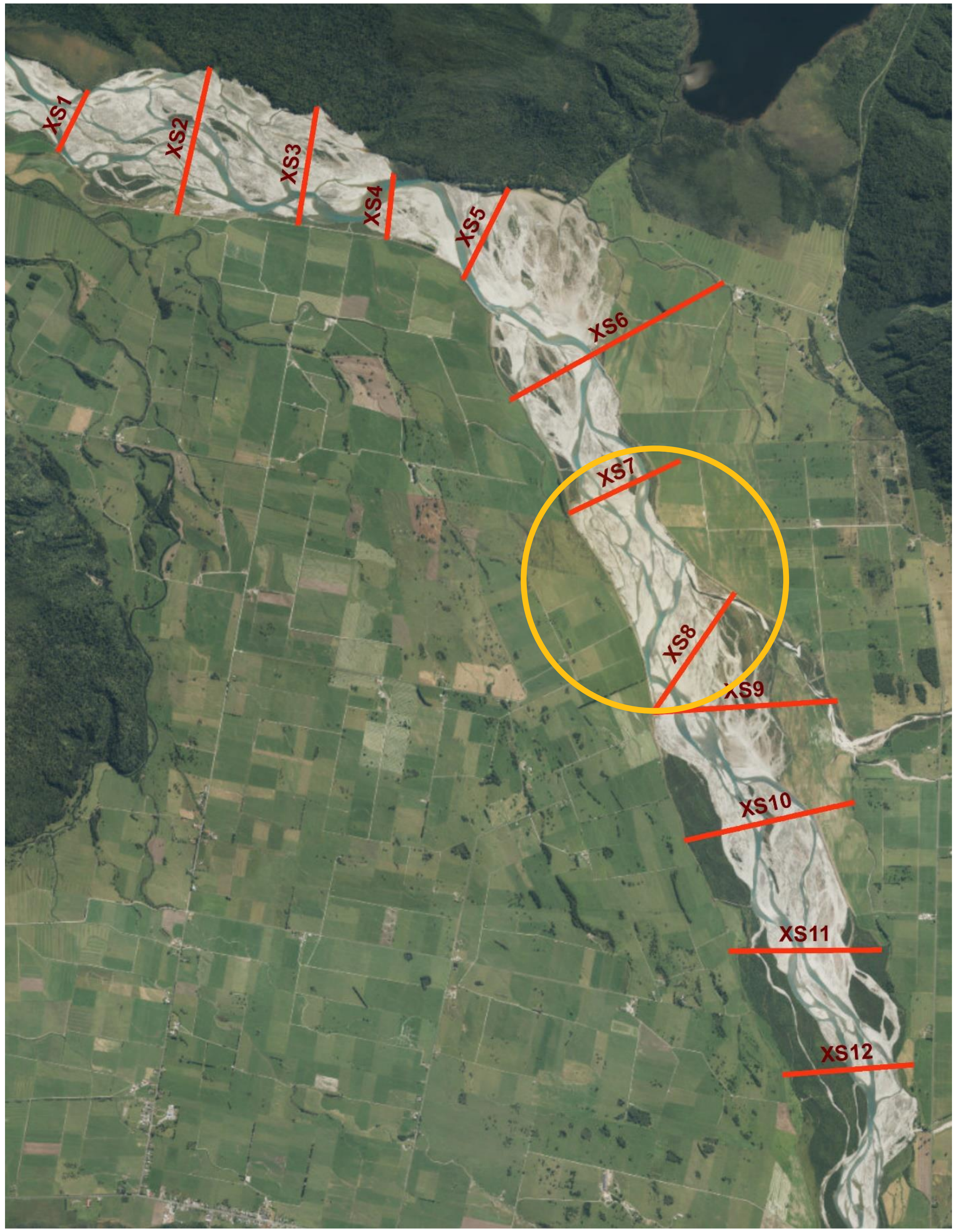
XS1
XS2
XS3
XS4
XS5
XS6
XS7
XS8
XS9
XS10
XS11
XS12

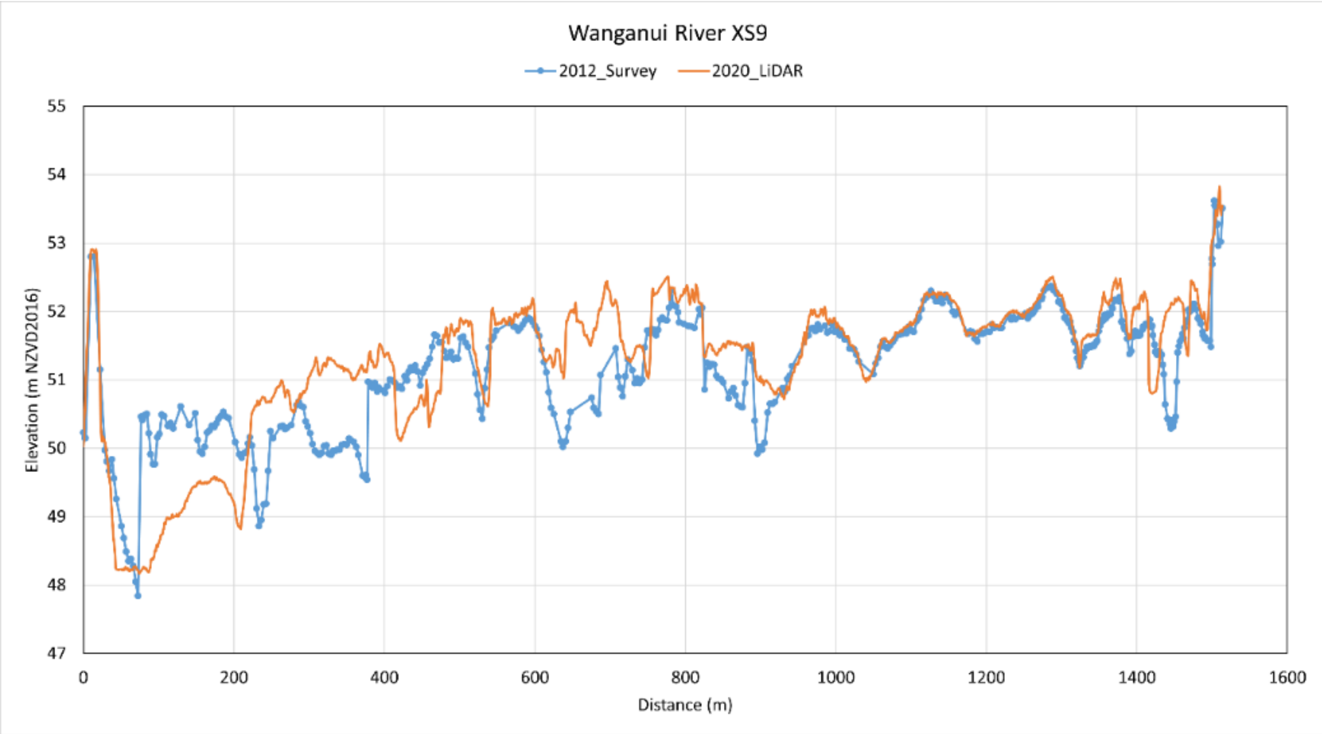
Wanganui River XS9
2012_Survey
2020_LiDAR
Elevation (m NZVD2016)
Distance (m)

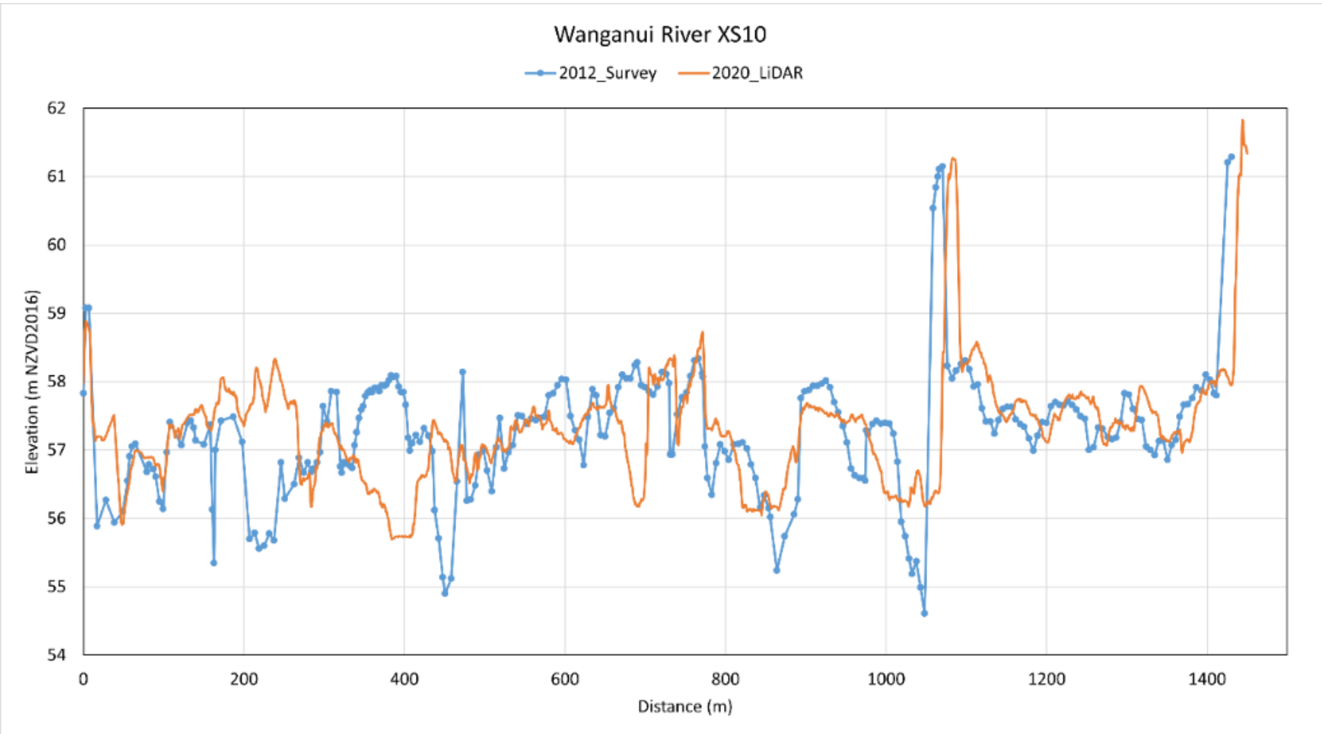
Wanganui River XS10
2012_Survey
2020_LiDAR
Elevation (m NZVD2016)
Distance (m)

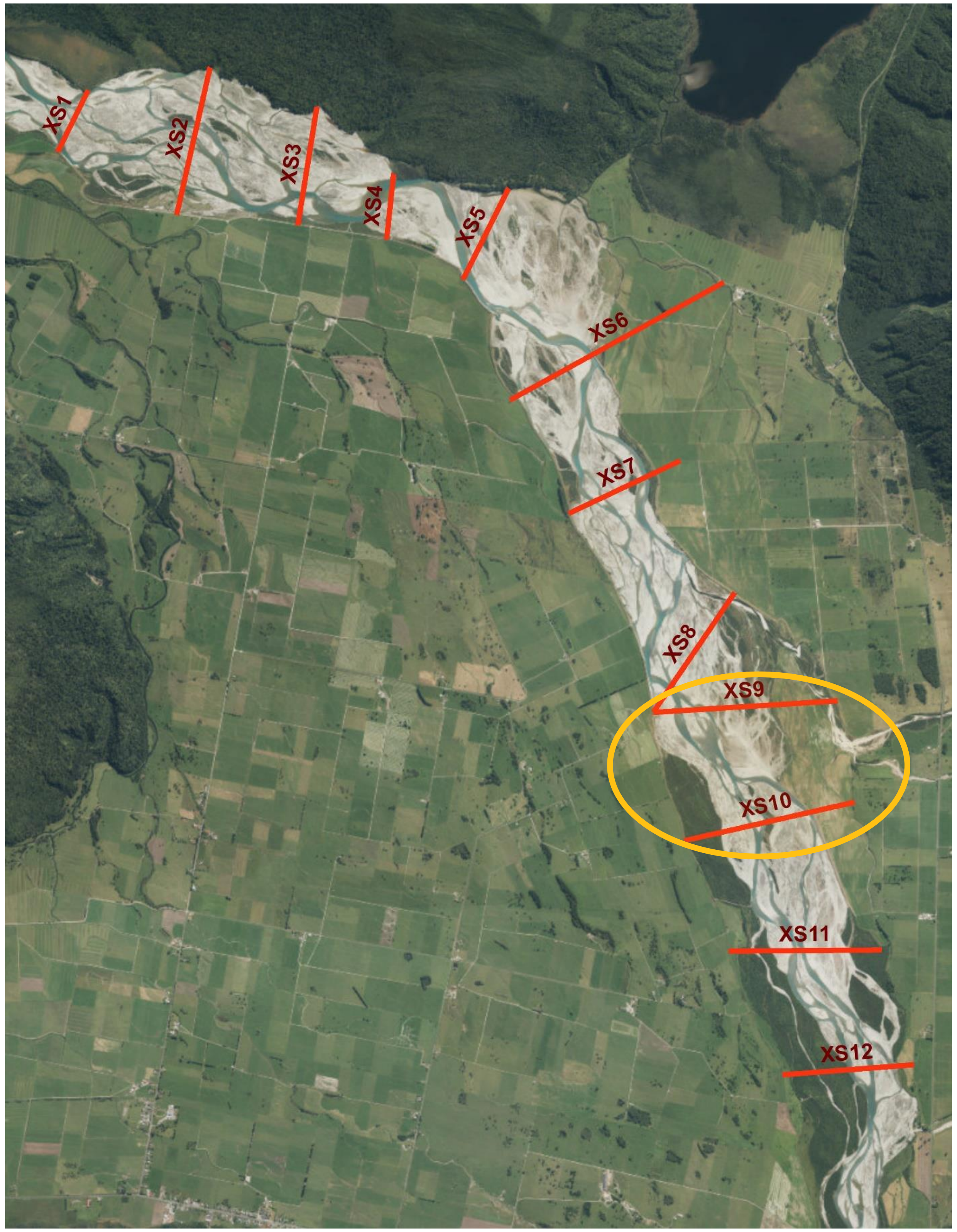
XS1
XS2
XS3
XS4
XS5
XS6
XS7
XS8
XS9
XS10
XS11
XS12

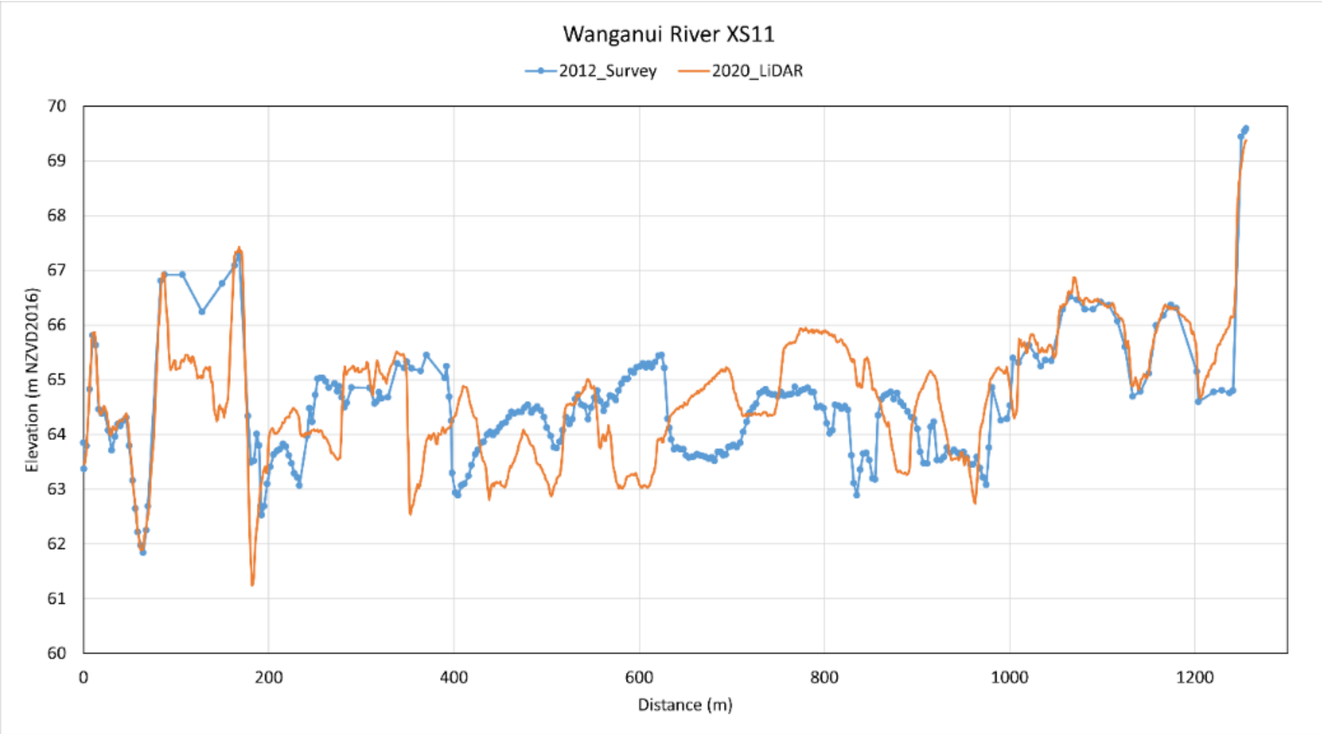
Wanganui River XS11
2012_Survey
2020_LiDAR
Elevation (m NZVD2016)
Distance (m)


Wanganui River XS12
2012_Survey
2020_LiDAR
Elevation (m NZVD2016)
Distance (m)

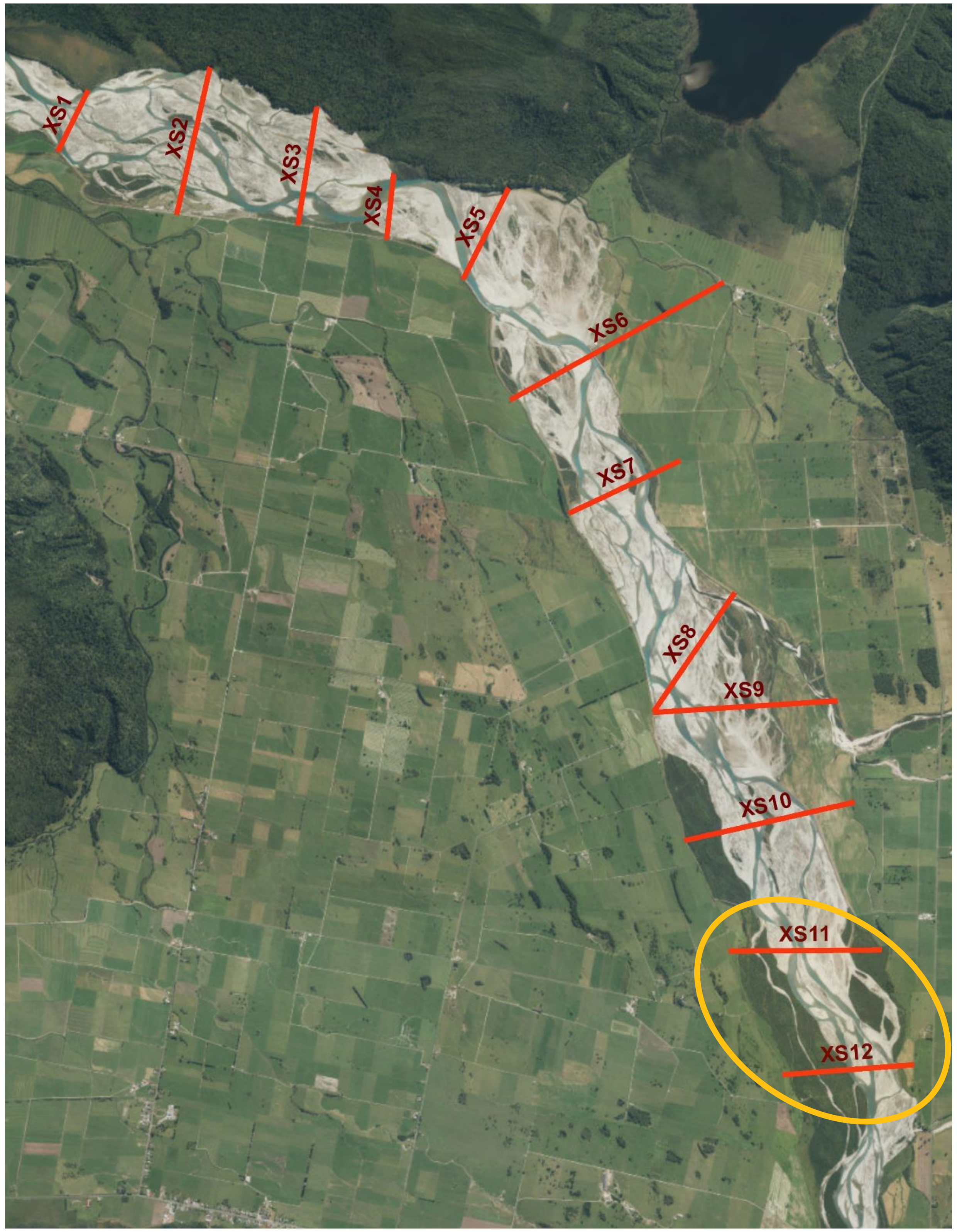
XS1
XS2
XS3
XS4
XS5
XS6
XS7
XS8
XS9
XS10
XS11
XS12